Institut für Nutzpflanzenwissenschaften und Ressourcenschutz - INRES
Abteilung Pflanzenernährung

Identification and characterization of evolutionarily conserved inositol pyrophosphate phosphohydrolases in plants

Dissertation

zur
Erlangung des Doktorgrades (Dr. agr.)
der
Landwirtschaftlichen Fakultät
der
Rheinischen Friedrich-Wilhelms-Universität Bonn

vorgelegt von

Philipp Gaugler
aus
Stuttgart

Bonn, 2023

Angefertigt mit Genehmigung der Landwirtschaftlichen
Fakultät der Rheinischen Friedrich-Wilhelms-Universität Bonn

Referent: Prof. Dr. Gabriel Schaaf
Koreferent: Prof. Dr. Peter Dörmann
Fachnahes Mitglied: Prof. Dr. Frank Hochholdinger
Vorsitzender: Prof. Dr. Andreas Meyer
Tag der mündlichen Prüfung: 19.09.2023

Contents

1. Summary

1.1. Summary

Inositol phosphates (InsPs), phosphate esters of *myo*-inositol, are cellular regulators with critical roles in a wide range of cellular processes in eukaryotes. Members of the subgroup containing at least one 'high-energy' phosphoanhydride group are termed inositol pyrophosphates (PP-InsPs) and have been of special interest in the last decades, especially for plant scientists. The biosynthesis of PP-InsPs has been uncovered in recent years, enabling the discovery of important functions in plant immunity, nutrient sensing and hormone signaling. However, one of the greatest challenges remains the reliable detection and quantification of these enigmatic molecules in plant extracts, primarily due to their low abundance and susceptibility to hydrolytic activities. The extraction of InsPs from plants labeled with [^{3}H]-*myo*-inositol and subsequent separation by strong anion exchange high-performance liquid chromatography (SAX-HPLC) is a method that has been frequently employed for the analysis of InsPs from all types of organisms, due to its high sensitivity and relative simplicity. Still, many parameters need optimization and a detailed description of the set-up and workflow of this method is critical for success. Therefore, the set-up of a suitable SAX-HPLC system, as well as the complete workflow covering plant cultivation, radiolabeling, InsP extraction, separation via SAX-HPLC and subsequent data analysis was described in a detailed step-by-step protocol and visualized by video documentation. The protocol allowed the discrimination and quantification of various InsP species, including multiple non-enantiomeric isomers and various PP-InsPs from the established model plant *Arabdiopsis thaliana*. The versatility of this method was exemplified by the first analysis of InsPs from *Lotus japonicus*. Multiple differences in InsP levels between *Arabidopsis* and *Lotus* give new hints for future studies of InsPs in plant systems, whereas the described method represents an optimized and standardized tool to help elucidate the biological roles of InsPs *in planta*. In addition to these methodological challenges, several aspects of PP-InsP biosynthesis in plants remain elusive. For instance, very little is known about the identity of PP-InsP phosphohydrolases, despite the apparent rapid hydrolysis of PP-InsPs in plant extracts. Therefore, the *Arabidopsis* members of the Plant and Fungi Atypical Dual Specificity Phosphatases (PFA-DSP), which are homologs of the recently identified yeast PP-InsP phosphohydrolase Siw14, were characterized. All five homologs, similarly to recombinant Siw14, displayed phosphohydrolase activity *in vitro*, with high specificity for the 5-β-phosphate of PP-InsPs and minor to minimal activity against 4/6-InsP$_7$ or 1/3-InsP$_7$, respectively. Furthermore, heterologous expression of either one of the homologs rescued wortmannin sensitivity of the *siw14⊿* yeast deletion mutant and restored elevated InsP$_7$ levels to wild-type levels. Genetic interaction analyses of InsP and PP-InsP kinases with *SIW14*, revealed that the wortmannin sensitivity of *siw14⊿* depends on the presence of Kcs1-derived PP-InsPs like 5-InsP$_7$. Although the *Arabidopsis* PFA-DSPs appear to be at least partially redundant *in vitro*, as well as *in vivo*, SAX-HPLC analyses of the *Arabidopsis* T-DNA insertion line *pfa-dsp1-6*, in which *PFA-DSP1* is overexpressed, showed a clear reduction of InsP$_7$ levels compared to Col-*0*. This finding was strengthened by heterologous expression of *PFA-DSP1* in *Nicotiana bethamiana* leaves, which resulted in a specific reduction of 5-InsP$_7$. In conclusion, these experiments showed that the *Arabidopsis* PFA-DSPs are evolutionarily conserved and are highly specific 5-β-phosphate PP-InsP phosphohydrolases with very similar *in vitro* and apparently also *in vivo* activities. These findings not only broaden the knowledge of PP-InsP degradation in yeast and in plants, but also provide additional genetic tools to uncover the roles of PP-InsPs in plant physiology and plant development.

1.2. Zusammenfassung

Inositolphosphate (InsPs), Phosphorsäureester von *myo*-Inositol, sind zelluläre Regulatoren mit kritischen Funktionen in vielzähligen zellulären Prozessen in Eukaryoten. Die Untergruppe, welche mindestens eine 'hochenergetische' Phosphoranhydrid Gruppe besitzt, wird Insositolpyrophosphate (PP-InsPs) genannt und war, speziell für Pflanzenbiologen, in den vergangenen Jahrzenten von besonderem Interesse. Die Biosynthese von PP-InsPs wurde in den vergangen Jahren entschlüsselt, was die Enthüllung von wichtigen Funktionen in der pflanzlichen Immunabwehr, der Nährstofferkennung und hormonellen Signalwegen ermöglicht hat. Allerdings bleibt eine der größten Herausforderungen die zuverlässige Detektion und Quantifizierung dieser enigmatischen Moleküle in Pflanzenextrakten, hauptsächlich aufgrund zu geringer Mengen und ihrer Anfälligkeit für hydrolytische Aktivitäten. Die Extraktion von InsPs aus [^{3}H]-*myo*-Inositol markierten Planzen und anschließende Trennung durch Anionenaustausch-Hochleistungsflüssigkeitschromatographie (SAX-HPLC) ist eine Methode, die aufgrund ihrer hohen Sensitivität und verhältnismäßigen Einfachheit häufig angewendet wurde, um InsPs aus verschiedenen Eukaryoten zu analysieren. Dennoch haben einige Parameter Optimierungsbedarf und eine detailierte Beschreibung des Aufbaus und des Arbeitsablaufs ist kritisch für den Erfolg dieser Methode. Deshalb wurde der Aufbau eines geeigneten SAX-HPLC Systems, sowie der gesamte Arbeitsablauf von der Pflanzenanzucht, der radioaktiven Markierung, der Extraktion der InsPs über die Auftrennung via SAX-HPLC und die anschließende Datenanalyse in einem detailierten Protokol Schritt für Schritt beschrieben und durch Videodokumentation visualisiert. Das Protokoll ermöglichte die Unterscheidung und Quantifizierung verschiedenster InsP Spezies, inklusive mehrerer nicht-enantiomerer Isomere sowie verschiedener PP-InsPs. Die Vielseitigkeit der Methode wurde durch die erstmalige Analyse von InsPs aus *Lotus japonicus* verdeutlicht. Mehrere Unterschiede in den InsP Werten zwischen *Arabidopsis* und *Lotus* geben neue Hinweise für zukünftige Studien über InsPs in pflanzlichen Systemen, wohingegen die beschriebene Methode ein optimiertes und standardisiertes Werkzeug darstellt, um die biologischen Rollen von InsPs *in planta* weiter zu untersuchen. Zusätzlich zu den genannten methodischen Herausforderungen, sind auch weiterhin weite Teile der PP-InsP Biosynthese nicht aufgedeckt. Beispielsweise ist nur sehr wenig über die Identität von PP-InsP Phosphohydrolasen bekannt, obwohl PP-InsPs in Pflanzenextrakten sehr schnell hydrolysiert werden. Deshalb wurden die Mitglieder der 'Plant and Fungi Atypical Dual Specificty' Phospatasen (PFA-DSP) aus *Arabidopsis*, welche Homologe der kürzlich identifizierten Hefe PP-InsP Phosphohydrolase Siw14 sind, charakterisiert. Alle fünf Homologe zeigten, sehr ähnlich zu rekombinatem Siw14, Phosphohydrolaseaktivität *in vitro*, mit hoher Spezifität für das 5-β-Phosphat der PP-InsPs und nur geringer bis minimaler Aktivität gegen 4/6-InsP$_7$ beziehungsweise 1/3-InsP$_7$. Darüber hinaus konnte heterologe Expression jedes Homologs die Sensitivität der Hefe *siw14⊿* Deletionsmutante gegenüber Wortmannin aufheben sowie die erhöhten InsP$_7$ Werte auf wildtypisches Niveau senken. Analysen genetischer Interaktionen zwischen *SIW14* und den InsP/PP-InsP Kinasen zeigten, dass die Sensitivität von *siw14⊿* gegenüber Wortmannin von Kcs1 abhängigen PP-InsPs wie 5-InsP$_7$ kontrolliert wird. Obwohl die biochemischen Aktivitäten von *Arabidopsis* PFA-DSPs *in vitro* ähnlich sind und *in vivo* teilweise redundant erscheinen, zeigten SAX-HPLC Analysen der *Arabidopsis* T-DNA Insertionslinie *pfa-dsp1-6*, welche *PFA-DSP1* überexprimiert, eine deutliche Reduktion der InsP$_7$ Werte im Vergleich zu Col-0. Diese Entdeckung wurde durch die heterologe Expression von *PFA-DSP1* in *Nicotiana benthamiana* Blättern, welche in einer spezifischen Reduktion von 5-InsP$_7$ resultierte, bestärkt. Zusammenfassend zeigten diese Experimente, dass die *Arabidopsis* PFA-DSPs evolutionär konservierte und hochspezifische 5-β-Phosphat PP-InsP Phosphohydrolasen mit sehr ähnlichen *in vitro* und scheinbar auch *in vivo* Aktivitäten sind. Diese Kenntnisse erweitern nicht nur das Wissen über den Abbau von PP-InsP in Hefe und Pflanzen, sondern liefern auch zusätzliche Werkzeuge, um die Rollen von PP-InsPs in der Physiologie und Entwicklung von Pflanzen aufzudecken.

2. Introduction

2.1. Chemistry and analysis of inositol phosphates

Inositol phosphates (InsPs) came into spotlight as signaling molecules almost four decades ago, after Ins(1,4,5)P_3, or simplified InsP_3, was identified as a second messenger activating the receptor-mediated release of Ca^{2+} in animal cells (Berridge & Irvine, 1989; Streb et al., 1983). InsPs are esterified derivatives of *myo*-inositol (Ins) with unique patterns of monophosphates (P) and high-energy di-phospho bonds (PP). InsPs containing at least one of these diphosphates are therefore termed inositol pyrophosphates (PP-InsPs) and have been described as versatile messengers in eukaryotes (Menniti et al., 1993; Stephens et al., 1993; Thota & Bhandari, 2015; Shears, 2018; Laha et al., 2015, 2016, 2022; Wild et al., 2016; Couso et al., 2016; Dong et al., 2019; Zhu et al., 2019; Riemer et al., 2021; Gulabani et al., 2021). For multiple reasons, the major methodological challenge for scientists interested in these enigmatic molecules is their reliable and precise detection, as well as quantification. First, a wide variety of *myo*-inositol phosphate species has already been identified in nature, with many more (63, excluding the pyrophosphate species) theoretically possible (Agranoff, 2009). Second, most of the identified ones are present at relatively low levels in the cells (Gaugler et al., 2020; Laha et al., 2021; Qiu et al., 2020; Qiu et al., 2021). And lastly, *myo*-inositol is a meso compound with a plane of symmetry dissecting the C2 and C5 positions, which is the reason why InsP species with (pyro)phosphorylations at either position C1 or C3, or at position C4 or C6 are enantiomers (Irvine & Schell, 2001; Blüher et al., 2017). Therefore, the methods developed and employed for the analysis of InsPs are similarly diverse. Different mass spectrometry-based methods have been used in the past to detect InsPs and PP-InsPs in cell extracts, but most of them failed to differentiate distinct isomers (Couso et al., 2016; Ito et al., 2018). Recently, a new method based on capillary electrophoresis (CE) coupled to electrospray ionization mass spectrometry (ESI-MS) has been developed, which enabled the detection and quantification of a large diversity of InsP and PP-InsP isomers, including the InsP_7 isomers, in a wide variety of cell extracts (Qiu et al., 2020, 2021). However, discrimination between enantiomers (e.g., 1/3 or 4/6-InsP_7) has still not been achieved and the method itself is quite demanding in terms of technical requirements. A much simpler method is based on polyacrylamide gel electrophoresis (PAGE). There, InsPs are extracted from cell lysates with TiO_2 beads and subsequently eluted. This step is identical to the sample preparation for the previously mentioned CE-ESI-MS analysis (Qiu et al., 2020). After separation on PAGE, the InsPs can be stained by either toluidine blue or DAPI (Dong et al., 2019; Wilson & Saiardi, 2018; Loss et al., 2011). Reliable detection of InsPs lower than InsP_5 and discrimination between isomers remain challenging with this method.

In contrast, another rather sophisticated method developed a few years ago allowed the detection of 5-$InsP_7$, as well as the discrimination of non-enantiomeric $InsP_5$ isomers (Harmel et al., 2019). This method is based on nuclear magnetic resonance (NMR) analysis using [^{13}C]-*myo*-inositol as labeling agent, a chemically synthesized and so far commercially unavailable compound. So far, the method of choice was in most cases strong anion exchange high-performance liquid chromatography (SAX-HPLC) of samples radiolabeled with [^{3}H]-*myo*-inositol (Azevedo & Saiardi, 2006; Shears, 2020; Wilson & Saiardi, 2017). The radioactive *myo*-inositol is taken up by the cells/organism and converted into InsPs by dedicated cellular kinases and phosphatases. With increasing labeling time, a steady-state isotopic equilibrium is reached, after which the obtained InsP profiles should represent the lipid-dependent InsP status of the organism (Azevedo & Saiardi, 2006). These labeled InsPs can then be extracted with perchloric acid and fractionated during SAX-HPLC, where the negatively charged InsPs strongly interact with the positively charged stationary phase of the SAX column. Elution is then achieved through an increasing phosphate buffer gradient with the elution times that vary depending on the charge and geometry of the respective InsP species. The resulting fractions are collected and the β-decay of tritium (^{3}H) can be measured in a liquid scintillation counter. Because only non-enantiomeric isomers can be separated, radiolabeled standards are necessary to assign a specific InsP isomer to its corresponding peak in the chromatogram. Thankfully, various laboratories have helped assigning peaks to certain InsP species and narrowing down isomeric identities by generating labeled, as well as unlabeled standards (Kuo et al., 2018; Stevenson-Paulik et al., 2002, 2005, 2006; Brearley & Hanke, 1996a, 1996b; Liu et al., 2001; Hughes et al., 1989; Shears et al., 1987; Stephens et al., 1989; Saiardi et al., 2000, 2001; Azevedo et al., 2010). The recent discoveries of the enzymatic pathways leading to the formation of PP-InsPs in plants, as well as of seemingly unrelated proteins like a bacterial type III effector with a specific 1-phytase activity, will allow for the generation of further useful standards (Blüher et al., 2017; Laha et al., 2015, 2016, 2019, 2022; Riemer et al., 2021). The basics of the SAX-HPLC based method have been described quite some time ago, but difficulties in the reliable detection of low abundant PP-InsPs species like $InsP_8$, especially *in planta*, underline the urgent need for further improvements of this SAX-HPLC-based method (Stevenson-Paulik et al., 2005, 2006; Brearley & Hanke, 1996a; Azevedo & Saiardi, 2006).

2.2. Biosynthesis of inositol pyrophosphates in yeast and plants

The biosynthesis of PP-InsPs is widely conserved among eukaryotes, but there are important distinctions between yeast/animals and plants. PP-InsPs are generally synthesized from a fully phosphorylated inositol ring, which is then termed $InsP_6$ (inositol hexakisphosphate or phytic acid).

In yeast and animals, the Kcs1/IP6K ($InsP_6$ Kinase)-type proteins phosphorylate the C5 position leading to the generation of 5-$InsP_7$, while the Vip1/PPIP5K kinases phosphorylate the C1 position of either $InsP_6$ or 5-$InsP_7$, which results in the formation of 1-$InsP_7$ or 1,5-$InsP_8$, respectively (Lin et al., 2009; Mulugu et al., 2007; Saiardi et al., 1999; Wang et al., 2012). With the use of the previously mentioned SAX-HPLC analyses of [^{3}H]-*myo*-inositol labeled plants, PP-InsPs have been detected in plant extracts in the past (Laha et al., 2015; Desai et al., 2014; Flores & Smart, 2000; Lemtiri-Chlieh et al., 2000). In *Arabidopsis*, $InsP_8$ and presumably 1/3-$InsP_7$ is synthesized by the PPIP5K isoforms VIH1 and VIH2 (Laha et al., 2015; Zhu et al., 2019). However, Kcs1/IP6K-type proteins have so far not been detected in any land plant. Work on *Arabidopsis* inositol (1,3,4) triphosphate 5/6 kinases ITPK1 and ITPK2 has partially shed some light on the synthesis of 5-$InsP_7$ *in planta*. Both enzymes were reported to catalyze the synthesis of 5-$InsP_7$ from $InsP_6$ *in vitro* (Riemer et al., 2021; Laha et al., 2022). In line with this finding, *itpk1* mutant plants display reduced 5-$InsP_7$ levels *in vivo* (Figure 1) (Riemer et al., 2021, 2022; Laha et al., 2022).

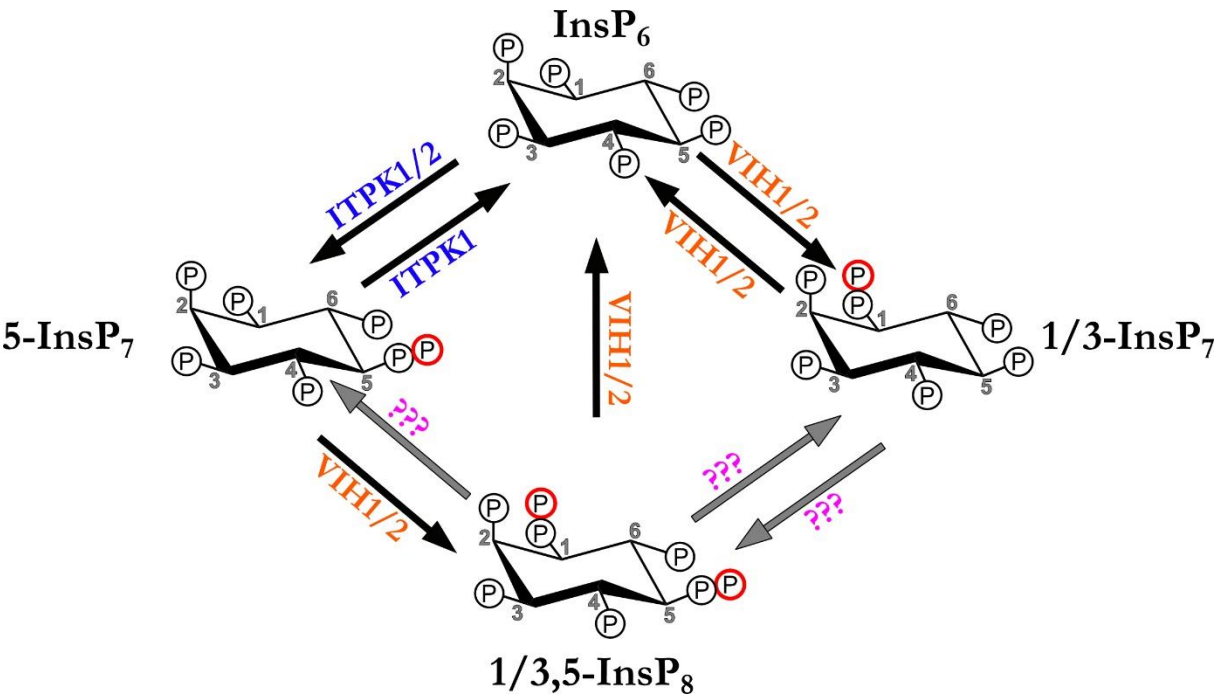

Figure 1: Inositol pyrophosphate biosynthesis pathways in plants.
$InsP_6$ is either phosphorylated by ITPK1/2 to 5-$InsP_7$ or by VIH1/2 to 1-$InsP_7$. VIH1/2 use 5-$InsP_7$ as substrate to generate $InsP_8$. The isomeric identity of the latter remains so far unresolved but presumably represents 1,5-$InsP_8$ or the enantiomeric 3,5-$InsP_8$. Both $InsP_8$ isomers, as well as 1/3-$InsP_7$ can be hydrolyzed to $InsP_6$ by the phosphatase domains of VIH1/2. ITPK1 is also able to catalyze the reverse reaction from 5-$InsP_7$ to $InsP_6$ in the presence of ADP at low adenylate charge. The gray arrows and question marks denote alternative routes of 1/3-$InsP_7$ and 1/3,5-$InsP_8$ synthesis and hydrolysis, for which the responsible enzymes are so far unknown (Figure modified from Riemer et al., 2022)

Interestingly, the use of the mentioned CE-ESI-MS method allowed for the detection of 4/6-$InsP_7$, an $InsP_7$ isomer so far unknown in plants and whose synthesis still needs to be elucidated (Riemer et al., 2021).

2.3. Inositol pyrophosphate phosphohydrolases in eukaryotes

Although the biosynthesis of PP-InsPs in plants is now better understood, very little is known about the (active) degradation of these molecules. All known Vip1/PPIP5K proteins are bifunctional enzymes, which consist of an N-terminal ATP-grasp kinase domain and a C-terminal phosphatase domain (Laha et al., 2015; Zhu et al., 2019; Mulugu et al., 2007; Wang et al., 2012; Fridy et al., 2007). A few years before the phosphatase activity of the respective domain was demonstrated, a cryptic pleckstrin homology (PH) domain was identified in the phosphatase domain of PPIP5K2, which allows the PtdIns 3-kinase pathway dependent translocation of the enzyme to the plasma membrane via binding of PtdIns(3,4,5)P_3 in mammalian cells (Gokhale et al., 2011). *In vitro*, this phosphatase domain of *Arabidopsis* VIH2 hydrolyzes PP-InsPs to $InsP_6$, as it has also been shown for fission yeast and mammalian PPIP5Ks (Zhu et al., 2019; Wang et al., 2015; Pascual-Ortiz et al., 2018; Gu et al., 2017). On the other hand, Kcs1/IP6Ks and ITPKs do not possess a defined phosphatase domain. However, under conditions of low adenylate charge, *Arabidopsis* ITPK1 can shift its activity from kinase to ADP phosphotransferase activity using its primary product 5-$InsP_7$, but no other $InsP_7$ isomer, *in vitro* (Riemer et al., 2021; Whitfield et al., 2020). Mammalian IP6Ks were shown *in vitro* to hydrolyze their primary substrate $InsP_6$ to $InsP_5$ under low adenylate charge as well (Wundenberg et al., 2014). Aside from these dual activities of the PP-InsP kinases, PP-InsPs may also be degraded by specialized phosphohydrolases. As such, diphosphoinositol polyphosphate phosphohydrolases (DIPPs), which are members of the larger family of the so called nudix hydrolases, have been demonstrated to catalyze the hydrolysis of the diphosphate groups of $InsP_7$ and $InsP_8$ at both C1 and C5 position, in animal cells (Shears, 2018; Kilari et al., 2013; Caffrey et al., 1999). The baker's yeast *S. cerevisiae* harbors one single homolog of DIPP1, termed Ddp1 (diadenosine and diphosphoinositol polyphosphate phosphohydrolase), which is active against various substrates like diadenosine polyphosphates, PP-InsPs like $InsP_8$, 5-$InsP_7$ and 1-$InsP_7$, as well as inorganic polyphosphates (poly-P), with a clear preference for the latter two (Safrany et al., 1999; Andreeva et al., 2019; Lonetti et al., 2011). Additionally, and in contrast to animal cells, yeast also has a PP-InsP phosphohydrolase with a high specificity for the diphosphate group of 5-$InsP_7$ named Siw14 or Oca3, alternatively (Steidle et al., 2016; Wang et al., 2018).

Siw14 is a member of the Plant and Fungi Atypical Dual Specificity Phosphatases (PFA-DSPs), which belong to the even larger family of protein tyrosine phosphatases (PTPs) (Wang et al., 2018; Romá-Mateo et al., 2007, 2011). The genome of *Arabidopsis thaliana* encodes five PFA-DSP proteins, out of which PFA-DSP1 shares 61 % amino acid identity and 76 % similarity with the yeast homolog Siw14 (Romá-Mateo et al., 2007, 2011). In PFA-DSP1, the predicted catalytic cysteine Cys^{150} resides at the bottom of a positively charged pocket and the protein itself adopts an α/β-fold, which is typical for cysteine phosphatases, as revealed by X-ray crystallography (Romá-Mateo et al., 2011; Aceti et al., 2008). *In vitro* studies showed, that recombinant *At*PFA-DSP1 is highly active against inorganic polyphosphates and deoxyribo-/ribonucleoside triphosphates and less active against phosphotyrosine-containing peptides or phosphoinositides (Aceti et al., 2008). However, InsPs and PP-InsPs have so far not been tested as potential substrates for any other PFA-DSP protein besides the previously mentioned yeast Siw14.

2.4. Functions of inositol pyrophosphates in plants

As mentioned before, InsPs emerged as signaling molecules after $InsP_3$ was shown to be responsible for the receptor-mediated Ca^{2+} release in animal cells. However, no $InsP_3$ receptor has been identified *in planta* until now, questioning a direct and prominent role of $InsP_3$ as signaling molecule (Krinke et al., 2007). Nevertheless, $InsP_3$ is a precursor for higher InsP species, which are then involved in various developmental processes and signaling pathways (Thota & Bhandari, 2015; Shears, 2018; Laha et al., 2015, 2016, 2022; Wild et al., 2016; Couso et al., 2016). $InsP_3$ can be further phosphorylated to $InsP_6$ or phytic acid, which represents not only a major storage of phosphate and cations, but also plays crucial roles in plant defense, mRNA export and phosphate homeostasis (Laha et al., 2015; Dong et al., 2019; Zhu et al., 2019; Riemer et al., 2021; Gulabani et al., 2021). In addition, $InsP_6$ is the precursor for PP-InsPs, which are still quite enigmatic molecules, despite several seminal works in plants (Figure 2) (Desai et al., 2014; Laha et al., 2015, 2016, 2019, 2022; Dong et al., 2019; Zhu et al., 2019; Riemer et al., 2021, 2022; Couso et al., 2016; Flores & Smart, 2000; Brearley & Hanke, 1996a).

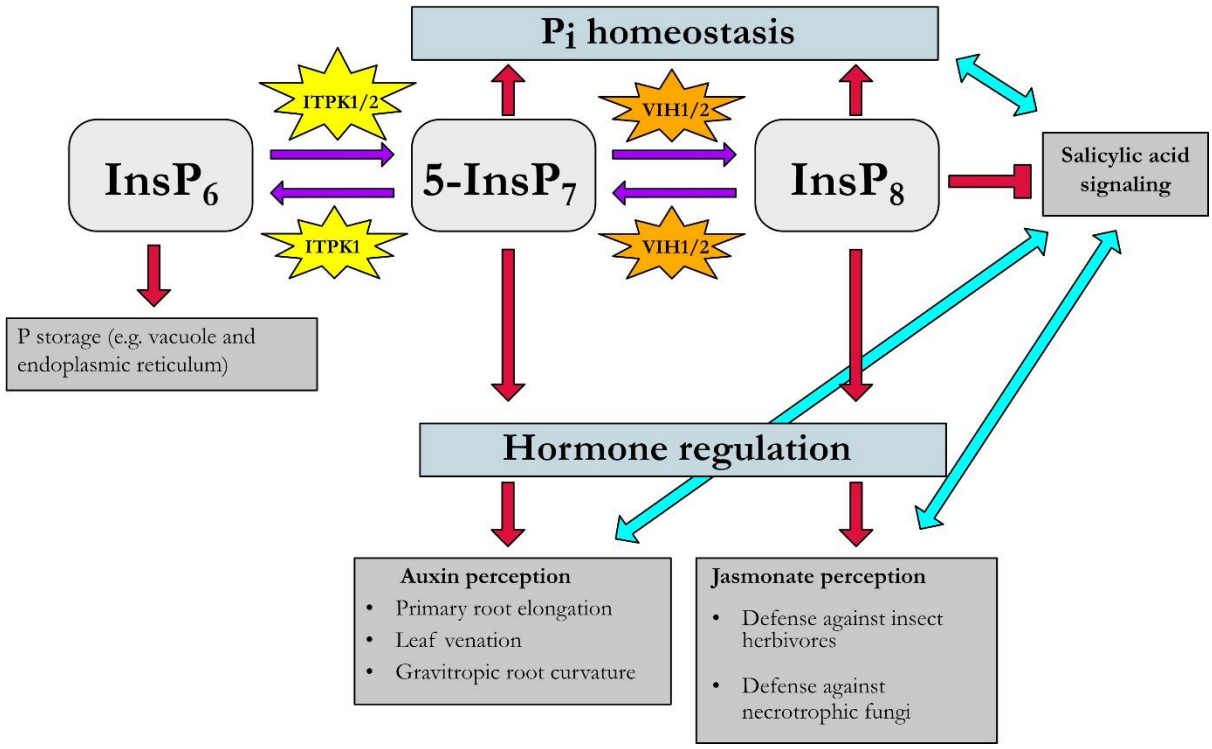

Figure 2: Manifold roles of inositol phosphates in biotic and abiotic stress responses. The roles of PP-InsPs in Pi homeostasis and hormone regulation are shown. Purple arrows indicate the kinase/phosphatase activity of the respective enzymes. Crimson arrows and T-shaped line indicate promotion and suppression of specific InsPs and PP-InsPs, whereas cyan arrows depict the interplay between the individual plant hormones (Figure modified from Riemer et al., 2022).

For example, cellular $InsP_8$ is proposed to regulate plant defenses against insect herbivores and necrotrophic fungi as a co-ligand via coincidence detection of $InsP_8$ and active jasmonate by the ASK1-COI1-JAZ receptor complex (Laha et al., 2015, 2016). Similarly, 5-$InsP_7$ is proposed to be a co-ligand together with auxin of the auxin receptor complex (Laha et al., 2022). Furthermore, disturbances of $InsP_7$/$InsP_8$ synthesis have been shown to result in defects in the salicylic acid-dependent plant immunity (Gulabani et al., 2021). Interestingly, $InsP_8$ and other PP-InsPs have been shown to be involved in energy homeostasis, nutrient sensing and phosphate (Pi) homeostasis, not only in plants, but also in other eukaryotes like yeast and animal cells (Dong et al., 2019; Zhu et al., 2019; Couso et al., 2016; Riemer et al., 2021; Wang et al., 2021; Wild et al., 2016; Li et al., 2020). PP-InsPs can bind to so-called SPX proteins, which act as the receptors in Pi signaling (Wild et al., 2016; Dong et al., 2019; Zhu et al., 2019; Gerasimaite et al., 2017; Ried et al., 2021; Zhou et al., 2021). *In planta*, $InsP_8$ appears to be the preferred ligand for these SPX proteins, which then inactivate the MYB-type transcription factors PHR1 and PHL1, altering the expression of Pi-starvation induced (PSI) genes and ultimately leading to the metabolic and developmental adaptions needed during Pi deficiency (Zhu et al., 2019; Dong et al., 2019; Ried et al., 2021; Rubio et al., 2001; Bustos et al., 2010; Puga et al., 2014).

Consequently, the levels of InsPs and especially of 5-InsP$_7$ and InsP$_8$ in plant tissues respond sensitively and quickly to the Pi status of the plant, suggesting a tight regulation of their synthesis and degradation (Figure 3) (Dong et al., 2019; Riemer et al., 2021, 2022).

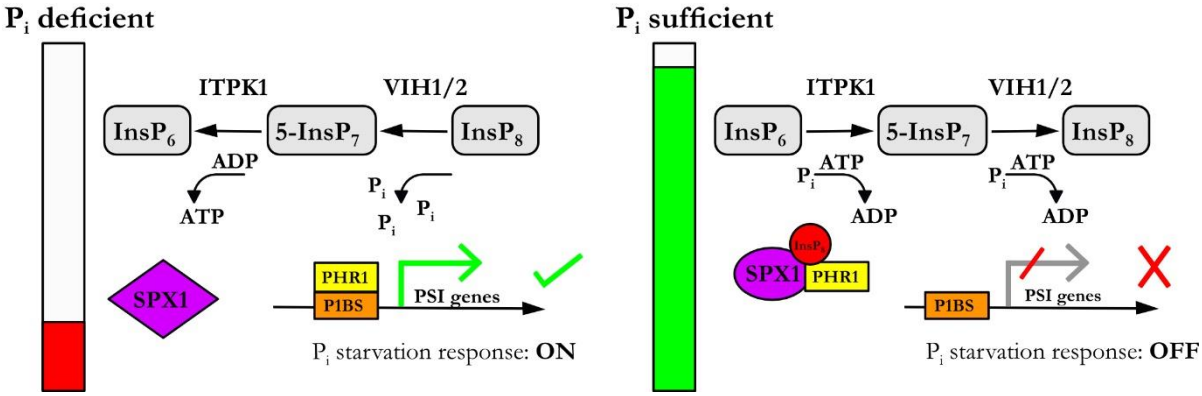

Figure 3: Model of PP-InsP regulated Pi homeostasis.
Pi-deficiency causes a drop in intracellular ATP levels, which stimulates ITPK1 to transfer the β-phosphate from 5-InsP$_7$ to ADP, which in turn leads to local ATP generation and decrease of 5-InsP$_7$. In addition, low Pi levels and low adenylate charge triggers the switch from kinase to phosphatase activity of VIH1 and 2, which then decreases InsP$_8$ levels. The lack of PP-InsPs then destabilizes the interaction of PHR1 and SPX1, ultimately activating the Pi starvation response by the binding of PHR1 to P1BS motifs in the promoters of respective PSI genes. Rising intracellular Pi levels revert this effect by activation of kinase activities and the generation of PP-InsPs, which suppress the Pi starvation response by facilitating the binding of SPX1 to PHR1 (Figure modified from Riemer et al., 2022).

2.5. Aims of this study

This study had two main foci, i) a methodological improvement for the detection of P-InsPs in plant extracts, and ii) to broaden the knowledge of PP-InsP degradation in yeast and *in planta*.

In more detail, the following objectives were pursued:

1. Optimization of SAX-HPLC analyses of [^{3}H]-*myo*-inositol labeled plants
    a. To adapt of the published protocols to increase reproducibility and sensitivity, while increasing time and cost efficiency
    b. To employ the optimized protocol for the so far never analyzed plant species *Lotus japonicus* as proof of concept
    c. To standardize the evaluation procedure
    d. To publish the optimized method with a highly detailed protocol, accompanied by a video documentation

2. Identification and characterization of putative PP-InsP phosphohydrolases
    a. *In vitro* characterization of *Arabidopsis* PFA-DSPs and yeast Siw14
    b. Utilization of yeast as a model organism to study the *in vivo* activities of *Arabidopsis* PFA-DSPs
    c. *In vivo* characterization of Siw14 functions
    d. Isolation and characterization of *Arabidopsis pfa-dsp1* T-DNA insertion lines
    e. Heterologous expression of *PFA-DSP1* in *Nicotiana benthamiana* to study its activity *in planta*

3. Results

3.1. Optimization of SAX-HPLC analyses of [^{3}H]-*myo*-inositol labeled plants

To optimize the method overall, different aspects were addressed individually to illustrate how different actions or prerequisites influence the outcome of the analysis. First, the impact of using an older, aged SAX-HPLC column, which has been used for more than 40 individual sample runs, was assessed. The resulting chromatogram in this case was strikingly different compared to a run of an identical sample, but using a much newer column. The use of the older column resulted in a strong reduction of $InsP_6$ detection and a complete absence of PP-InsPs. Another challenging aspect of this method is the fact that the HPLC run itself is quite time consuming, with around 125 minutes run time per sample, limiting the amount of samples that can be analyzed per work day. Although already available protocols describe the possibility to store extracted samples in the fridge for up to two weeks (Azevedo & Saiardi, 2006), this has never been tested for plant extracts . Therefore, the effect of freezing and storing extracted plant samples was evaluated by splitting one extracted sample and analyzing the first half immediately afterwards, and the second half on the day after with storage at -80°C. Neither the freezing, nor the waiting time for sample and HPLC machine had a significant impact on the obtained results, which additionally highlighted the reproducibility of the method itself. Additionally, other parts of the originally available protocols were optimized. The standard volume of culture media for the seedlings was reduced by 33 % and at the same time, the required amount of [^{3}H]-*myo*-inositol, a highly expensive chemical, was reduced to 22,5 $\mu Ci\ mL^{-1}$, a reduction of 25 %. Radiolabeled waste, was reduced accordingly by this change. Importantly, also the whole evaluation process was improved and standardized. While most evaluations relied on comparative analyzes based on overlay of runs, precise quantifications of experiments performed with this method are rare. The use of tritium as a low-energy beta emitter and the overall rather low activities prevent the successful use of on-line detectors, and thereby of measurements in real-time. This can be partially overcome by simple calculations in Excel or, as described here, by using a software designed for evaluating chromatograms. As shown in this study, the use of this software leads to reliable, relative quantifications.

Lastly, the optimized protocol was used to analyze InsPs from *Lotus japonicus*, a plant species that has not been used for InsP analyses before. Even without any additional optimization, aside from the initial plant cultivation on plates, the use of this protocol successfully resulted in the first InsP profile reported for this species. A side-by-side comparison with an *Arabidopsis* profile revealed multiple differences regarding the amounts of certain InsP species. However, based on the number of peaks and their elution times, no InsP species is absent or additionally present in *L. japonicus*.

The whole workflow, starting from the setup of the equipment to plant cultivation and labeling, InsP extraction and the SAX-HPLC run itself, as well as the subsequent analysis was presented in a detailed protocol and additional video documentation.

These results and experimental details are described in the following publication:

Gaugler, P.; Gaugler, V.; Kamleitner, M.; Schaaf, G. Extraction and Quantification of Soluble, Radiolabeled Inositol Polyphosphates from Different Plant Species using SAX-HPLC. *Journal of Visualized Experiments*. 2020, 160, No. e61495 https://doi.org/10.3791/61495

3.2. Identification and characterization of putative PP-InsP phosphohydrolases

The five *Arabidopsis* homologs of the yeast PP-InsP phosphohydrolase Siw14, all of which had been identified previously (Romá-Matteo et al., 2007), were amplified from *Arabidopsis* cDNA and cloned into various expression constructs for later use in *in vitro* and *in vivo* experiments. Additionally, *SIW14* was also amplified from yeast genomic DNA and cloned into the respective expression vectors. Sequence alignments of the Siw14 and PFA-DSP1 proteins revealed the high level of conservation, as well as the location of the essential cysteine residue in the conserved PTP (Protein Tyrosine Phosphatase) signature motif HC(X)5R of both proteins, as published previously (Romá-Matteo et al., 2007, Steidle et al., 2016).

3.2.1. *In vitro* characterization of *Arabidopsis* PFA-DSPs and yeast Siw14

All five PFA-DSP proteins could be expressed as soluble, recombinant translational fusion proteins with an N-terminal hexahistidine tag and additional maltose-binding protein (MBP) in bacteria. Recombinant His-MBP-Siw14 and free His-MBP served as controls in the following *in vitro* experiments. In the presence of Mg^{2+} cations, PFA-DSP1 displayed robust hydrolytic activity against 5-$InsP_7$ but not 1-$InsP_7$, resulting in the generation of $InsP_6$ as confirmed by CE-ESI-MS analysis. Other cations (Zn^{2+}, Mn^{2+}, Ca^{2+}) tested prevented this hydrolysis, while the absence of any divalent cation allowed the hydrolysis of both $InsP_7$ isomers. Then, all PFA-DSPs, as well as Siw14, were tested against all six $InsP_7$ isomers. With the exception of PFA-DSP5, all proteins displayed robust activity and high-specificity towards 5-$InsP_7$. This also confirmed earlier reports that Siw14 prefers 5-$InsP_7$ over 1-$InsP_7$ as substrate (Steidle et al., 2016; Wang et al., 2018). Partial hydrolytic activities were detectable against the enantiomers 4-$InsP_7$ and 6-$InsP_7$ and only minor activities against the enantiomers 1-$InsP_7$ and 3-$InsP_7$, again with the exception of PFA-DSP5, which showed no activity. Increasing incubation time and enzyme concentration of PFA-DSP5, however, resulted in activities and a specificity similar to the other homologs. For all $InsP_7$ isomers, the reaction product was $InsP_6$, as deduced from CE-ESI-MS analyses. Interestingly, 2-$InsP_7$ was completely resistant to any protein activity under any assay condition, with only minor hydrolysis detectable even after 24 h incubation. Under these conditions, all other $InsP_7$ isomers were hydrolyzed. Furthermore, and again with the exception of PFA-DSP5, all of the proteins could hydrolyze the enantiomeric $InsP_8$ isomers 1,5-$InsP_8$ and 3,5-$InsP_8$ to either 1-$InsP_7$ or 3-$InsP_7$. Taken together, these experiments showed a very similar *in vitro* behavior of Siw14 and its *Arabidopsis* counterparts.

3.2.2. Complementation of yeast *siw14⊿* defects by expression of *PFA-DSPs*

The yeast *siw14⊿* deletion strain was used as a tool to investigate potential *in vivo* activities of *Arabidopsis* PFA-DSPs by heterologous expression. The fungal toxin wortmannin is known to cause severe growth defects of the *siw14⊿* strain (Brown et al., 2006). This growth defect was fully complemented by expression of *SIW14* or any of the *PFA-DSP* homologs. Additionally, heterologous expression of either one of the *PFA-DSP* genes restored the increased $InsP_7/InsP_6$ ratio to wild-type levels, indicating that Siw14 and PFA-DSPs are functionally highly similar. $InsP_7$ was the only InsP isomer that was consistently affected, either by the loss of *SIW14* or by the heterologous expression of *PFA-DSP* genes. In addition, substitutions of the catalytic cysteine in Siw14 or PFA-DSP1 by serine residues resulted in proteins that were unable to complement any of the *siw14⊿* defects, despite being stably expressed. This illustrates the importance of the catalytic activity for wortmannin resistance and $InsP_7$ homeostasis.

3.2.3. *In vivo* characterization of Siw14 functions

While this and other studies (Brown et al., 2006) show the sensitivity of *siw14⊿* to wortmannin, the yeast deletion mutant *kcs1⊿* was reported to be resistant to wortmannin (Saiardi et al., 2005), suggesting a connection between the activities of both proteins. Therefore, genetic interactions between Siw14 and different InsP kinases were investigated. The growth of a *vip1⊿* deletion strain, as well as of a *kcs1⊿* strain on media containing wortmannin was comparable to wild-type yeast, with *kcs1⊿* showing an increased resistance on even higher wortmannin doses. However, a *vip1⊿ siw14⊿* double mutant displayed a severe growth defect, comparable to the *siw14⊿* single mutant. On the other hand, *kcs1⊿ siw14⊿* double mutants were as resistant to wortmannin as the respective *kcs1⊿* single mutants. To answer the question whether the presence of the Kcs1 protein itself or Kcs1-dependent PP-InsPs are relevant for *siw14⊿*-associated wortmannin sensitivity, an *ipk2⊿* mutant and an *ipk2⊿ siw14⊿* double mutant were tested on wortmannin-containing media. Both mutants lack Ipk2, which sequentially phosphorylates $InsP_3$ to $InsP_5$ and thus delivers the precursors for PP-InsP synthesis by Kcs1 (Estevez et al., 1994; Saiardi et al., 2005). Notably, neither of these strains showed growth defects compared to wild-type, suggesting that the presence of Kcs1-dependent PP-InsPs is essential for the sensitivity of *siw14⊿* to wortmannin.

3.2.4. Isolation and characterization of *Arabidopsis pfa-dsp1* T-DNA insertion lines

In order to gain a better understanding of PFA-DSP functions *in planta*, *Arabidopsis* T-DNA insertion lines for *PFA-DSP1* were searched and three homozygous lines could be isolated.

Under standard growth conditions, none of these lines displayed obvious growth phenotypes that were distinguishable from wild-type plants. SAX-HPLC analyses of the *pfa-dsp1-3* and *pfa-dsp1-4* insertion lines could not reveal any relevant difference in the InsP profiles compared to the respective wild-types. Interestingly, analyses of the *pfa-dsp1-6* line revealed a significant reduction of the $InsP_7/InsP_6$ ratio of 36 % on average compared to Col-0, whereas the other InsP species remained unaffected in this mutant. Further analysis of the *pfa-dsp1-6* line indicated that the insertion of the T-DNA is just a few basepairs upstream of the start codon, causing an approx. 6-fold increase of full-length *PFA-DSP1* expression compared to Col-0.

3.2.5. Heterologous expression of *PFA-DSP1* in *Nicotiana benthamiana* to study its activity *in planta*

Analyses of the *pfa-dsp1-6* T-DNA insertion line suggest that increased PFA-DSP1 activity leads to decreased $InsP_7$ levels. To further strengthen this hypothesis, *PFA-DSP1* was transiently expressed in *N. benthamiana* and the resulting InsP profile evaluated. As a control, the catalytically inactive *PFA-DSP1*^{C150S} version was also expressed. PAGE analyses of extracted and purified InsPs showed no effect of *PFA-DSP1* expression on $InsP_6$ levels, but a visible reduction of $InsP_7$ in plants expressing the functional PFA-DSP1 protein. Subsequent CE-ESI-MS analyses did not reveal any difference in the 1/3-$InsP_7/InsP_6$ or 4/6-$InsP_7/InsP_6$ ratios between plants expressing the active, inactive or no PFA-DSP1 protein at all. However, the 5-$InsP_7/InsP_6$ ratio was significantly reduced in plants expressing *PFA-DSP1* compared to both controls. Consequently, the $InsP_8/InsP_6$ ratio was strongly reduced by the expression of *PFA-DSP1* as well. Together with the previous results, these experiments demonstrate that ectopic expression of *Arabidopsis PFA-DSP1* results in a specific decrease of 5-$InsP_7$ and $InsP_8$ *in planta*.

These results and experimental details are described in the following publication

Gaugler, P., Schneider, R., Liu, G., Qiu, D., Weber, J., Schmid, J., Jork, N., Häner, M., Ritter, K., Fernández-Rebollo, N., Giehl, R.F.H., Trung, M.N., Yadav, R., Fiedler, D., Gaugler, V., Jessen, H.J., Schaaf, G., Laha, D. *Arabidopsis* PFA-DSP-Type Phosphohydrolases Target Specific Inositol Pyrophosphate Messengers. *Biochemistry.* 2022 Jun 21;61(12):1213-1227
https://doi.org/10.1021/acs.biochem.2c00145

4. Discussion

While both parts of this thesis can be viewed independently, they are still directly connected. One of the biggest challenges in understanding the manifold roles of InsPs and PP-InsPs in the different eukaryotic systems is the elucidation of InsP and especially PP-InsP biosynthesis itself. This, however, depends on another major difficulty, which is the reliable and precise detection of these molecules in a way that it is as native and non-invasive as possible, but ideally sensitive enough to allow for the discrimination of as many isomers as possible. Both challenges were addressed during this thesis.

4.1. Optimization of SAX-HPLC analyses of [^{3}H]-*myo*-inositol labeled plants

The protocol described here provides the possibility to set up the whole workflow from the very beginning, including details on the equipment and tools needed. It also illustrated the most critical points and possibilities for either mistakes or technical failures. Generally, most of the deviations from the ideal state will lead to a reduction or complete loss of higher InsP species, like $InsP_7$ and $InsP_8$ in the chromatogram. The analysis of plant extracts using an older or aged column exemplified that. But there are more reasons that have, in the past, resulted in such an observation, like microbial contamination, insufficient deactivation of endogenous PP-InsP phosphohydrolases or inaccurate pH adjustments. Therefore, meticulous preparation and handling of the samples, as well as proper maintenance of the HPLC components is crucial for accurate and reproducible results. The seamless implementation of a new and different sample like *L. japonicus* additionally illustrates the versatility of the workflow. Another major point this study addressed, is the general lack of precise, software-based analysis and evaluation of the detected radioactive signals. The use of the rather weak beta emitter tritium, combined with the overall low abundance of especially PP-InsPs in cell extracts, prevents the successful use of on-line scintillation counters and measurements in real-time. Furthermore, while graphs of HPLC runs can be easily prepared in softwares like Excel, it does not allow background subtraction and peak integration, which is necessary for precise quantification and comparison of independent SAX-HPLC runs and individual InsP peaks. The here described use of software like OriginPro overcomes this weakness.

Nevertheless, this SAX-HPLC-based method clearly has drawbacks. The labeling with [^{3}H]-*myo*-inositol needs to be performed in sterile liquid culture, which does not reflect a physiological environment for land plants. It also limits the size and age of the plants, although leaf infiltration of soil-grown plants with [^{3}H]-*myo*-inositol is in principle possible (Blüher et al., 2017). Most importantly, the use of radioactive *myo*-inositol hides other possible types and sources of InsPs in cells, such as other inositol isomers like *scyllo*-inositol, which have been identified in certain plant

species (Pollard et al., 1961). There is also a completely different biosynthetic pathway of InsPs present in eukaryotes. While the pool of InsPs radiolabeled with [^{3}H]-*myo*-inositol results from the lipid-dependent pathway and the activity of Phospholipase C (PLC), which cleaves PtdIns(4,5)P_2 and/or PtdIns(4)P into diacylglycerol and Ins(1,4,5)P_3 and Ins(1,4)P_2 respectively (Munnik, 2014; Zhang et al., 2018), a lipid-independent pathway is also present. In this case, an enzyme called L-*myo*-inositol 1-phosphate synthase (MIPS) fuels the InsP biosynthesis via the isomerization of glucose-6-phosphate to L-*myo*-inositol 1-phosphate (Loewus & Murthy, 2000; Donahue et al., 2010; Fleet et al., 2018; Desfougeres et al., 2019). This could be the reason for the discrepancy, in some cases, between SAX-HPLC and PAGE or CE-ESI-MS analyses of InsPs purified from extracts with TiO_2 pulldown, a technique that should in principle purify and detect all types of InsPs, independently from their cellular source. A recent study could not only show that, in human cancer cell lines, $InsP_6$ and PP-InsPs are almost exclusively synthesized via ITPK1 in the lipid-independent pathway, but also that significant differences in the InsP levels can be seen when comparing SAX-HPLC analyses of [^{3}H] radiolabeled cells with PAGE analyses of total InsPs (Desfougeres et al., 2019). A similar situation is plausible for plants, which also possess all of the necessary enzymes for these two seemingly independent biosynthetic pathways. There is one more important challenge shared by the method described here and every other available method for InsP analysis, e.g., CE-ESI-MS. All of them are unable to distinguish enantiomers (Laha et al., 2015; Blüher et al., 2017; Qiu et al., 2020). The addition of chiral selectors, e.g., the enantiopure L-arginine amide, can tackle this challenge, as they can interact with the enantiomeric InsP molecules and thereby form diastereomeric complexes, which can then be separated. However, this has only been achieved once with an NMR-based method (Blüher et al., 2017). To date, there is no successful report of the implementation of chiral SAX-HPLC or CE-ESI-MS analyses for InsP detection.

4.2. Identification and characterization of putative PP-InsP phosphohydrolases

In recent years, the identity and activity of $InsP_6$/PP-InsP kinases in plants have been elucidated and diverse roles in nutrient sensing, hormone signaling and immunity were discovered (Laha et al., 2015, 2016, 2019, 2022; Desai et al., 2014; Riemer et al., 2021). What remained sparse is the information on the degradation of PP-InsPs *in planta* and the enzymes involved, although some data has been gathered from yeast and animal cells (Menniti et al., 1993; Kilari et al., 2013; Lonetti et al., 2011; Steidle et al., 2016; Safrany et al., 1998). Here, the homologs of the yeast PP-InsP phosphohydrolase from *Arabidopsis*, namely the five PFA-DSP proteins, were characterized.

The *in vitro* experiments not only corroborated the previous findings from Steidle et al., 2016, which showed that Siw14 is active against 5-InsP$_7$ and not 1-InsP$_7$, but also highlighted that Siw14 and all of the PFA-DSP proteins are highly similar in their *in vitro* activity. They all have their highest activity against 5-InsP$_7$, clearly reduced activity against the enantiomers 4/6-InsP$_7$, minimal activity against the enantiomers 1/3-InsP$_7$ and virtually no activity against 2-InsP$_7$. The latter could be resistant for a couple of reasons. It could be that 2-InsP$_7$ does not fit accurately into the active site of PFA-DSP proteins due to the axial position of the pyrophosphate moiety, whereas the other InsP$_7$ isomers possess planar positioned pyrophosphates. Alternatively, it could be that 2-InsP$_7$ does fit well but cannot be efficiently hydrolyzed, leaving the possibility open that 2-InsP$_7$ could be an antagonist of 5-InsP$_7$ or, in other words, an inhibitor of PFA-DSP proteins. However, 2-InsP$_7$ has so far been detected only in mammalian cells, despite the recent analyses of *Arabidopsis*, rice, yeast and *Dictyostelium* with the highly sensitive CE-ESI-MS-based method (Qiu et al., 2020, 2022; Riemer et al., 2021; Desfougeres et al., 2022). Furthermore, the proteins were all highly active and specific against the 5-β-phosphate moiety of the enantiomers 1,5-InsP$_8$ and 3,5-InsP$_8$. PFA-DSP5 stood out, as it displayed much less activity overall, but the pattern remained similar to the other proteins and the reduced activity did not translate to the later yeast *in vivo* experiments. The finding that Mg^{2+} is needed as a cofactor to reduce promiscuous activities *in vitro* is in line with other cases, where enzymes like phosphatases need metal ions like Mg^{2+} for their function or substrate specificity (Baier et al., 2015; Barrozo et al., 2017). Furthermore, a recent publication demonstrated the influence of Mg^{2+} on the conformational change between the equatorial position to the "flipped" axial conformation of 1,5-InsP$_8$ (Kurz et al., 2023).

During the final stage of this work, a different study reported crystal structures of *Arabidopsis* PFA-DSP1 in complex with 5-InsP$_7$ and 6-InsP$_7$. In agreement with the findings described here, the authors demonstrated efficient *in vitro* phosphatase activity of PFA-DSP1 against 5-InsP$_7$ and the enantiomers 4/6-InsP$_7$ (Wang et al., 2022).

As published previously (Steidle et al., 2016), the *siw14*⊿ yeast strain accumulated InsP$_7$ and this defect could be complemented by heterologous expression of either one of the *Arabidopsis PFA-DSP*s. This shows that the previous *in vitro* results, where recombinant PFA-DSP5 had only minimal hydrolytic activity, were likely caused by suboptimal assay conditions or missing posttranslational modifications of the protein, rather than PP-InsPs not being a substrate of PFA-DSP5. SAX-HPLC analyses of *siw14*⊿ transformants expressing either Siw14^{C214S} or PFA-DSP1^{C150S} demonstrated that catalytic activity of the proteins themselves is crucial for restoring the InsP$_7$/InsP$_6$ ratio to wild-type levels.

The subsequent search for growth phenotypes of *siw14*⊿ led to the use of wortmannin, a chemical that is already directly linked to PP-InsPs, since the *kcs1*⊿ yeast mutant displayed increased resistance against this drug (Saiardi et al., 2005). Loss of *SIW14* resulted in robust sensitivity of the yeast against wortmannin, compared to wild-type, a defect that could be fully complemented by heterologous expression of either one of the *Arabidopsis* homologs. Collectively, these data provide strong evidence that *Arabidopsis* PFA-DSPs are PP-InsP phosphohydrolases *in vitro* and functional Siw14 homologs in yeast.

To gain a better understanding of the growth defects caused by wortmannin and the potential role of Siw14 in this process, yeast mutants of different InsP and PP-InsP kinases, as well as double mutants combining the loss of the respective kinase with *siw14*⊿ were analyzed. As it has been published before, *kcs1*⊿ and *ipk2*⊿ were not sensitive to wortmannin (Saiardi et al., 2005). However, the loss of *SIW14* rendered *vip1*⊿ highly sensitive to wortmannin, whereas the *kcs1*⊿ *siw14*⊿ and *ipk2*⊿ *siw14*⊿ mutants remained resistant. This indicates that the function of Siw14 in the response to wortmannin depends on the presence of Kcs1 and, thus, likely Kcs1-derived 5-$InsP_7$. Previous studies have linked Kcs1 and Kcs1-derived PP-InsPs with the PI3K-related enzymes Mec1 (human ATR) and Tel1 (human ATM) (Saiardi et al., 2005; York et al., 2005). Both enzymes represent critical kinases involved in the DNA damage response (DDR), such as regulating telomere length (Cussiol et al., 2019). Kcs1-derived PP-InsPs are thought to be inhibitors of the Tel1- and possibly Mec1-mediated control of telomere length, which in turn could explain increased telomere length in *kcs1*⊿, as well as the increased wortmannin resistance (Saiardi et al., 2005). The findings that *vip1*⊿ is not sensitive to wortmannin, despite having strongly increased levels of 5-$InsP_7$, and that *siw14*⊿, which accumulates 5-$InsP_7$ to a similar extent, is highly sensitive, suggests that the role of Siw14 in the response to wortmannin is more specific than the regulation of global 5-$InsP_7$ levels in the cell (Steidle et al., 2016). The observations that *kcs1*⊿ is resistant to wortmannin and another PI3K inhibitor, caffeine, whereas *siw14*⊿ is sensitive to both, suggests that both enzymes are antagonists in the DDR (Care et al., 2004; Saiardi et al., 2005). Therefore, one possible explanation could be that Siw14 hydrolyzes 5-$InsP_7$ at a specific subcellular location or developmental stage, possibly facilitated by a direct interaction or association of Siw14 with components of DDR signaling, similar to the substrate channeling proposed for the IP6K2-mediated activation of CK2 in the DNA-PKcs/ATM-p53 cell death pathway (Rao et al., 2014). The finding that the *Arabidopsis* PFA-DSPs can fully substitute Siw14 in this process, leaves room for the possibility that the PFA-DSPs have a very similar role in plants and the regulation of DDR and telomere length, which are similarly regulated in plants (Gentric et al., 2021; Garcia et al., 2003; Nisa et al., 2019; Manova & Gruszka, 2015).

Notably, wortmannin, albeit generally seen as a PI3K inhibitor, based on data from mammalian cells, is a weak inhibitor of the yeast PI3K Vps34, but a very potent inhibitor of the yeast PI4K Stt4, both of which are kinases that phosphorylate phosphatidylinositol (PtdIns) at either position 3 or 4, resulting in phosphatidylinositol phosphate (PIP) (Arcaro and Wymann, 1993; Powis et al., 1994; Stack & Emr, 1994; Cutler et al., 1997). As wortmannin treatment phenocopies loss of SST4, resulting in a reduction of PtdIn(4)P and PtdIns(4,5)P_2 at the plasma membrane, these findings indicate that loss of *SIW14* and the increase in InsP_7 has an additional negative impact on yeast survival (Cutler et al., 1997). PIPs and PP-InsPs have been shown to compete for proteins containing Pleckstrin homology domains (PH domains), including proteins in the mammalian Akt signaling pathway (Luo et al., 2003; Chakraborty et al., 2010; Gokhale et al., 2013). It could very well be, that 5-InsP_7 antagonizes PtdIns(4,5)P_2 for recruiting certain proteins to the plasma membrane in yeast cells. Loss of Siw14 combined with the inhibitive effect of wortmannin on Stt4 could then prevent critical proteins from binding to and acting at the plasma membrane. In plants, PIPs, PP-InsPs and PIP-binding proteins can also be found (Lorenzo-Orts et al., 2020). To current knowledge, *Arabidopsis* possesses 59 proteins with a clearly defined PH-domain and many more proteins that have other types of lipid-binding domains and been shown to bind PIPs (de Jong and Munnik, 2021). However, so far, no PH domain from a plant protein has been tested for its ability to bind PP-InsPs (Lorenzo-Orts et al., 2020).

The experimental data presented here illustrates the striking biochemical similarities between *Arabidopsis* PFA-DSPs *in vitro*, as well as in yeast. These similarities might well explain redundancies of these enzymes and therefore the lack of obvious phenotypes in single *pfa-dsp1* loss-of-function lines in *Arabidopsis*. Interestingly, the T-DNA insertion line *pfa-dsp1-6* displayed a robust reduction in the InsP_7/InsP_6 ration. The insertion did not result in a reduction or absence of *PFA-DSP1* transcripts, but in a more than 6-fold increased expression, which in combination suggests that overexpression of *PFA-DSP1* causes increased hydrolysis of InsP_7. This hypothesis was strengthened by heterologous expression of *PFA-DSP1* in *N. benthamiana*. CE-ESI-MS analyses of transiently expressing plants revealed a specific reduction of 5-InsP_7. Consequently, the InsP_8/InsP_6 ratio was strongly reduced as well, in agreement with the activity of PFA-DSP1 against InsP_8, as well as with the finding that 5-InsP_7 is the major precursor for InsP_8 synthesis *in planta* (Riemer et al., 2021).

In conclusion, this study not only established the *Arabidopsis* Siw14 homologs, PFA-DSP1-5, as functional PP-InsP phosphohydrolases *in vitro* and *in vivo*, with overall strikingly similar biochemical properties. It also shed more light on the possible roles of 5-InsP_7 in wortmannin-related signaling pathways in yeast.

4.3. Outlook

The findings of this thesis lay the analytical, biochemical and genetic basis for future studies on the roles of PP-InsPs in physiology and development of yeast and plants. Although SAX-HPLC analyses of radiolabeled samples may eventually be replaced by the much newer, almost as sensitive but in many aspects superior CE-ESI-MES method, the technique will still be preferable in certain conditions and scientific rationales. Combining SAX-HPLC with chiral selectors could be a challenging, but rewarding future task.

On the other hand, the PFA-DSP proteins emerge with this thesis as novel plant PP-InsP phosphohydrolases, with high structural and biochemical similarity to the yeast homolog Siw14 and a strong preference for 5-$InsP_7$ as substrate not only *in vitro*, but also *in vivo*. Future studies will have to illuminate which physiological roles these proteins might have in the plant's development and metabolism. A first hint could be found in transcriptome analyses in this study, which revealed that *PFA-DSP1*, *2* and *4* are strongly induced by Pi deficiency. Together with the recent discovery that PP-InsPs disappear in tissues of Pi-starved plants, this finding could point to a direct role of PFA-DSP proteins in Pi signaling and homeostasis (Dong et al., 2019; Riemer et al., 2021). Future analyses of additional T-DNA insertion lines and/or CRISPR-Cas9-generated knockouts of *PFA-DSP* genes will not only determine whether 5-$InsP_7$ is the primary *in vivo* substrate of these proteins in *Arabidopsis*, but also which physiological roles these proteins might have. The findings described here, as well as recently published data, further emphasizes not only the need for detailed localization of the enzymes and the InsPs themselves, but also for increased efforts to dissect the lipid-dependent from the lipid-independent biosynthetic pathway in planta (Desfougeres et al., 2019). Moreover, a role of 5-$InsP_7$ and Siw14-type proteins in the DDR, as suggested by this study, has not yet been investigated *in planta* so far. However, since previous work suggests that ITPK1/2-derived 5-$InsP_7$ plays a critical role in Pi homeostasis and auxin perception, while VIH1/2-derived $InsP_8$ regulates both phosphate starvation responses and jasmonate perception, multiple, potentially antagonistic, roles of PFA-DSP proteins are possible (Laha et al., 2015, 2016, 2022; Dong et al., 2019; Zhu et al., 2019; Riemer et al., 2021). Furthermore, the high specificity of PFA-DSPs allows for their ideal use as tools to investigate physiological roles of 5-β-phosphate containing PP-InsPs, not only *in planta*, but also other eukaryotes. This will allow to answer many research questions about PP-InsPs in the future that could not be answered before.

5. References

Aceti, D. J.; Bitto, E.; Yakunin, A. F.; Proudfoot, M.; Bingman, C. A.; Frederick, R. O.; Sreenath, H. K.; Vojtik, F. C.; Wrobel, R. L.; Fox, B. G.; Markley, J. L.; Phillips, G. N. Structural and functional characterization of a novel phosphatase from the Arabidopsis thaliana gene locus At1g05000. *Proteins* 2008, 73, 241−253.

Adepoju, O.; Williams, S. P.; Craige, B.; Cridland, C. A.; Sharpe, A. K.; Brown, A. M.; Land, E.; Perera, I. Y.; Mena, D.; Sobrado, P.; Gillaspy, G. E. Inositol Trisphosphate Kinase and Diphosphoinositol Pentakisphosphate Kinase Enzymes Constitute the Inositol Pyrophosphate Synthesis Pathway in Plants, 2019. DOI: 10.1101/724914.

Agranoff B. W. Turtles All the Way: Reflections on myo-Inositol. *J. Biol. Chem.* 2009, 284(32), 21121–21126.

Andreeva, N.; Ledova, L.; Ryazanova, L.; Tomashevsky, A.; Kulakovskaya, T.; Eldarov, M. Ppn2 endopolyphosphatase overexpressed in Saccharomyces cerevisiae: Comparison with Ppn1, Ppx1, and Ddp1 polyphosphatases. *Biochimie* 2019, 163, 101−107.

Arcaro, A.; Wymann, M. P. Wortmannin is a potent phosphatidylinositol 3-kinase inhibitor: the role of phosphatidylinositol 3,4,5-trisphosphate in neutrophil responses. *Biochem. J.* 1993, 296, 297−301.

Azevedo, C., Burton, A., Bennett, M., Onnebo, S. M. N., Saiardi, A. in Inositol Phosphates and Lipids: Methods and Protocols (ed Christopher J. Barker). *Humana Press* 2010, 73-85.

Azevedo, C.; Saiardi, A. Extraction and analysis of soluble inositol polyphosphates from yeast. *Nat. Protoc.* 2006, 1, 2416−2422.

Baier, F., Chen, J., Solomonson, M., Strynadka, N. C., Tokuriki, N. Distinct Metal Isoforms Underlie Promiscuous Activity Profiles of Metalloenzymes. *ACS Chem. Biol.* 2015,10(7), 1684–1693.

Barrozo, A., Blaha-Nelson, D., Williams, N. H., Kamerlin, S. C. L. The effect of magnesium ions on triphosphate hydrolysis. *Pure Appl. Chem.* 2017, 89,6, 715-727.

Berridge, M. J., Irvine, R. F. Inositol Phosphates and Cell Signaling. *Nature* 1989, 341 (6239), 197-205.

Bhosale, R., Giri, J., Pandey, B. K., Giehl, R. F. H., Hartmann, A., Traini, R., Truskina, J., Leftley, N., Hanlon, M., Swarup, K., Rashed, A., Voss, U., Alonso, J., Stepanova, A., Yun, J., Ljung, K., Brown, K. M., Lynch, J. P., Dolan, L., Vernoux, T., Bishopp, A., Wells, D., von Wiren, N., Bennett, M. J., and Swarup, R. A mechanistic framework for auxin dependent Arabidopsis root hair elongation to low external phosphate, *Nat. Commun.* 2018, 9, 1409.

Blüher, D.; Laha, D.; Thieme, S.; Hofer, A.; Eschen-Lippold, L.; Masch, A.; Balcke, G.; Pavlovic, I.; Nagel, O.; Schonsky, A.; Hinkelmann, R.; Wörner, J.; Parvin, N.; Greiner, R.; Weber, S.; Tissier, A.; Schutkowski, M.; Lee, J.; Jessen, H.; Schaaf, G.; Bonas, U. A 1-phytase type III effector interferes with plant hormone signaling. *Nat. Commun.* 2017, 8, No. 2159.

Brearley, C. A., Hanke, D. E. Inositol phosphates in barley (Hordeum vulgare L) aleurone tissue are stereochemically similar to the products of breakdown of InsP(6) in vitro by wheat-bran phytase. *Biochem. J.* 1996, 318, 279-286.

Brearley, C. A., Hanke, D. E. Inositol phosphates in the duckweed Spirodela polyrhiza L. *Biochem. J.* 1996, 314 215-225.

Brown, J. A.; Sherlock, G.; Myers, C. L.; Burrows, N. M.; Deng, C.; Wu, H. I.; McCann, K. E.; Troyanskaya, O. G.; Brown, J. M. Global analysis of gene function in yeast by quantitative phenotypic profiling. *Mol. Syst. Biol.* 2006, 2, No. 2006.0001.

Bustos, R.; Castrillo, G.; Linhares, F.; Puga, M. I.; Rubio, V.; Perez-Perez, J.; Solano, R.; Leyva, A.; Paz-Ares, J. A Central Regulatory System Largely Controls Transcriptional Activation and Repression Responses to Phosphate Starvation in Arabidopsis. *PLoS Genet.* 2010, 6, No. e1001102.

Caffrey, J. J.; Hidaka, K.; Matsuda, M.; Hirata, M.; Shears, S. B. The human and rat forms of multiple inositol polyphosphate phosphatase: functional homology with a histidine acid phosphatase up-regulated during endochondral ossification. *FEBS Lett.* 1999, 442, 99−104.

Capolicchio, S.; Thakor, D. T.; Linden, A.; Jessen, H. J. Synthesis of unsymmetric diphospho-inositol polyphosphates. *Angew. Chem., Int. Ed.* 2013, 52, 6912−6916.

Capolicchio, S.; Wang, H.; Thakor, D. T.; Shears, S. B.; Jessen, H. J. Synthesis of Densely Phosphorylated Bis-1,5-Diphospho-myoInositol Tetrakisphosphate and its Enantiomer by Bidirectional PAnhydride Formation. *Angew. Chem., Int. Ed.* 2014, 53, 9508−9511.

Care, A., Vousden, K. A., Binley, K. M., Radcliffe, P., Trevethick, J., Mannazzu, I., Sudbery, P. E. A synthetic lethal screen identifies a role for the cortical actin patch/endocytosis complex in the response to nutrient deprivation in Saccharomyces cerevisiae. *Genetics* 2004, 166(2), 707–719.

Chakraborty, A., Koldobskiy, M. A., Bello, N. T., Maxwell, M., Potter, J. J., Juluri, K. R., Maag, D., Kim, S., Huang, A. S., Dailey, M. J., Saleh, M., Snowman, A. M., Moran, T. H., Mezey, E., Snyder, S. H. Inositol pyrophosphates inhibit Akt signaling, thereby regulating insulin sensitivity and weight gain. *Cell* 2010, 143(6), 897–910.

Couso, I.; Evans, B.; Li, J.; Liu, Y.; Ma, F.; Diamond, S.; Allen, D. K.; Umen, J. G. Synergism between inositol polyphosphates and TOR kinase signaling in nutrient sensing, growth control and lipid metabolism in Chlamydomonas. *Plant Cell* 2016, 28, 2026−2042.

Cussiol, J. R. R., Soares, B. L., Oliveira, F. M. B. From yeast to humans: Understanding the biology of DNA Damage Response (DDR) kinases. *Genet. Mol. Biol.* 2019, 43(1 suppl 1), e20190071.

Cutler, N. S., Heitman, J., Cardenas, M. E. STT4 is an essential phosphatidylinositol 4-kinase that is a target of wortmannin in Saccharomyces cerevisiae. *J. Biol. Chem.* 1997, 272(44), 27671–27677.

Desai, M.; Rangarajan, P.; Donahue, J. L.; Williams, S. P.; Land, E. S.; Mandal, M. K.; Phillippy, B. Q.; Perera, I. Y.; Raboy, V.; Gillaspy, G. E. Two inositol hexakisphosphate kinases drive inositol pyrophosphate synthesis in plants. *Plant J.* 2014, 80, 642−653.

Desfougères, Y., Portela-Torres, P., Qiu, D., Livermore, T. M., Harmel, R. K., Borghi, F., Jessen, H. J., Fiedler, D., Saiardi, A. The inositol pyrophosphate metabolism of Dictyostelium discoideum does not regulate inorganic polyphosphate (polyP) synthesis. *Adv. Biol. Regul.* 2022, 83, 100835.

Desfougeres, Y., Wilson, M. S. C., Laha, D., Miller, G. J., Saiardi, A. ITPK1 mediates the lipidindependent synthesis of inositol phosphates controlled by metabolism. *Proc. Natl. Acad. Sci. U.S.A.* 2019, 116 (49), 24551-24561.

Donahue, J. L., Alford, S. R., Torabinejad, J., Kerwin, R. E., Nourbakhsh, A., Ray, W. K., Hernick, M., Huang, X., Lyons, B. M., Hein, P. P., Gillaspy, G. E. The Arabidopsis thaliana Myoinositol 1-phosphate synthase1 gene is required for Myoinositol synthesis and suppression of cell death. *Plant Cell.* 2010, 22 (3), 888-903.

Dong, J.; Ma, G.; Sui, L.; Wei, M.; Satheesh, V.; Zhang, R.; Ge, S.; Li, J.; Zhang, T. E.; Wittwer, C.; Jessen, H. J.; Zhang, H.; An, G. Y.; Chao, D. Y.; Liu, D.; Lei, M. Inositol Pyrophosphate InsP8 Acts as an Intracellular Phosphate Signal in Arabidopsis. *Mol. Plant* 2019, 12, 1463−1473.

Dorsch, J. A., Cook, A., Young, K. A., Anderson, J. M., Bauman, A. T., Volkmann, C. J., Murthy, P. P., Raboy, V. Seed phosphorus and inositol phosphate phenotype of barley low phytic acid genotypes. *Phytochemistry* 2003, 62 (5), 691-706.

Estevez, F.; Pulford, D.; Stark, M. J.; Carter, A. N.; Downes, C. P. Inositol trisphosphate metabolism in Saccharomyces cerevisiae: identification, purification and properties of inositol 1,4,5-trisphosphate 6-kinase. *Biochem. J.* 1994, 302, 709−716.

Fleet, C.M., Yen, J.Y., Hill, E.A., Gillaspy, G.E. Co-suppression of AtMIPS demonstrates cooperation of MIPS1, MIPS2 and MIPS3 in maintaining myo-inositol synthesis. *Plant Mol. Biol.* 2018, 97: 253-263

Flores, S.; Smart, C. C. Abscisic acid-induced changes in inositol metabolism in Spirodela polyrrhiza. *Planta* 2000, 211, 823− 832.

Fridy, P. C.; Otto, J. C.; Dollins, D. E.; York, J. D. Cloning and characterization of two human VIP1-like inositol hexakisphosphate and diphosphoinositol pentakisphosphate kinases. *J. Biol. Chem.* 2007, 282, 30754−30762.

Garcia, V., Bruchet, H., Camescasse, D., Granier, F., Bouchez, D., Tissier, A. AtATM is essential for meiosis and the somatic response to DNA damage in plants. *Plant Cell* 2003, 15(1), 119–132.

Gaugler, P.; Gaugler, V.; Kamleitner, M.; Schaaf, G. Extraction and Quantification of Soluble, Radiolabeled Inositol Polyphosphates from Different Plant Species using SAX-HPLC. *J. Vis. Exp.* 2020, 160, No. e61495.

Gentric, N., Genschik, P., Noir, S. Connections between the Cell Cycle and the DNA Damage Response in Plants. *Int. J. Mol. Sci.* 2021, 22(17), 9558.

Gerasimaite, R.; Pavlovic, I.; Capolicchio, S.; Hofer, A.; Schmidt, A.; Jessen, H. J.; Mayer, A. Inositol Pyrophosphate Specificity of the SPX-Dependent Polyphosphate Polymerase VTC. *ACS Chem. Biol.* 2017, 12, 648−653.

Gietz, R. D.; Schiestl, R. H.; Willems, A. R.; Woods, R. A. Studies on the transformation of intact yeast cells by the LiAc/SSDNA/PEG procedure. *Yeast* 1995, 11, 355−360.

Gillaspy, G. E. in Lipid-mediated Protein Signaling (ed Daniel G. S. Capelluto). *Springer Netherlands* 2013, 141-157.

Gokhale, N. A., Zaremba, A., Shears, S. B. Receptor-dependent compartmentalization of PPIP5K1, a kinase with a cryptic polyphosphoinositide binding domain. *Biochem. J.* 2011, 434(3), 415–426.

Gokhale, N. A., Zaremba, A., Janoshazi, A. K., Weaver, J. D., Shears, S. B. PPIP5K1 modulates ligand competition between diphosphoinositol polyphosphates and PtdIns(3,4,5)P3 for polyphosphoinositide-binding domains. *Biochem. J.* 2013, 453(3), 413–426.

Gruber, B. D.; Giehl, R. F.; Friedel, S.; von Wiren, N. Plasticity of the Arabidopsis root system under nutrient deficiencies. *Plant Physiol.* 2013, 163, 161−179.

Gu, C., Nguyen, H. N., Hofer, A., Jessen, H. J., Dai, X., Wang, H., Shears, S. B.. The Significance of the Bifunctional Kinase/Phosphatase Activities of Diphosphoinositol Pentakisphosphate Kinases

(PPIP5Ks) for Coupling Inositol Pyrophosphate Cell Signaling to Cellular Phosphate Homeostasis. *J. Biol. Chem.* 2017, 292(11), 4544–4555.

Gueldener, U.; Heinisch, J.; Koehler, G. J.; Voss, D.; Hegemann, J. H. A second set of loxP marker cassettes for Cremediated multiple gene knockouts in budding yeast. *Nucleic Acids Res.* 2002, 30, No. e23.

Gulabani, H.; Goswami, K.; Walia, Y.; Roy, A.; Noor, J. J.; Ingole, K. D.; Kasera, M.; Laha, D.; Giehl, R. F. H.; Schaaf, G.; Bhattacharjee, S. Arabidopsis inositol polyphosphate kinases IPK1 and ITPK1 modulate crosstalk between SA-dependent immunity and phosphate-starvation responses. *Plant Cell Rep.* 2021, 41, 347−363.

Harmel, R. K., Puschmann, R., Nguyen Trung, M., Saiardi, A., Schmieder, P., Fiedler, D. Harnessing C-13-labeled myo-inositol to interrogate inositol phosphate messengers by NMR Electronic supplementary information (ESI) available. *Chem. Sci.* 2019, 10 (20), 5267-5274.

Hughes, P. J., Hughes, A. R., Putney, J. W., Shears, S. B. The regulation of the phosphorylation of inositol 1,3,4- trisphosphate in cell-free preparations and its relevance to the formation of inositol 1,3,4,6-tetrakisphosphate in agonist-stimulated rat parotid acinar cells. *J. Biol. Chem.* 1989, 264 (33), 19871-19878.

Irvine, R. F.; Schell, M. J. Back in the water: the return of the inositol phosphates. *Nat. Rev. Mol. Cell Biol.* 2001, 2, 327−338.

Ito, M., Fujii, N., Wittwer, C., Sasaki, A., Tanaka, M., Bittner, T., Jessen, H. J., Saiardi, A., Takizawa, S., Nagata, E. Hydrophilic interaction liquid chromatography-tandem mass spectrometry for the quantitative analysis of mammalian-derived inositol poly/ pyrophosphates. *J. Chromatogr. A.* 2018, 1573 87-97.

Kilari, R. S.; Weaver, J. D.; Shears, S. B.; Safrany, S. T. Understanding inositol pyrophosphate metabolism and function: Kinetic characterization of the DIPPs. *FEBS Lett.* 2013, 587, 3464− 3470.

Krinke, O., Novotna, Z., Valentova, O., Martinec, J. Inositol trisphosphate receptor in higher plants: is it real? *J. Exp. Bot.* 2007, 58 (3), 361-376.

Kuo, H. F., Chang, T. Y., Chiang, S. F., Wang, W. D., Charng, Y. Y., Chiou, T. J. Arabidopsis inositol pentakisphosphate 2-kinase, AtIPK1, is required for growth and modulates phosphate homeostasis at the transcriptional level. *Plant J.* 2014 80 (3), 503-515.

Kuo, H. F.; Hsu, Y. Y.; Lin, W. C.; Chen, K. Y.; Munnik, T.; Brearley, C. A.; Chiou, T. J. Arabidopsis inositol phosphate kinases IPK1 and ITPK1 constitute a metabolic pathway in maintaining phosphate homeostasis. *Plant J.* 2018, 95, 613−630.

Kurz, L.; Schmieder, P.; Veiga, N.; Fiedler, D. One Scaffold, Two Conformations: The Ring-Flip of the Messenger $InsP_8$ Occurs under Cytosolic Conditions. *Preprints* 2023, 2023030053. https://doi.org/10.20944/preprints202303.0053.v1.

Laha, N. P., Giehl, R. F. H., Riemer, E., Qiu, D., Pullagurla, N. J., Schneider, R., Dhir, Y. W., Yadav, R., Mihiret, Y. E., Gaugler, P., Gaugler, V., Mao, H., Zheng, N., von Wirén, N., Saiardi, A., Bhattacharjee, S., Jessen, H. J., Laha, D., Schaaf, G. INOSITOL (1,3,4) TRIPHOSPHATE 5/6 KINASE1-dependent inositol polyphosphates regulate auxin responses in Arabidopsis. *Plant physiol.* 2022, 190(4), 2722–2738.

Laha, D.; Johnen, P.; Azevedo, C.; Dynowski, M.; Weiss, M.; Capolicchio, S.; Mao, H.; Iven, T.; Steenbergen, M.; Freyer, M.; Gaugler, P.; de Campos, M. K.; Zheng, N.; Feussner, I.; Jessen, H. J.; Van Wees, S. C.; Saiardi, A.; Schaaf, G. VIH2 Regulates the Synthesis of Inositol Pyrophosphate InsP8 and Jasmonate-Dependent Defenses in Arabidopsis. *Plant Cell* 2015, 27, 1082−1097.

Laha, D.; Kamleitner, M.; Johnen, P.; Schaaf, G. Analyses of Inositol Phosphates and Phosphoinositides by Strong Anion Exchange (SAX)-HPLC. *Methods Mol. Biol.* 2021, 2295, 365−378.

Laha, D.; Parvin, N.; Dynowski, M.; Johnen, P.; Mao, H.; Bitters, S. T.; Zheng, N.; Schaaf, G. Inositol Polyphosphate Binding Specificity of the Jasmonate Receptor Complex. *Plant Physiol.* 2016, 171, 2364−2370.

Laha, D.; Parvin, N.; Hofer, A.; Giehl, R. F. H.; FernandezRebollo, N.; von Wiren, N.; Saiardi, A.; Jessen, H. J.; Schaaf, G. Arabidopsis ITPK1 and ITPK2 Have an Evolutionarily Conserved Phytic Acid Kinase Activity. *ACS Chem. Biol.* 2019, 14, 2127−2133.

Laha, N. P.; Dhir, Y. W.; Giehl, R. F. H.; Schäfer, E. M.; Gaugler, P.; Shishavan, Z. H.; Gulabani, H.; Mao, H.; Zheng, N.; von Wirén, N.; Jessen, H. J.; Saiardi, A.; Bhattacharjee, S.; Laha, D.; Schaaf, G. ITPK1-Dependent Inositol Polyphosphates Regulate Auxin Responses in Arabidopsis thaliana, 2020. DOI: 10.1101/ 2020.04.23.058487.

Lee, H. S., Lee, D. H., Cho, H. K., Kim, S. H., Auh, J. H., Pai, H. S. InsP6-sensitive variants of the Gle1 mRNA export factor rescue growth and fertility defects of the ipk1 low-phytic-acid mutation in Arabidopsis. *Plant Cell* 2015, 27 (2), 417-431.

Lemtiri-Chlieh, F.; MacRobbie, E. A.; Brearley, C. A. Inositol hexakisphosphate is a physiological signal regulating the K+-inward rectifying conductance in guard cells. *Proc. Natl. Acad. Sci. U.S.A.* 2000, 97, 8687−8692.

Li, X., Gu, C., Hostachy, S., Sahu, S., Wittwer, C., Jessen, H. J., Fiedler, D., Wang, H., Shears, S. B. Control of XPR1-dependent cellular phosphate efflux by $InsP_8$ is an exemplar for functionally-exclusive inositol pyrophosphate signaling. *Proc. Natl. Acad. Sci. U. S. A.* 2020, 117(7), 3568–3574.

Lin, H.; Fridy, P. C.; Ribeiro, A. A.; Choi, J. H.; Barma, D. K.; Vogel, G.; Falck, J. R.; Shears, S. B.; York, J. D.; Mayr, G. W. Structural analysis and detection of biological inositol pyrophosphates reveal that the family of VIP/diphosphoinositol pentakisphosphate kinases are 1/3-kinases. *J. Biol. Chem.* 2009, 284, 1863−1872.

Liu, C., Riley, A. M., Yang, X., Shears, S. B., Potter, B. V. L. Synthesis and Biological Activity of d- and l-chiro-Inositol 2,3,4,5-Tetrakisphosphate: Design of a Novel and Potent Inhibitor of Ins(3,4,5,6)P4 1-Kinase/ Ins(1,3,4)P3 5/6-Kinase. *J. Med. Chem.* 2001, 44 (18), 2984-2989.

Loewus, F.A., Murthy, P.P.N. myo-Inositol metabolism in plants. *Plant Sci.* 2000, 150: 1-19

Lonetti, A.; Szijgyarto, Z.; Bosch, D.; Loss, O.; Azevedo, C.; Saiardi, A. Identification of an Evolutionarily Conserved Family of Inorganic Polyphosphate Endopolyphosphatases. *J. Biol. Chem.* 2011, 286, 31966−31974.

Loqué, D.; Lalonde, S.; Looger, L. L.; von Wiren, N.; Frommer, W. B. A cytosolic trans-activation domain essential for ammonium uptake. *Nature* 2007, 446, 195−198.

Lorenzo-Orts, L., Couto, D., Hothorn, M. Identity and functions of inorganic and inositol polyphosphates in plants. *New Phytol.* 2020, 225(2), 637–652.

Loss, O., Azevedo, C., Szijgyarto, Z., Bosch, D., Saiardi, A. Preparation of Quality Inositol Pyrophosphates. *J. Vis. Exp.* 2011, UNSP e3027 (55).

Luo, H. R., Huang, Y. E., Chen, J. C., Saiardi, A., Iijima, M., Ye, K., Huang, Y., Nagata, E., Devreotes, P., Snyder, S. H. Inositol pyrophosphates mediate chemotaxis in Dictyostelium via pleckstrin homology domain-PtdIns(3,4,5)P3 interactions. *Cell* 2003, 114(5), 559–572.

Manova, V., Gruszka, D. DNA damage and repair in plants - from models to crops. *Front. Plant Sci.* 2015, 6, 885.

Menniti, F. S.; Miller, R. N.; Putney, J. W., Jr.; Shears, S. B. Turnover of inositol polyphosphate pyrophosphates in pancreatoma cells. *J. Biol. Chem. 1993*, 268, 3850−3856.

Mulugu, S.; Bai, W.; Fridy, P. C.; Bastidas, R. J.; Otto, J. C.; Dollins, D. E.; Haystead, T. A.; Ribeiro, A. A.; York, J. D. A conserved family of enzymes that phosphorylate inositol hexakisphosphate. *Science* 2007, 316, 106−109.

Munnik, T. PI-PLC: Phosphoinositide-Phospholipase C in Plant Signaling. In: Wang, X. (eds) *Phospholipases in Plant Signaling. Signaling and Communication in Plants*, 2014 vol 20. Springer, Berlin, Heidelberg.

Murphy, A. M., Otto, B., Brearley, C. A., Carr, J. P., Hanke, D. E. A role for inositol hexakisphosphate in the maintenance of basal resistance to plant pathogens. *Plant J.* 2008, 56 (4), 638-652.

Nagy, R.; Grob, H.; Weder, B.; Green, P.; Klein, M.; FreletBarrand, A.; Schjoerring, J. K.; Brearley, C.; Martinoia, E. The Arabidopsis ATP-binding cassette protein AtMRP5/AtABCC5 is a high affinity inositol hexakisphosphate transporter involved in guard cell signaling and phytate storage. *J. Biol. Chem.* 2009, 284, 33614− 33622.

Nakamura, S.; Mano, S.; Tanaka, Y.; Ohnishi, M.; Nakamori, C.; Araki, M.; Niwa, T.; Nishimura, M.; Kaminaka, H.; Nakagawa, T.; Sato, Y.; Ishiguro, S. Gateway Binary Vectors with the Bialaphos Resistance Gene, as a Selection Marker for Plant Transformation. *Biosci., Biotechnol., Biochem.* 2010, 74, 1315−1319.

Nisa, M. U., Huang, Y., Benhamed, M., Raynaud, C. The Plant DNA Damage Response: Signaling Pathways Leading to Growth Inhibition and Putative Role in Response to Stress Conditions. *Front. Plant Sci.* 2019, 10, 653.

Onnebo, S. M.; Saiardi, A. Inositol pyrophosphates modulate hydrogen peroxide signalling. *Biochem. J.* 2009, 423, 109−118.

Osada, S.; Kageyama, K.; Ohnishi, Y.; Nishikawa, J.; Nishihara, T.; Imagawa, M. Inositol phosphate kinase Vip1p interacts with histone chaperone Asf1p in Saccharomyces cerevisiae. *Mol. Biol. Rep.* 2012, 39, 4989−4996.

Pascual-Ortiz, M.; Saiardi, A.; Walla, E.; Jakopec, V.; Kunzel, N. A.; Span, I.; Vangala, A.; Fleig, U. Asp1 Bifunctional Activity Modulates Spindle Function via Controlling Cellular Inositol Pyrophosphate Levels in Schizosaccharomyces pombe. *Mol. Cell. Biol.* 2018, 38, No. e00047-18.

Pollard, J. K., Steward, F. C., Shantz, E. M. Hexitols in Coconut Milk - Their Role in Nurture of Dividing Cells. *Plant Physiol.* 1961, 36 (4), 492.

Poon, J. S. Y., Le Fevre, R. E., Carr, J. P., Hanke, D. E., Murphy, A. M. Inositol hexakisphosphate biosynthesis underpins PAMP-triggered immunity to Pseudomonas syringae pv. tomato in Arabidopsis thaliana but is dispensable for establishment of systemic acquired resistance. *Mol. Plant Pathol.* 2020, 21 (3), 376-387.

Powis, G., Bonjouklian, R., Berggren, M. M., Gallegos, A., Abraham, R., Ashendel, C., Zalkow, L., Matter, W. F., Dodge, J., Grindey, G. Wortmannin, a potent and selective inhibitor of phosphatidylinositol-3-kinase. *Cancer Res.* 1994, 54(9), 2419–2423.

Puga, M. I.; Mateos, I.; Charukesi, R.; Wang, Z.; FrancoZorrilla, J. M.; de Lorenzo, L.; Irigoye, M. L.; Masiero, S.; Bustos, R.; Rodriguez, J.; Leyva, A.; Rubio, V.; Sommer, H.; Paz-Ares, J. SPX1 is a phosphate-dependent inhibitor of PHOSPHATE STARVATION RESPONSE 1 in Arabidopsis. *Proc. Natl. Acad. Sci. U.S.A.* 2014, 111, 14947−14952.

Qiu, D., Gu, C., Liu, G., Ritter, K., Eisenbeis, V. B., Bittner, T., Gruzdev, A., Seidel, L., Bengsch, B., Shears, S. B., & Jessen, H. J. (2022). Capillary electrophoresis mass spectrometry identifies new isomers of inositol pyrophosphates in mammalian tissues. *Chem. Sci.*, *14*(3), 658–667.

Qiu, D. Y.; Eisenbeis, V. B.; Saiardi, A.; Jessen, H. J. Absolute Quantitation of Inositol Pyrophosphates by Capillary Electrophoresis Electrospray Ionization Mass Spectrometry. *J. Vis. Exp.* 2021, 174, No. e62847.

Qiu, D. Y.; Wilson, M. S.; Eisenbeis, V. B.; Harmel, R. K.; Riemer, E.; Haas, T. M.; Wittwer, C.; Jork, N.; Gu, C. F.; Shears, S. B.; Schaaf, G.; Kammerer, B.; Fiedler, D.; Saiardi, A.; Jessen, H. J. Analysis of inositol phosphate metabolism by capillary electrophoresis electrospray ionization mass spectrometry. *Nat. Commun.* 2020, 11, No. 6035.

Rao, F., Cha, J., Xu, J., Xu, R., Vandiver, M. S., Tyagi, R., Tokhunts, R., Koldobskiy, M. A., Fu, C., Barrow, R., Wu, M., Fiedler, D., Barrow, J. C., Snyder, S. H. Inositol Pyrophosphates Mediate the DNA-PK/ATM-p53 Cell Death Pathway by Regulating CK2 Phosphorylation of Tti1/Tel2. *Mol. Cell* 2014, 79(4), 702.

Ried, M. K.; Wild, R.; Zhu, J. S.; Pipercevic, J.; Sturm, K.; Broger, L.; Harmel, R. K.; Abriata, L. A.; Hothorn, L. A.; Fiedler, D.; Hiller, S.; Hothorn, M. Inositol pyrophosphates promote the interaction of SPX domains with the coiled-coil motif of PHR transcription factors to regulate plant phosphate homeostasis. *Nat. Commun.* 2021, 12, No. 384.

Riemer, E.; Qiu, D.; Laha, D.; Harmel, R. K.; Gaugler, P.; Gaugler, V.; Frei, M.; Hajirezaei, M. R.; Laha, N. P.; Krusenbaum, L.; Schneider, R.; Saiardi, A.; Fiedler, D.; Jessen, H. J.; Schaaf, G.; Giehl, R. F. H. ITPK1 is an InsP6/ADP phosphotransferase that controls phosphate signaling in Arabidopsis. *Mol. Plant* 2021, 14, 1864−1880.

Romá-Mateo, C.; Rios, P.; Tabernero, L.; Attwood, T. K.; Pulido, R. A novel phosphatase family, structurally related to dualspecificity phosphatases, that displays unique amino acid sequence and substrate specificity. *J. Mol. Biol.* 2007, 374, 899−909.

Romá-Mateo, C.; Sacristan-Reviriego, A.; Beresford, N. J.; Caparros-Martin, J. A.; Culianez-Macia, F. A.; Martin, H.; Molina, M.; Tabernero, L.; Pulido, R. Phylogenetic and genetic linkage between novel atypical dual-specificity phosphatases from non-metazoan organisms. *Mol. Genet. Genomics* 2011, 285, 341−354.

Rubio, V.; Linhares, F.; Solano, R.; Martin, A. C.; Iglesias, J.; Leyva, A.; Paz-Ares, J. A conserved MYB transcription factor involved in phosphate starvation signaling both in vascular plants and in unicellular algae. *Genes Dev.* 2001, 15, 2122−2133.

Safrany, S. T.; Caffrey, J. J.; Yang, X.; Bembenek, M. E.; Moyer, M. B.; Burkhart, W. A.; Shears, S. B. A novel context for the 'MutT' module, a guardian of cell integrity, in a diphosphoinositol polyphosphate phosphohydrolase. *EMBO J.* 1998, 17, 6599−6607.

Safrany, S. T.; Ingram, S. W.; Cartwright, J. L.; Falck, J. R.; McLennan, A. G.; Barnes, L. D.; Shears, S. B. The diadenosine hexaphosphate hydrolases from Schizosaccharomyces pombe and Saccharomyces cerevisiae are homologues of the human diphosphoinositol polyphosphate phosphohydrolase - Overlapping substrate specificities in a MutT-type protein. *J. Biol. Chem.* 1999, 274, 21735− 21740.

Saiardi, A., Nagata, E., Luo, H. R., Sawa, A., Luo, X., Snowman, A. M., Snyder, S. H. Mammalian inositol polyphosphate multikinase synthesizes inositol 1,4,5-trisphosphate and an inositol pyrophosphate. *Proc. Natl. Acad. Sci. U.S.A.* 2001, 98 (5), 2306.

Saiardi, A., Caffrey, J. J., Snyder, S. H., Shears, S. B. The Inositol Hexakisphosphate Kinase Family: CATALYTIC FLEXIBILITY AND FUNCTION IN YEAST VACUOLE BIOGENESIS. *J. Biol. Chem.* 2000, 275 (32), 24686-24692.

Saiardi, A.; Erdjument-Bromage, H.; Snowman, A. M.; Tempst, P.; Snyder, S. H. Synthesis of diphosphoinositol pentakisphosphate by a newly identified family of higher inositol polyphosphate kinases. *Curr. Biol.* 1999, 9, 1323−1326.

Saiardi, A.; Resnick, A. C.; Snowman, A. M.; Wendland, B.; Snyder, S. H. Inositol pyrophosphates regulate cell death and telomere length through phosphoinositide 3-kinase-related protein kinases. *Proc. Natl. Acad. Sci. U.S.A.* 2005, 102, 1911−1914.

Schaaf, G.; Betts, L.; Garrett, T. A.; Raetz, C. R.; Bankaitis, V. A. Crystallization and preliminary X-ray diffraction analysis of phospholipid-bound Sfh1p, a member of the Saccharomyces cerevisiae Sec. 14p-like phosphatidylinositol transfer protein family. *Acta Crystallogr.*, Sect. F 2006, 62, 1156−1160.

Shears, S. B. in Inositol Phosphates: Methods and Protocols (ed Gregory J. Miller) 1-28 *Springer US*. 2020.

Shears, S. B. Inositol pyrophosphates: Why so many phosphates? *Adv. Biol. Regul.* 2015, 57 203-216.

Shears, S. B. Intimate connections: Inositol pyrophosphates at the interface of metabolic regulation and cell signaling. *J. Cell. Physiol.* 2018, 233, 1897−1912.

Shears, S. B., Kirk, C. J., Michell, R. H. The pathway of myo-inositol 1,3,4-trisphosphate dephosphorylation in liver. Biochem. J. 1987, 248 (3), 977-980.

Stack, J. H., Emr, S. D. Vps34p required for yeast vacuolar protein sorting is a multiple specificity kinase that exhibits both protein kinase and phosphatidylinositol-specific PI 3-kinase activities. *J Biol. Chem.* 1994, 269(50), 31552–31562.

Steidle, E. A.; Chong, L. S.; Wu, M.; Crooke, E.; Fiedler, D.; Resnick, A. C.; Rolfes, R. J. A Novel Inositol Pyrophosphate Phosphatase in Saccharomyces cerevisiae: Siw14 PROTEIN SELECTIVELY CLEAVES THE beta-PHOSPHATE FROM 5-DIPHOSPHOINOSITOL PENTAKISPHOSPHATE (5PP-IP5). *J. Biol. Chem.* 2016, 291, 6772−6783.

Steidle, E. A.; Morrissette, V. A.; Fujimaki, K.; Chong, L.; Resnick, A. C.; Capaldi, A. P.; Rolfes, R. J. The InsP7 phosphatase Siw14 regulates inositol pyrophosphate levels to control localization of the general stress response transcription factor Msn2. *J. Biol. Chem.* 2020, 295, 2043−2056.

Stephens, L. R., Hawkins, P. T., Downes, C. P. An analysis of myo-[3H]inositol trisphosphates found in myo-[3H]inositol prelabelled avian erythrocytes. *Biochem. J.* 1989, 262 (3), 727-737.

Stephens, L.; Radenberg, T.; Thiel, U.; Vogel, G.; Khoo, K. H.; Dell, A.; Jackson, T. R.; Hawkins, P. T.; Mayr, G. W. The detection, purification, structural characterization, and metabolism of diphosphoinositol pentakisphosphate(s) and bisdiphosphoinositol tetrakisphosphate(s). *J. Biol. Chem.* 1993, 268, 4009−4015.

Stevenson-Paulik, J., Chiou, S. T., Frederick, J. P., dela Cruz, J., Seeds, A. M., Otto, J. C., York, J. D. Inositol phosphate metabolomics: Merging genetic perturbation with modernized radiolabeling methods. *Methods.* 2006, 39 (2), 112-121.

Stevenson-Paulik, J., Odom, A. R., York, J. D. Molecular and Biochemical Characterization of Two Plant Inositol Polyphosphate 6-/3-/5-Kinases. *J. Biol. Chem.* 2002, 277 (45), 42711-42718.

Stevenson-Paulik, J.; Bastidas, R. J.; Chiou, S. T.; Frye, R. A.; York, J. D. Generation of phytate-free seeds in Arabidopsis through disruption of inositol polyphosphate kinases. *Proc. Natl. Acad. Sci. U.S.A.* 2005, 102, 12612−12617.

Streb, H., Irvine, R. F., Berridge, M. J., Schulz, I. Release of Ca-2+ from a Nonmitochondrial Intracellular Store in Pancreatic Acinar-Cells by Inositol-1,4,5-Trisphosphate. *Nature.* 1983, 306 (5938), 67-69.

Thota, S. G.; Bhandari, R. The emerging roles of inositol pyrophosphates in eukaryotic cell physiology. *J. Biosci.* 2015, 40, 593− 605

Wang, H.; Falck, J. R.; Hall, T. M.; Shears, S. B. Structural basis for an inositol pyrophosphate kinase surmounting phosphate crowding. *Nat. Chem. Biol.* 2012, 8, 111−116.

Wang, H.; Gu, C.; Rolfes, R. J.; Jessen, H. J.; Shears, S. B. Structural and biochemical characterization of Siw14: A proteintyrosine phosphatase fold that metabolizes inositol pyrophosphates. *J. Biol. Chem.* 2018, 293, 6905−6914.

Wang, H.; Nair, V. S.; Holland, A. A.; Capolicchio, S.; Jessen, H. J.; Johnson, M. K.; Shears, S. B. Asp1 from Schizosaccharomyces pombe binds a [2Fe-2S](2+) cluster which inhibits inositol pyrophosphate 1-phosphatase activity. *Biochemistry* 2015, 54, 6462− 6474.

Wang, H.; Perera, L.; Jork, N.; Zong, G.; Riley, A. M.; Potter, B. V. L.; Jessen, H. J.; Shears, S. B. A structural expose of noncanonical molecular reactivity within the protein tyrosine phosphatase WPD loop. *Nat. Commun.* 2022, 13, No. 2231.

Wang, Z. R.; Kuo, H. F.; Chiou, T. J. Intracellular phosphate sensing and regulation of phosphate transport systems in plants. *Plant Physiol.* 2021, 187, 2043−2055.

Whitfield, H.; White, G.; Sprigg, C.; Riley, A. M.; Potter, B. V. L.; Hemmings, A. M.; Brearley, C. A. An ATP-responsive metabolic cassette comprised of inositol tris/tetrakisphosphate kinase 1 (ITPK1) and inositol pentakisphosphate 2-kinase (IPK1) buffers diphosphosphoinositol phosphate levels. *Biochem. J.* 2020, 477, 2621−2638.

Wild, R.; Gerasimaite, R.; Jung, J. Y.; Truffault, V.; Pavlovic, I.; Schmidt, A.; Saiardi, A.; Jessen, H. J.; Poirier, Y.; Hothorn, M.; Mayer, A. Control of eukaryotic phosphate homeostasis by inositol polyphosphate sensor domains. *Science* 2016, 352, 986−990.

Wilson, M. S. C., Saiardi, A. Importance of Radioactive Labelling to Elucidate Inositol Polyphosphate Signalling. *Top. Curr. Chem.* 2017, 375 (1).

Wilson, M. S. C., Saiardi, A. Inositol Phosphates Purification Using Titanium Dioxide Beads. *Bio Protoc.* 2018, 8 (15).

Wundenberg, T., Grabinski, N., Lin, H., Mayr, G. W. Discovery of InsP6-kinases as InsP6-dephosphorylating enzymes provides a new mechanism of cytosolic InsP6 degradation driven by the cellular ATP/ADP ratio. *Biochem. J* 2014, 462(1), 173–184.

York, S. J., Armbruster, B. N., Greenwell, P., Petes, T. D., York, J. D. Inositol diphosphate signaling regulates telomere length. *J. Biol. Chem.* 2005, 280(6), 4264–4269.

Zhang, Q., van Wijk, R., Shahbaz, M., Roels, W., Schooten, B. V., Vermeer, J. E. M., Zarza, X., Guardia, A., Scuffi, D., García-Mata, C., Laha, D., Williams, P., Willems, L. A. J., Ligterink, W., Hoffmann-Benning, S., Gillaspy, G., Schaaf, G., Haring, M. A., Laxalt, A. M., Munnik, T. Arabidopsis Phospholipase C3 is Involved in Lateral Root Initiation and ABA Responses in Seed Germination and Stomatal Closure. *Plant Cell Physiol.* 2018, 59(3), 469–486.

Zhou, J.; Hu, Q.; Xiao, X.; Yao, D.; Ge, S.; Ye, J.; Li, H.; Cai, R.; Liu, R.; Meng, F.; Wang, C.; Zhu, J. K.; Lei, M.; Xing, W. Mechanism of phosphate sensing and signaling revealed by rice SPX1-PHR2 complex structure. *Nat. Commun.* 2021, 12, No. 7040.

Zhu, J.; Lau, K.; Puschmann, R.; Harmel, R. K.; Zhang, Y.; Pries, V.; Gaugler, P.; Broger, L.; Dutta, A. K.; Jessen, H. J.; Schaaf, G.; Fernie, A. R.; Hothorn, L. A.; Fiedler, D.; Hothorn, M. Two bifunctional inositol pyrophosphate kinases/phosphatases control plant phosphate homeostasis. *eLife* 2019, 8, No. e43582.

Zonneveld, B. J. M. B.J.M. Zonneveld. 1986. Cheap and simple yeast media. *J. Microb. Methods* 1986, 4, 287−291.

6. Publications

6.1. Gaugler, P.; Gaugler, V.; Kamleitner, M.; Schaaf, G. Extraction and Quantification of Soluble, Radiolabeled Inositol Polyphosphates from Different Plant Species using SAX-HPLC. *Journal of Visualized Experiments*. 2020, 160, No. e61495

https://doi.org/10.3791/61495

Own contribution: Conceived the study. Performed and analyzed all experiments. Prepared the figure and wrote the manuscript with the help of all authors.

6.2. Gaugler, P., Schneider, R., Liu, G., Qiu, D., Weber, J., Schmid, J., Jork, N., Häner, M., Ritter, K., Fernández-Rebollo, N., Giehl, R.F.H., Trung, M.N., Yadav, R., Fiedler, D., Gaugler, V., Jessen, H.J., Schaaf, G., Laha, D. *Arabidopsis* PFA-DSP-Type Phosphohydrolases Target Specific Inositol Pyrophosphate Messengers. *Biochemistry*. 2022 Jun 21;61(12):1213-1227

https://doi.org/10.1021/acs.biochem.2c00145

Own contribution: Conceived the study with D.L. and G.S. Designed most of the experiments, generated yeast mutants and performed all yeast experiments, generated constructs, isolated T-DNA insertion lines, performed HPLC analyses of plants, performed qPCR analyses, performed plant infiltration and TiO_2 pulldowns, and analyzed most of the experiments. Prepared the figures and wrote the manuscript with G.S., R.S., R.Y. and D.L. with input from all authors.

Extraction and Quantification of Soluble, Radiolabeled Inositol Polyphosphates from Different Plant Species using SAX-HPLC

Gaugler, P.; Gaugler, V.; Kamleitner, M.; Schaaf, G.

Journal of Visualized Experiments. 2020, 160, No. e61495 https://doi.org/10.3791/61495

Highlights:

- Existing protocols were optimized in regards of reproducibility, time and costs
- A standardized approach for data evaluation is proposed
- A detailed step by step protocol from set-up, preparations, performance to analysis is described and visualized
- The first inositol phosphate profile of *Lotus japonicus* is reported

jove

Extraction and Quantification of Soluble, Radiolabeled Inositol Polyphosphates from Different Plant Species using SAX-HPLC

Philipp Gaugler[1], **Verena Gaugler**[1], **Marília Kamleitner**[1], **Gabriel Schaaf**[1]

[1] Department of Plant Nutrition, Institute of Crop Science and Resource Conservation, University of Bonn

Corresponding Author

Philipp Gaugler
pgaugler@uni-bonn.de

Citation

Gaugler, P., Gaugler, V., Kamleitner, M., Schaaf, G. Extraction and Quantification of Soluble, Radiolabeled Inositol Polyphosphates from Different Plant Species using SAX-HPLC. *J. Vis. Exp.* (160), e61495, doi:10.3791/61495 (2020).

Date Published

June 26, 2020

DOI

10.3791/61495

URL

jove.com/video/61495

Abstract

The phosphate esters of *myo*-inositol, also termed inositol phosphates (InsPs), are a class of cellular regulators playing important roles in plant physiology. Due to their negative charge, low abundance and susceptibility to hydrolytic activities, the detection and quantification of these molecules is challenging. This is particularly the case for highly phosphorylated forms containing 'high-energy' diphospho bonds, also termed inositol pyrophosphates (PP-InsPs). Due to its high sensitivity, strong anion exchange high-performance liquid chromatography (SAX-HPLC) of plants labeled with [^{3}H]-*myo*-inositol is currently the method of choice to analyze these molecules. By using [^{3}H]-*myo*-inositol to radiolabel plant seedlings, various InsP species including several non-enantiomeric isomers can be detected and discriminated with high sensitivity. Here, the setup of a suitable SAX-HPLC system is described, as well as the complete workflow from plant cultivation, radiolabeling and InsP extraction to the SAX-HPLC run and subsequent data analysis. The protocol presented here allows the discrimination and quantification of various InsP species, including several non-enantiomeric isomers and of the PP-InsPs, $InsP_7$ and $InsP_8$, and can be easily adapted to other plant species. As examples, SAX-HPLC analyses of *Arabidopsis thaliana* and *Lotus japonicus* seedlings are performed and complete InsP profiles are presented and discussed. The method described here represents a promising tool to better understand the biological roles of InsPs in plants.

Introduction

Almost four decades ago, inositol phosphates (InsPs) emerged as signaling molecules, after Ins(1,4,5)P_3 ($InsP_3$) was identified as a second messenger that activates the receptor-mediated release of Ca^{2+} in animal cells[1,2]. To date, no $InsP_3$ receptor (IP3-R) has been identified in plants, which questions a direct signaling role for $InsP_3$ in plant cells[3]. Regardless, $InsP_3$ serves as a precursor for other InsPs involved in several plant developmental

processes, including the regulation of specific signaling pathways[3,4,5,6,7,8]. For instance, $InsP_3$ can be further phosphorylated to $InsP_6$, also known as "phytic acid", which represents a major source of phosphate, *myo*-inositol and cations, and was shown to play key roles in plant defense against pathogens, mRNA export and phosphate homeostasis[5,9,10,11,12].

Inositol pyrophosphates (PP-InsPs) are a class of InsPs that contain at least one high-energy di-phospho bond, initially identified in animal cells, amoeba and yeast, where they play critical roles in various cellular processes[13,14,15]. Despite seminal work on PP-InsPs in plants[16,17,18,19,20,21,22,23,24,25,26], the biological functions and isomer identity of these molecules still remain largely enigmatic. In the model plant *Arabidopsis thaliana*, cellular $InsP_8$ was proposed to regulate defenses against insect herbivores and necrotrophic fungi via coincidence-detection of $InsP_8$ and active jasmonate by the ASK1-COI1-JAZ receptor complex[17]. Furthermore, roles of $InsP_8$ and other PP-InsPs in energy homeostasis and nutrient sensing, as well as phosphate homeostasis have been proposed[17,23,24,25,26].

Regardless of the biological system employed, one major methodological challenge when studying InsPs has been the reliable detection and precise quantification of these molecules. Mass spectrometry-based methods have been used to detect InsPs, including PP-InsPs, from cell extracts. However, those studies failed to differentiate distinct isomers[26,27]. Another approach to analyze InsPs employs pull-down of InsPs from cell lysates using TiO_2 beads, followed by polyacrylamide gel electrophoresis (PAGE) of the eluted InsPs. The InsPs can then be stained by either toluidine blue or DAPI[24,28,29]. However, it is so far not possible to reliably detect InsPs lower than $InsP_5$ from plant extracts using this method. Recently, a method using [^{13}C]-*myo*-inositol for nuclear magnetic resonance (NMR) analysis of InsPs was published as an alternative to strong anion exchange high-performance liquid chromatography (SAX-HPLC)[30]. This technique has been reported to achieve a similar sensitivity compared to SAX-HPLC and to allow the detection of 5-$InsP_7$, as well as the discrimination of different non-enantiomeric $InsP_5$ isomers from cell extracts. However, the implementation of the NMR-based method requires chemically synthesized and commercially not available [^{13}C]-*myo*-inositol. Therefore, the method employed in most cases is radiolabeling samples with [^{3}H]-*myo*-inositol, followed by SAX-HPLC[31,32,33]. This technique is based on the uptake of radioactive *myo*-inositol into the plant and its conversion into different InsPs by the combined activity of dedicated cellular kinases and phosphatases.

The [^{3}H]-labeled InsPs are then acid-extracted and fractionated using SAX-HPLC. Because of their negative charge, the InsPs strongly interact with the positively charged stationary phase of the SAX-HPLC column and can be eluted with a buffer gradient containing increasing phosphate concentrations to outcompete InsPs from the column. Elution times thus depend on charge and geometry of the InsP species to be separated. In the absence of chiral columns, only non-enantiomeric isomers can by separated by this protocol. However, radiolabeled standards can be used to assign the isomeric nature of a specific InsP peak. Multiple efforts in the past by various laboratories to generate labeled and unlabeled standards with (bio)chemical methods or to purify them from various cells and organisms have helped assigning peaks to certain InsP species, and also to narrow down the isomeric identity of individual InsP species[5,7,21,34,35,36,37,38,39,40,41,42,43]. Also, the

recent elucidation of enzymatic pathways leading to the formation of PP-InsPs in plants, as well as the discovery of a bacterial type III effector with a specific 1-phytase activity, provide information on how to generate useful standards for these analyses[10, 17, 18, 22, 23].

The resulting fractions can be measured in a liquid scintillation counter due to the β-decay of tritium (^{3}H). With increasing labeling time, a steady-state isotopic equilibrium is reached, after which the obtained InsP profiles should represent the InsP status of the plant[31]. The major advantage of this protocol in comparison to other available techniques is the high sensitivity achieved by the use of the direct precursor for InsPs and the measurement of a radioactive signal.

SAX-HPLC of samples extracted from [^{3}H]-*myo*-inositol-labeled plants or other organisms is commonly used for the detection and quantification of InsPs ranging from lower InsP species to PP-InsPs, representing a valuable tool to better understand the metabolism, function and modes of action of InsPs. So far, this method is also the most appropriate choice for researchers with special interest in lower InsP species. While the basics of this procedure, on which the protocol described here builds on, have been previously described[7, 21, 31, 34], a detailed protocol tailored to the analysis of plant-derived InsPs and especially of PP-InsPs is still missing. Previous publications reported difficulties to reliably detect the low abundant PP-InsPs, especially $InsP_8$, due to one or more of the following factors: relatively low amounts of plant material, [^{3}H]-*myo*-inositol with low specific activity (> 20 Ci/mmol), usage of extraction buffers that are either not based on perchloric acid or are less concentrated than 1 M, different neutralizing buffers, as well as sub-optimal gradients or detection of [^{3}H] with an on-line detector. In comparison to those studies, the protocol presented here is designed for the reliable detection of PP-InsPs[7, 21, 34].

Here we present a detailed workflow, starting from the setup of the equipment to plant cultivation and labeling, InsP extraction and the SAX-HPLC run itself. Although the method was optimized to the model plant *A. thaliana*, it can be easily modified to study other plant species, as shown here with the first reported InsP profile of the model legume *Lotus japonicus*. Although the use of a different plant species might require some optimization, we envisage that those will be minor, making this protocol a good starting point for further research in plant InsPs. In order to facilitate possible optimizations, we indicate every step within the protocol in which modifications are possible, as well as all critical steps that may be challenging when establishing the method for the first time. Additionally, we report how data obtained by this method can be used for the quantification of specific InsPs and how different samples can be analyzed and compared.

Protocol

1. Setting up the HPLC system

1. Set up a system consisting of two independent HPLC pumps (binary pump), one for each buffer. Both pumps need to be controlled together via a computer with respective software or by having a master pump. Implement a piston seal wash for both pumps, either via gravitational force or through a third low pressure pump. Designate one pump for buffer A (termed pump A) and one for buffer B (termed pump B).
   NOTE: Both have to be able to generate pressures up to 60 bar (6 MPa) and flow rates of at least 0.5 mL/min.
2. Connect both pumps to a dynamic mixer.

3. Connect the mixer to an injection valve with a sample loop of at least 1 mL capacity.
4. Connect the injection valve to the column with a capillary via the corresponding end fittings.
5. Connect the column to the fraction collector by using a capillary with an appropriate length.

   NOTE: This description is based on our HPLC system (see the **Table of Materials**), which requires more manual steps than newer and more sophisticated systems. Our system allows easy access and modification of all components. Quaternary pumps (with the binary gradient described here) can also be used and will lead to elution profiles and overall quality of the analyses similar to those achieved with binary pumps.

2. Preparation of buffers, column and HPLC system

1. Prepare the buffers for the extraction of soluble InsPs: extraction buffer (1 M $HClO_4$) and neutralization buffer (1 M K_2CO_3). Prepare both buffers with ultra-pure deionized water. They are stable at room temperature for several months. Immediately prior to extraction, add EDTA to both solutions to a final concentration of 3 mM (e.g., from a filtered 250 mM EDTA stock solution).

   CAUTION: $HClO_4$ (perchloric acid) is strongly corrosive.
2. Prepare the buffers for the SAX-HPLC run: buffer A (1 mM EDTA) and buffer B (1 mM EDTA, 1.3 M $(NH_4)_2HPO_4$; pH 3.8 with H_3PO_4). Prepare both using ultra-pure deionized water followed by vacuum filtration with 0.2 µm pore-sized membrane filters. These are stable at room temperature for several months.

   NOTE: EDTA should be included in all buffers to prevent interactions of cations with InsPs, which could result in altered InsP charge or even insoluble InsP salt complexes.
3. Program the gradient as follows: 0–2 min, 0% buffer B; 2–7 min, up to 10% buffer B; 7–68 min, up to 84% buffer B; 68–82 min, up to 100% buffer B; 82–100 min, 100% buffer B, 100–101 min, down to 0% buffer B; 101–125 min, 0% buffer B. The optimal flow-rate for this gradient is 0.5 mL/min.
   1. During the run, collect fractions every minute, starting from minute 1 to minute 96. The remaining 30 min of the gradient serve to wash the column and the system, and do not have to be collected for scintillation counting.
4. If possible, set the maximal reachable pressure before the emergency shutdown of the HPLC pumps to 80 bar (8 MPa). This prevents **critical damage** to the column's resin.
5. When using a new SAX HPLC column, **wash** it **thoroughly** (>50 mL) with filtered ultra-pure deionized water before the first use.

   NOTE: This will ensure removal of the contained methanol, thus preventing salt precipitation in later steps. If possible, use a separate HPLC pump. If this is not available, make sure that the HPLC has flushed with water before washing the column. The flow-rate should not exceed 2 mL/min. After washing, the column is ready for the analysis and, when properly handled, can be **used for 20–40 runs**. After that, the resolution will successively decrease. Prolonged washing with buffer A (>1 h) and performing step 2.6 can help increase the lifetime of the column. If the decrease in resolution persists, the column needs to be exchanged. The gradient can be adjusted to increase the separation between specific

inositol polyphosphate species or to decrease the overall runtime. Using different HPLC systems (with different void volume or different volume of the capillaries) will strongly affect the retention times. Also, column changes have minor effects on the retention times.

6. Perform a "mock run". Instead of an extracted sample, inject filtered ultra-pure deionized water in the HPLC system and run the standard gradient. The fractions do not have to be collected.

   NOTE: Step 2.6 is optional. However, it should be performed if one of the following situations apply: A new column is installed; The HPLC system has been used for a different method beforehand; The HPLC system has not been used for longer than 3 days; There was a problem with the preceding run.

3. Plant cultivation and labeling with [^{3}H]-*myo*-inositol

NOTE: The following steps should be performed with **sterile components** and under **sterile conditions**, while wearing gloves to protect hands from contamination with the radiolabel. Plant media, especially when containing sucrose, are prone to microbial contamination.

1. Sterilize *A. thaliana* seeds with 1 mL of 1.2% sodium hypochlorite for 3 min followed by 1 mL of 70% ethanol for 3 min. Then add 1 mL of 100% ethanol, pipette the seeds with the ethanol onto a circular filter paper and allow them to air-dry under a laminar-flow on a clean bench.
   1. When using *L. japonicus* seeds, place them in a mortar and scrub seeds with sandpaper before sterilization to ensure a sufficient germination rate.
2. Sow out *Arabidopsis* seeds in 1–2 rows on square Petri dishes filled with solid growth media consisting of half-strength Murashige and Skoog (MS) salt solution, 1% sucrose, 0.7% gellan gum in deionized water adjusted to pH 5.7 with KOH and allow them to stratify for at least 1 day at 4 °C in the dark.
   1. For *Lotus* seeds, sow them out in 1 row on square Petri dishes filled with solid growth media consisting of 0.8% bacteriological agar in deionized water and allow them to stratify for at least 3 days at 4 °C in the dark.
3. Place the plates vertically in a growth incubator or climate chamber and allow them to grow for 10–12 days under short-day conditions (8 h light at 22 °C, 16 h dark at 20 °C).
4. Transfer 10–20 seedlings into one well of a 12-well clear flat-bottomed cell culture plate filled with 2 mL of half-strength MS salt solution supplemented with 1% sucrose and adjusted to pH 5.7.
5. Add 45 µCi of [^{3}H]-*myo*-inositol (30–80 Ci/mmol, dissolved in 90% ethanol) and mix by gentle swirling. Cover the plate with the corresponding lid and seal it with microporous surgical tape (e.g., micropore or leucopore tape), placing it back into the growth incubator.

   CAUTION: [^{3}H] is a low-energy beta emitter that can be a harmful radiation hazard when inhaled, ingested or absorbed through bare skin. **Always** wear gloves when handling radioactive material or equipment that has direct or indirect contact to radioactive material. Also follow the local rules for safe handling of radiochemicals (e.g., wearing additional protective clothes, use of a dosimeter and surveys of surfaces for contaminations on a regular basis).
6. After 5 days of labeling, remove seedlings from the media and wash them briefly with deionized water. Dry

them with paper towels and transfer them into a 1.5 mL microcentrifuge tube. **Do not overfill** the tube, and place no more than 100 mg FW/tube, which corresponds to approximately 10–20 17-day-old seedlings.

NOTE: An excess of plant material will dilute the acid during the extraction process and will strongly decrease the extraction efficiency.

1. Snap-freeze the tube in liquid nitrogen and store it at -80 °C until extraction.

   NOTE: Samples can be kept at -80 °C for several weeks without compromising sample quality. The growth conditions (media, light, temperature, time) can be modified according to the needs of a specific experiment or plant species. However, care should be taken when diluting the [^{3}H]-*myo*-inositol, in order to ensure quantifiable SAX-HPLC runs of good quality. Therefore, it is recommended to start with the [^{3}H]-*myo*-inositol concentrations stated here and reduce it stepwise if desired. During labeling time, plants can be submitted to different treatments (e.g., environmental stresses or chemical agents) to assess the impact of those conditions on global InsPs. To reach steady-state labeling, we recommend to label plants for at least 5 days.

4. Extraction of soluble InsPs

NOTE: Keep samples and reagents on ice during the whole extraction process. **Always wear gloves and protective glasses** due to the high risk of contact with radioactive material, especially during grinding. Everything that gets in contact with samples is considered as **radioactive waste** and should be disposed of according to the local rules for safe disposal of radioactive material.

1. Prepare the working solutions for the extraction and neutralization buffer as in step 2.1. Each sample will require 600 µL of extraction buffer and 400 µL of neutralization buffer. Store the buffers on ice.
2. Take the samples from -80 °C freezer and keep them in liquid nitrogen until further processing. Grind the samples with a microcentrifuge tube pestle until they start thawing and add 500 µL of ice-cold extraction buffer. Continue grinding until sample is completely homogenized and the solution has a deep green color (if leaves are present in the sample).
3. Centrifuge the samples for 10 min at 4 °C at ≥ 18000 x *g*. Transfer the supernatant into a fresh 1.5 mL tube. Keep in mind that the tubes used for extraction are considered solid radioactive waste and need to be disposed of accordingly.
4. **Carefully** add 300 µL of neutralization buffer to the extract. Precipitation of proteins and bubbling will start immediately. Mix by swirling with a pipette tip after a minute and wait for a few seconds before pipetting a small amount (5 µL) on pH paper (ideally range of pH 6–9). The pH should be between pH 7 and 8 in the end.
   1. If necessary, add small amounts (typically 10–20 µL) of either neutralization buffer or extraction buffer until the desired pH is reached. Let the samples rest on ice for at least 1 h with an open lid.
5. Centrifuge the samples for 10 min at 4 °C at ≥ 18,000 x *g*. Transfer the supernatant into a fresh 1.5 mL tube.

   NOTE: The samples can be either directly used in a SAX-HPLC run or kept on ice (if used later on the same day) or frozen in liquid nitrogen and stored at -80 °C for 2–4 weeks. To ensure a high reproducibility and comparability, it is recommended to always freeze the

samples in liquid nitrogen for 5 min, even if they will be directly used afterwards. Longer term storage of extracted samples at -80 °C is possible as long as samples are only thawed once. If frozen samples are used for the analysis, make sure that **no particles** are visible after thawing. Otherwise, centrifuge again for 10 min at 4 °C at ≥ 18,000 x *g* and transfer the supernatant into a fresh 1.5 mL tube.

5. Performing the HPLC run

1. Equip the fraction collector with 96 small scintillation vials (capacity of ~6 mL) and fill each vial with 2 mL of a suitable scintillation cocktail (e.g., Ultima-Flo AP liquid scintillation cocktail) compatible with buffers with low pH and high ammonium phosphate concentration (see **Table of Materials**).

   NOTE: The number of vials and the size of the vials depend on the fraction collector and scintillation counter used. It is important to at least collect the **first 90 fractions**, if the gradient described here is used, to obtain a full inositol polyphosphate profile. Also make sure to **properly label** every vial and its respective lid, to prevent mix-up of fractions or samples.

2. Start the HPLC system/pumps and have it ready to run. Activate the piston seal wash and keep it activated during the whole run. Load the sample by manually injecting the complete supernatant from step 4.5 (approximately 750 µL) using a suitable syringe (see **Table of Materials**). If automatic injection is possible, transfer the sample to the corresponding sample vial. Turn the valve from “load” to “inject” position and start the gradient and the fraction collector.

   NOTE: Depending on the HPLC system used, the starting procedure might differ, especially when comparing older systems (as described here) with a fully software-controlled newer model. It is very important to ensure that the gradient, the sample injection and fraction collection start simultaneously.

3. While the HPLC run is ongoing, check the pressure regularly. The starting pressure should be around 18–24 bar (1.8–2.4 MPa) and should slowly rise to 50–60 bar (5–6 MPa) once 100% buffer B is reached.

   CAUTION: Decreased pressure might indicate a leak in the system while increased pressure indicates a blockage. Pressure fluctuations (≥ 3 bar in a few seconds) can indicate the presence of air in the system. Keep in mind that everything that leaves the column, as well as every leakage that occurs at the injector or afterwards is **radioactive**.

   NOTE: The pressure also depends on the HPLC system and can be lower or higher than stated here. It will slowly increase after approximately 15–20 runs. However, this does not necessarily influence the quality of the obtained runs.

4. After the run, close the vials tightly and mix the fractions with the scintillation cocktail by vigorous shaking. Proceed directly with the measurement or keep the vials in an upright position, ideally in the dark.

   NOTE: Fractions mixed with scintillation cocktail are stable for weeks and can be measured later. Since the half-life of tritium is 12.32 years, the signal loss is negligible.

5. Once the run of the last sample of the day is finished, stop both HPLC pumps.

6. (Optional) To increase the longevity of the system, especially when it is not used regularly, wash pump B and capillaries by placing the capillary from buffer B into a bottle with buffer A and let the pump run for 10–15 min.

Before the next use, **remember** to replace the capillary into buffer B and to uncouple pump B from the mixer to flush it with buffer B. Once the pump and capillaries are filled again with buffer B, reconnect it with the mixer and the system is ready to use.

6. Measuring the fractions

1. Insert the vials into scintillation counter racks and measure each vial for 5 min in a liquid scintillation counter.
2. Ideally, use racks that directly fit small vials and avoid hanging in the vials in bigger (e.g., 20 mL) vials to reduce counting errors. The software settings used in this protocol are shown in **Supplemental Figure 1**.
   NOTE: Regularly perform an SNC (self-normalization and calibration) protocol using unquenched [^{3}H] standards. Shorter counting times (1–5 min) are possible to reduce the waiting time. However, to ensure a high counting reproducibility and accuracy, 5 min are recommended.

7. Data analysis

1. Export the measurements from the scintillation counter as a spreadsheet file or a compatible/convertible file format. Evaluate the data with a computer equipped with Excel or similar software, and a suitable analysis software like Origin.
2. Prepare a 2-D line chart where the measured counts per minutes (cpm) are plotted against the retention time (see **Figure 1**, **Figure 2**).
3. To compare samples with each other, **normalize the data** by summing up the cpm from each eluted fraction from minute 25 to 96 for each individual sample.
   NOTE: Minute 25 is used as cut-off to exclude unincorporated [^{3}H]-*myo*-inositol, $InsP_1$ and $InsP_2$ from the analysis, as those tend to fluctuate strongly and cannot be well separated (at least with the gradient proposed in this protocol) and thus strongly change the normalization factor due to their high activity.
4. Normalize all data to the sample with the lowest total cpm (in fractions 25–96) by dividing the total cpm from the sample with the lowest cpm (in fractions 25–96) by the total cpm (in fractions 25–96) of the other samples. The resulting factor can then be used to normalize the cpm from each fraction by multiplying the cpm of each fraction with the factor.
   NOTE: In the end, the sum of the cpm values from minute 25 to the end should be equal for all samples compared with each other. Only normalized runs should be presented in the same graph/figure (when presented as actual profiles). **Supplemental Figure 2** shows an example of how these calculation steps are made (using only fractions 25–35 of two samples for simplification). However, in some cases it is not necessary to normalize data. For instance, when peaks are quantified according to step 7.4 and presented as percentages of total InsPs (as shown in **Figure 3D**). As stated before, when presenting multiple analyses side by side as profiles, or when the actual measured activity is used for conclusions (e.g., treatment a) increases $InsP_7$ by x% compared to control, referring to the cpm values of $InsP_7$ of both samples and not to their percentage of total InsPs) normalization is needed. To analyze the effect of genotype or treatment differences on labeling efficiency, it is important **not** to **normalize**, as this would invalidate these differences. However, absolute quantification with this method is challenging because the extraction efficiency with this protocol can be variable for various reasons and are sometimes even observed when

replica of same genotype and treatment are analyzed. Keep in mind that depending on the HPLC system, column and gradient used for the analyses, the cut-off might need to be changed.

5. To **perform relative quantifications** of certain inositol polyphosphate peaks and to subsequently create **bar graphs** that contain data of replications for statistical analyses, continue the analysis with a specialized software that can calculate peak areas of chromatograms (e.g., Origin). See **Supplemental Figure 3**.

   NOTE: Most HPLC systems that are software-controlled are supplied with a respective software capable of this task. Peaks are determined as the fractions with cpm values above background (that varies to a certain degree between runs) and retention times that are similar to previously published data. The retention time of a specific peak is determined in spreadsheet software (e.g., Excel) and used to assign peaks for calculation of definite integrals (e.g., in Origin). **Supplemental Figure 3** illustrates this process of peak determination, background subtraction and integration of peaks.

Representative Results

The results shown here aim to illustrate possible outcomes obtained according to variations at technical and biological levels. The first is exemplified by analyses using new versus aged columns (**Figure 1**) and fresh versus stored samples (**Figure 3**), and the second by evaluating extracts from two different plant systems, *A. thaliana* (**Figure 1**, **Figure 3**) and *L. japonicus* (**Figure 2**).

An optimal SAX-HPLC run is depicted on **Figure 1A–C**, which shows a complete inositol polyphosphate spectrum obtained from *A. thaliana* extracts after scintillation counting. Note that peaks are nicely separated and can be assigned to different isomers (or enantiomer-pairs) based on chromatographic mobilities described earlier[5,7].

Figure 2 shows the representative result of a SAX-HPLC analysis of *L. japonicus* seedlings that were grown and labeled under the same conditions as the *Arabidopsis* seedlings. While presumably all InsP species and peaks that are known from *Arabidopsis* can be seen, there are substantial differences regarding the relative (e.g., ratios between isomers) amount of specific InsP isomers, when comparing the profiles of both species. For instance, the Lotus extracts showed increased $InsP_{3c}$, $InsP_{4b}$, $InsP_{5b}$ and reduced $InsP_{3a}$, $InsP_{4a}$, $InsP_{5a}$ and $InsP_{5c}$ compared to *Arabidopsis* which leaves room for further investigations. **Figure 2D** illustrates the different ratios between InsP isomers between *Arabidopsis* and *Lotus*.

Figure 3 shows two InsP profiles of a sample that was split after the extraction. The first half was immediately analyzed and the second half one day later, after storage at -80 °C. Note that only minor differences are observed between the different samples (i.e., black and red lines on **Figure 3A–C**, and **Figure 3D**). This illustrates that one freeze-thaw cycle does not harm the sample and that the method itself generates reproducible results.

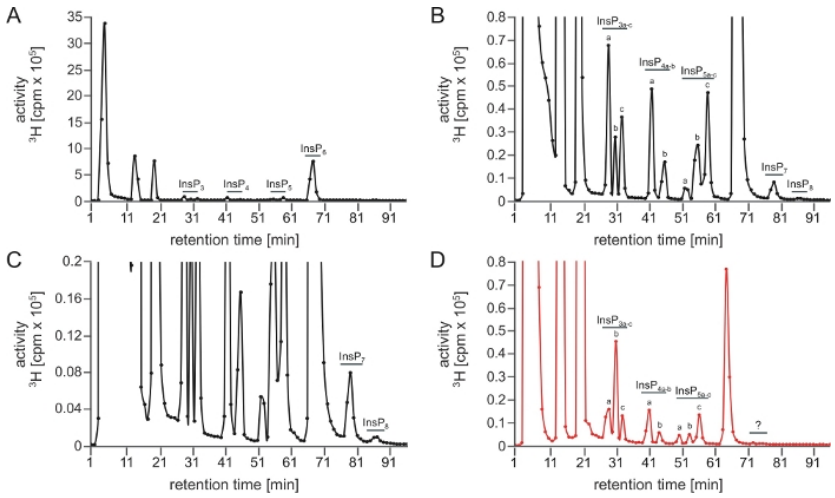

Figure 1: Typical InsP profile of a successful and of an unsuccessful SAX-HPLC analysis performed with this protocol. (**A**–**C**) SAX-HPLC profile of 17-day-old wild-type (Col-*0*) *Arabidopsis* seedlings radiolabeled with [^{3} H]-*myo*-inositol. Global InsP extraction and SAX-HPLC run were performed on the same day. (**A**) Full spectra; (**B**, **C**) Zoom-ins of the profile shown in A. All visible peaks are highlighted and assigned to the corresponding InsP species. Based on published chromatographic mobilities[5,7], $InsP_{4a}$ likely represents Ins(1,4,5,6)P_4 or Ins(3,4,5,6)P_4, $InsP_{5a}$ represents $InsP_5$ [2-OH], $InsP_{5b}$ represents $InsP_5$ [4-OH] or its enantiomeric form $InsP_5$ [6-OH], and $InsP_{5c}$ represents $InsP_5$ [1-OH] or its enantiomeric form $InsP_5$ [3-OH]. The isomeric natures of $InsP_{3a-c}$, $InsP_{4b}$, $InsP_7$, and $InsP_8$ are still unknown. Panel (**D**) shows a SAX-HPLC profile of identically grown plants but using an aged column (>40 runs). A clear reduction of $InsP_6$ compared to other InsP species and the absence of PP-InsPs is visible. Please click here to view a larger version of this figure.

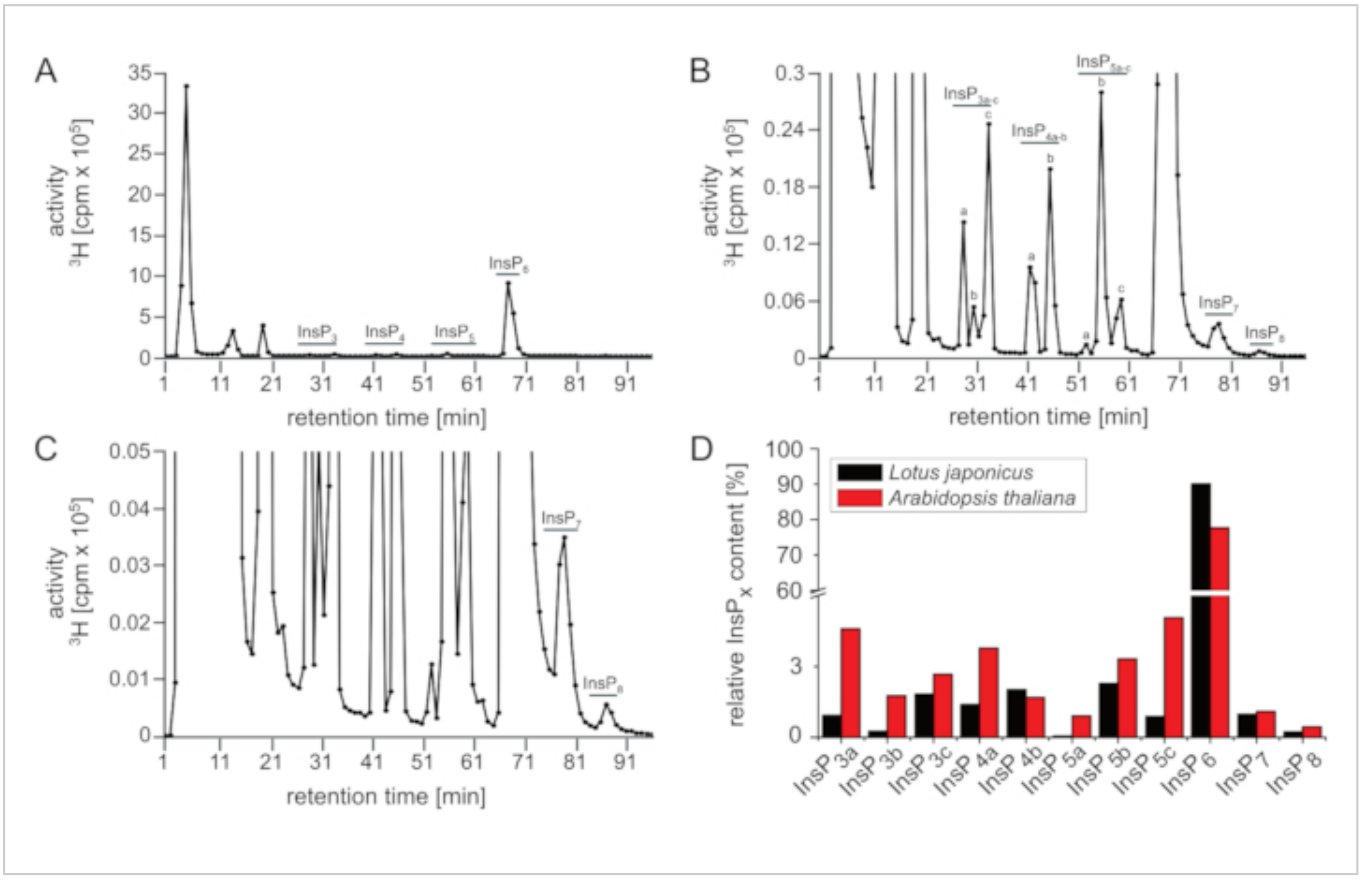

Figure 2: Representative InsP profile of *L. japonicus* plants. SAX-HPLC profile (**A**–**C**) of 17-day-old wild-type (Gifu) *L. japonicus* seedlings radiolabeled with [^{3} H]-*myo*-inositol. (**A**) Full spectra; (**B**, **C**) Zoom-ins of the profile shown in A. All visible peaks are highlighted and assigned to the corresponding InsP species. Based on published chromatographic mobilities[5,7], $InsP_{4a}$ likely represents Ins(1,4,5,6)P_4 or Ins(3,4,5,6)P_4, $InsP_{5b}$ likely represents $InsP_5$ [4-OH] or its enantiomeric form $InsP_5$ [6-OH], and $InsP_{5c}$ likely represents $InsP_5$ [1-OH] or its enantiomeric form $InsP_5$ [3-OH]. The isomeric natures of $InsP_{3a-c}$, $InsP_{4b}$, $InsP_7$, and $InsP_8$ are unknown. (**D**) Comparison between the individual InsP species (in % of total activity from elution 25–96) of *A. thaliana* (data from **Figure 1A–C**) and *L. japonicus* (data from **Figure 2A–C**). Please click here to view a larger version of this figure.

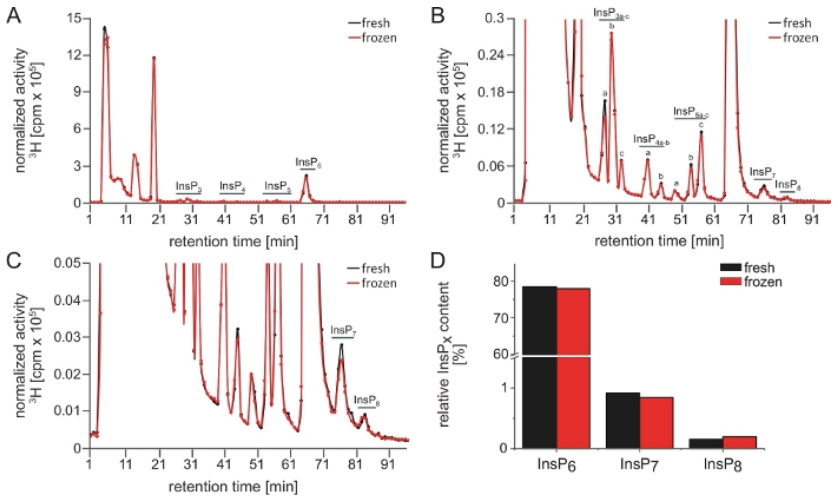

Figure 3: InsP profiles of a split sample illustrating the reproducibility of SAX-HPLC analyses. (**A**–**C**) SAX-HPLC profiles of 17-day-old wild-type (Col-*0*) *Arabidopsis* seedlings radiolabeled with [^{3} H]-*myo*-inositol. Prior the run, the sample was split and one half run immediately and the other half one day later after storage at -80 °C. (**A**) Full spectra; (**B**, **C**) Zoom-ins of the profile shown in A. All visible peaks are highlighted and assigned to the corresponding InsP species. Based on published chromatographic mobilities[5,7], InsP$_{4a}$ likely represents Ins(1,4,5,6)P$_4$ or Ins(3,4,5,6)P$_4$, InsP$_{5a}$ represents InsP$_5$ [2-OH], InsP$_{5a}$ represents InsP$_5$ [2-OH], InsP$_{5b}$ represents InsP$_5$ [4-OH] or its enantiomeric form InsP$_5$ [6-OH], and InsP$_{5c}$ represents InsP$_5$ [1-OH] or its enantiomeric form InsP$_5$ [3-OH]. The isomeric natures of InsP$_{3a-c}$, InsP$_{4b}$, InsP$_7$, and InsP$_8$ are still unknown. Panel **D** shows the quantification of InsP$_6$ and the PP-InsPs InsP$_7$ and InsP$_8$ of both runs. The values represent the amount (in %) of the respective InsP species relative to all InsP (total activity from elution 25–96). Please click here to view a larger version of this figure.

Supplemental Figure 1: Software settings for liquid scintillation counting using a light scintillation counter. Screenshots showing the software version, as well as settings used for scintillation counting of [^{3} H] samples performed with this protocol are depicted. Please click here to download this figure.

Supplemental Figure 2: Representative example of data normalization. A screenshot of a worksheet shows all steps and formulas used to normalize SAX-HPLC runs to each other. For simplification, only fractions 25–35 of samples are shown. Please click here to download this figure.

Supplemental Figure 3: Peak determination, background subtraction and integration using analysis software. (**A**) Data from SAX-HPLC analysis is loaded into the software (minutes 28–96) and the peak analyzer tool is selected. (**B**–**E**) The baseline is defined manually by setting points between individual peaks and the background is subtracted. (**F**) Peaks are determined manually based on appearance and published chromatographic mobilities[5,7]. (**G**) Peak ranges

are defined manually by cpm values. (**H**) Peaks are integrated and calculated as % of all peaks. Please click here to download this figure.

Discussion

Here we present a versatile and sensitive method to quantify InsPs including PP-InsPs in plant extracts and provide practical tips on how to get this method established. Even though the protocol is generally robust, suboptimal runs and analyses can occur. In most cases, those runs can be identified by a strong reduction or even complete loss of highly phosphorylated InsPs, especially the PP-InsP species $InsP_7$ and $InsP_8$. Possible reasons can be microbial contaminations of the plant material and insufficient deactivation of endogenous plant PP-InsP hydrolases during extraction due to insufficient grinding and thawing of plant material that will not be in immediate contact with extraction buffer. Further reasons include inaccurate pH adjustment by insufficient or excess addition of neutralization buffer, or simply insufficient sample material. The latter can make it difficult to detect PP-InsPs, since those are often present in very low amounts in the cells. An excess of sample material or inefficient drying during step 3.5 may cause dilution of the perchloric acid, therefore also leading to insufficient enzyme deactivation and a specific loss of $InsP_6$ and PP-InsPs. The amount of plant material, as well as radiolabel used in this protocol were optimized based on costs and performance, and is therefore close to the lowest amount that is still sufficient for providing optimal results. In addition, the column resin will gradually loose its resolution capacity. The first sign of this process is (for reasons not entirely clear to the authors) a specific loss of higher phosphorylated InsP species like the PP-InsPs in the HPLC spectrum. With further aging, even $InsP_6$ will not be resolved properly by the column (**Figure 1D**). Therefore, the use of an adequate column, as well as meticulous handling of the sample and proper maintenance of the HPLC components is crucial for ensuring accurate results.

When comparing samples and runs, especially when generated with different equipment (e.g., HPLC systems and columns) or on different days, it is crucial to normalize the samples to each other (as described in step 7.3) and to analyze them in the same way. Only through normalization it is possible and accurate to show multiple samples in the same graph (**Figure 3**). For quantification of individual InsPs relative to total InsPs, or to another specific InsP species, it is not necessary to normalize, as long as only relative values and not absolute values are shown. Ideally, both the InsP profiles and the quantifications are shown. However, in some cases it is not possible to adequately show two or more runs in the same graph. Different retention times or different levels of background activity can make it difficult to compare unquantified SAX-HPLC profiles alone. The same is the true when many samples need to be compared. In such cases, a further evaluation using an additional software (e.g., Origin) for individual peak quantification is necessary.

The authors are aware that the protocol described here can be optimized and needs to be adapted to each individual research question. Although being optimized for *Arabidopsis* extracts[7,17] in this protocol, this method is versatile and can help determining InsP profiles of other plant species as well. Here we exemplify this possibility by presenting for the first time a InsP profile for *L. japonicus*, which required no modifications of the labeling conditions, InsP extraction or SAX-HPLC run (**Figure 2**). Notably, while overall similar, differences are observed between *L. japonicus* and *Arabidopsis* InsP profiles. For instance, in *L. japonicus* $InsP_5$ [4-OH] or its enantiomeric form $InsP_5$ [6-OH] are more abundant than $InsP_5$ [1-OH] or its enantiomeric form $InsP_5$

[3-OH] in comparison to *Arabidopsis*, where $InsP_5$ [1-OH] or its enantiomeric form $InsP_5$ [3-OH] are the dominant $InsP_5$ species. Likewise, we anticipate that alterations in the media composition, [^{3}H]-*myo*-inositol concentration, plant age, environmental conditions (e.g., light and temperature), addition of chemical compounds or analyses of plant-microbial interactions among other factors, might need to be tested and adapted.

One important drawback of this method that needs to be considered is that the labeling is done in a (sterile) liquid culture, which does not represent a physiological environment for most land plants. In addition, due to the high costs of [³H]-*myo*-inositol, the volume of the labeling solution and the size of the culture vessel is generally limited, which also restricts the size of the plants that can be used. Cultivation in liquid culture can be avoided by directly infiltrating for instance leaves of soil-grown plants with [³H]-*myo*-inositol and subsequently following the protocol described here, as previously reported[10].

There are several drawbacks of this protocol in comparison to alternative methods, such as TiO_2 pull-down followed by PAGE or mass spectrometry based techniques. Due to the [^{3}H]-*myo*-inositol labeling, only InsP species that directly originate from radiolabeled *myo*-inositol will be detected in the end. The method described here is blind to other Ins isomers such as *scyllo*-inositol and other isomers some of which have been identified in certain plants[44]. Furthermore, *myo*-InsPs derived from other pathways will be excluded, including those synthesized by *de novo* synthesis of *myo*-inositol and *myo*-inositol-3-phosphate via isomerization of glucose-6-phosphate, catalyzed by *myo*-inositol-3-phosphate synthase (MIPS) proteins[45]. Although [^{32}P] or [^{33}P]-*ortho*-phosphate can be used as alternative labels, their use poses a major disadvantage, since every phosphate-containing molecule, including the abundant nucleotides and its derivatives, will be labeled. Those molecules can also be extracted with this protocol and bind to the SAX column, which will result in a high level of background activity that will interfere with the identification of individual InsP peaks[5]. In addition, quantification of [^{32}P]- or [^{33}P] -labeled InsPs and PP-InsPs can be strongly influenced by phosphate and pyrophosphate moiety turnover and might not report a mass readout for inositol species.

On the other hand, [^{3}H]-*myo*-inositol specifically labels *myo*-inositol-containing molecules. InsPs, inositol-containing lipids, such as phosphoinositides, and galactinol are in this case labeled. However, only InsPs will be analyzed with this protocol, since lipids are insoluble in the extraction buffer and galactinol does not bind to the SAX column.

So far, the differences from a plant InsP profile generated by [^{3}H]-*myo*-inositol labeling compared with one determined by TiO_2 pulldown/PAGE remains unknown, since such comparisons have not been performed in plants. A recent study in animal cells addressed this question[46]. In that work, a pool of $InsP_6$ that is invisible by [^{3}H]-*myo*-inositol labeling, which should thereby be directly derived from glucose-6-phosphate, was identified by comparing SAX-HPLC profiles with PAGE gels of mammalian cell lines. 24 h of phosphate starvation resulted in a 150% increase of $InsP_6$ when quantifying PAGE gels of InsPs purified using TiO_2 pulldown. SAX-HPLC analyses of [^{3}H]-*myo*-inositol-labeled cells that were treated identically only showed an increase by 15% of [^{3}H]-$InsP_6$. As previously mentioned, InsPs lower than $InsP_5$ are undetectable with PAGE analysis in most cases. Radiolabeling followed by SAX-HPLC appears to be the method of choice, as long as mass spectrometric protocols

are not optimized to detect this group of highly negatively charged molecules.

Another remaining challenge is to distinguish enantiomers in SAX-HPLC analyses (or in any other method for InsP analysis)[10,17]. This challenge can be tackled by the addition of chiral selectors, i.e., enantiopure compounds like L-arginine amide that interact with the respective enantiomeric molecules to form diastereomeric complexes that can be separated[10]. To our knowledge, this approach has only been implemented to discriminate the enantiomeric $InsP_5$ isomers $InsP_5$ [1-OH] and $InsP_5$ [3-OH] by NMR analyses[10]. Discrimination of other enantiomeric pairs or successful discrimination of enantiomers by chiral SAX-HPLC analysis or chiral PAGE-based methods have not yet been reported and should be further developed. Considering the conserved synthesis and the conserved regulation of PP-InsPs by phosphorous availability, we envision that especially non-radioactive methods such as PAGE or MS-based methods, together with nutrient analyses, will help ground truthing efforts to calibrate remote sensing data designed to diagnose nutrient deficiencies in crops[17,18,24,25]. However, the method presented here can currently still be considered the gold standard for InsP analyses and will be instrumental to discover new functions of these intriguing messengers in plants.

Disclosures

The authors have nothing to disclose.

Acknowledgments

This work was funded by the Deutsche Forschungsgemeinschaft (DFG, German Research Foundation) under Germany's Excellence Strategy - EXC-2070 – 390732324 (PhenoRob), the Research Training Group GRK2064 and individual research grants SCHA1274/4-1 and SCHA1274/5-1 to G.S.. We also thank Li Schlüter and Brigitte Ueberbach for technical assistance.

References

1. Berridge, M. J., Irvine, R. F. Inositol Phosphates and Cell Signaling. *Nature.* **341** (6239), 197-205, (1989).
2. Streb, H., Irvine, R. F., Berridge, M. J., Schulz, I. Release of Ca-2+ from a Nonmitochondrial Intracellular Store in Pancreatic Acinar-Cells by Inositol-1,4,5-Trisphosphate. *Nature.* **306** (5938), 67-69, (1983).
3. Krinke, O., Novotna, Z., Valentova, O., Martinec, J. Inositol trisphosphate receptor in higher plants: is it real? *Journal of Experimental Botany.* **58** (3), 361-376, (2007).
4. Kuo, H. F. *et al.* Arabidopsis inositol pentakisphosphate 2-kinase, AtIPK1, is required for growth and modulates phosphate homeostasis at the transcriptional level. *Plant Journal.* **80** (3), 503-515, (2014).
5. Kuo, H. F. *et al.* Arabidopsis inositol phosphate kinases IPK1 and ITPK1 constitute a metabolic pathway in maintaining phosphate homeostasis. *Plant Journal.* **95** (4), 613-630, (2018).
6. Gillaspy, G. E. in *Lipid-mediated Protein Signaling* (ed Daniel G. S. Capelluto) 141-157 *Springer Netherlands.* (2013).
7. Stevenson-Paulik, J., Bastidas, R. J., Chiou, S. T., Frye, R. A., York, J. D. Generation of phytate-free seeds in Arabidopsis through disruption of inositol polyphosphate kinases. *Proceedings of the National Academy of Sciences of the United States of America.* **102** (35), 12612-12617, (2005).

8. Lemtiri-Chlieh, F., MacRobbie, E. A. C., Brearley, C. A. Inositol hexakisphosphate is a physiological signal regulating the K+-inward rectifying conductance in guard cells. *Proceedings of the National Academy of Sciences.* **97** (15), 8687-8692, (2000).
9. Lee, H. S. *et al.* InsP6-sensitive variants of the Gle1 mRNA export factor rescue growth and fertility defects of the ipk1 low-phytic-acid mutation in Arabidopsis. *Plant Cell.* **27** (2), 417-431, (2015).
10. Blüher, D. *et al.* A 1-phytase type III effector interferes with plant hormone signaling. *Nature Communications.* **8**, (2017).
11. Murphy, A. M., Otto, B., Brearley, C. A., Carr, J. P., Hanke, D. E. A role for inositol hexakisphosphate in the maintenance of basal resistance to plant pathogens. *Plant Journal.* **56** (4), 638-652, (2008).
12. Poon, J. S. Y., Le Fevre, R. E., Carr, J. P., Hanke, D. E., Murphy, A. M. Inositol hexakisphosphate biosynthesis underpins PAMP-triggered immunity to Pseudomonas syringae pv. tomato in Arabidopsis thaliana but is dispensable for establishment of systemic acquired resistance. *Molecular Plant Pathology.* **21** (3), 376-387, (2020).
13. Wild, R. *et al.* Control of eukaryotic phosphate homeostasis by inositol polyphosphate sensor domains. *Science.* **352** (6288), 986-990, (2016).
14. Shears, S. B. Inositol pyrophosphates: Why so many phosphates? *Advances in Biological Regulation.* **57** 203-216, (2015).
15. Shears, S. B. Intimate connections: Inositol pyrophosphates at the interface of metabolic regulation and cell signaling. *Journal of Cellular Physiology.* **233** (3), 1897-1912, (2018).
16. Desai, M. *et al.* Two inositol hexakisphosphate kinases drive inositol pyrophosphate synthesis in plants. *Plant Journal.* **80** (4), 642-653, (2014).
17. Laha, D. *et al.* VIH2 Regulates the Synthesis of Inositol Pyrophosphate InsP8 and Jasmonate-Dependent Defenses in Arabidopsis. *Plant Cell.* **27** (4), 1082-1097, (2015).
18. Laha, D. *et al.* Arabidopsis ITPK1 and ITPK2 Have an Evolutionarily Conserved Phytic Acid Kinase Activity. *Acs Chemical Biology.* **14** (10), 2127-2133, (2019).
19. Dorsch, J. A. *et al.* Seed phosphorus and inositol phosphate phenotype of barley low phytic acid genotypes. *Phytochemistry.* **62** (5), 691-706, (2003).
20. Flores, S., Smart, C. C. Abscisic acid-induced changes in inositol metabolism in Spirodela polyrrhiza. *Planta.* **211** (6), 823-832, (2000).
21. Brearley, C. A., Hanke, D. E. Inositol phosphates in barley (Hordeum vulgare L) aleurone tissue are stereochemically similar to the products of breakdown of InsP(6) in vitro by wheat-bran phytase. *Biochemical Journal.* **318** 279-286, (1996).
22. Laha, N. P. *et al.* ITPK1-Dependent Inositol Polyphosphates Regulate Auxin Responses in *Arabidopsis thaliana. bioRxiv.* (2020).
23. Laha, D. *et al.* Inositol Polyphosphate Binding Specificity of the Jasmonate Receptor Complex. *Plant Physiology.* **171** (4), 2364-2370, (2016).
24. Dong, J. S. *et al.* Inositol Pyrophosphate InsP(8) Acts as an Intracellular Phosphate Signal in Arabidopsis. *Molecular Plant.* **12** (11), 1463-1473, (2019).

25. Zhu, J. *et al.* Two bifunctional inositol pyrophosphate kinases/phosphatases control plant phosphate homeostasis. *Elife.* **8**, (2019).
26. Couso, I. *et al.* Synergism between Inositol Polyphosphates and TOR Kinase Signaling in Nutrient Sensing, Growth Control, and Lipid Metabolism in Chlamydomonas. *Plant Cell.* **28** (9), 2026-2042, (2016).
27. Ito, M. *et al.* Hydrophilic interaction liquid chromatography-tandem mass spectrometry for the quantitative analysis of mammalian-derived inositol poly/pyrophosphates. *Journal of Chromatography A.* **1573** 87-97, (2018).
28. Wilson, M. S. C., Saiardi, A. Inositol Phosphates Purification Using Titanium Dioxide Beads. *Bio-Protocol.* **8** (15), (2018).
29. Loss, O., Azevedo, C., Szijgyarto, Z., Bosch, D., Saiardi, A. Preparation of Quality Inositol Pyrophosphates. *Jove-Journal of Visualized Experiments.* UNSP e3027 (55), (2011).
30. Harmel, R. K. *et al.* Harnessing C-13-labeled myo-inositol to interrogate inositol phosphate messengers by NMR Electronic supplementary information (ESI) available. *Chemical Science.* **10** (20), 5267-5274, (2019).
31. Azevedo, C., Saiardi, A. Extraction and analysis of soluble inositol polyphosphates from yeast. *Nature Protocols.* **1** (5), 2416-2422, (2006).
32. Shears, S. B. in *Inositol Phosphates: Methods and Protocols* (ed Gregory J. Miller) 1-28 *Springer US.* (2020).
33. Wilson, M. S. C., Saiardi, A. Importance of Radioactive Labelling to Elucidate Inositol Polyphosphate Signalling. *Topics in Current Chemistry.* **375** (1), (2017).
34. Stevenson-Paulik, J. *et al.* Inositol phosphate metabolomics: Merging genetic perturbation with modernized radiolabeling methods. *Methods.* **39** (2), 112-121, (2006).
35. Liu, C., Riley, A. M., Yang, X., Shears, S. B., Potter, B. V. L. Synthesis and Biological Activity of d- and l-chiro-Inositol 2,3,4,5-Tetrakisphosphate: Design of a Novel and Potent Inhibitor of Ins(3,4,5,6)P4 1-Kinase/ Ins(1,3,4)P3 5/6-Kinase. *Journal of Medicinal Chemistry.* **44** (18), 2984-2989, (2001).
36. Hughes, P. J., Hughes, A. R., Putney, J. W., Shears, S. B. The regulation of the phosphorylation of inositol 1,3,4-trisphosphate in cell-free preparations and its relevance to the formation of inositol 1,3,4,6-tetrakisphosphate in agonist-stimulated rat parotid acinar cells. *Journal of Biological Chemistry.* **264** (33), 19871-19878, (1989).
37. Shears, S. B., Kirk, C. J., Michell, R. H. The pathway of myo-inositol 1,3,4-trisphosphate dephosphorylation in liver. *The Biochemical journal.* **248** (3), 977-980, (1987).
38. Stevenson-Paulik, J., Odom, A. R., York, J. D. Molecular and Biochemical Characterization of Two Plant Inositol Polyphosphate 6-/3-/5-Kinases. *Journal of Biological Chemistry.* **277** (45), 42711-42718, (2002).
39. Stephens, L. R., Hawkins, P. T., Downes, C. P. An analysis of myo-[3H]inositol trisphosphates found in myo-[3H]inositol prelabelled avian erythrocytes. *The Biochemical journal.* **262** (3), 727-737, (1989).
40. Saiardi, A. *et al.* Mammalian inositol polyphosphate multikinase synthesizes inositol 1,4,5-trisphosphate and an inositol pyrophosphate. *Proceedings of the National Academy of Sciences.* **98** (5), 2306, (2001).

41. Azevedo, C., Burton, A., Bennett, M., Onnebo, S. M. N., Saiardi, A. in *Inositol Phosphates and Lipids: Methods and Protocols* (ed Christopher J. Barker) 73-85 *Humana Press.* (2010).

42. Saiardi, A., Caffrey, J. J., Snyder, S. H., Shears, S. B. The Inositol Hexakisphosphate Kinase Family: CATALYTIC FLEXIBILITY AND FUNCTION IN YEAST VACUOLE BIOGENESIS. *Journal of Biological Chemistry.* **275** (32), 24686-24692, (2000).

43. Brearley, C. A., Hanke, D. E. Inositol phosphates in the duckweed Spirodela polyrhiza L. *Biochemical Journal.* **314** 215-225, (1996).

44. Pollard, J. K., Steward, F. C., Shantz, E. M. Hexitols in Coconut Milk - Their Role in Nurture of Dividing Cells. *Plant Physiology.* **36** (4), 492-&, (1961).

45. Donahue, J. L. *et al.* The Arabidopsis thaliana Myo-inositol 1-phosphate synthase1 gene is required for Myo-inositol synthesis and suppression of cell death. *Plant Cell.* **22** (3), 888-903, (2010).

46. Desfougeres, Y., Wilson, M. S. C., Laha, D., Miller, G. J., Saiardi, A. ITPK1 mediates the lipid-independent synthesis of inositol phosphates controlled by metabolism. *Proceedings of the National Academy of Sciences of the United States of America.* **116** (49), 24551-24561, (2019).

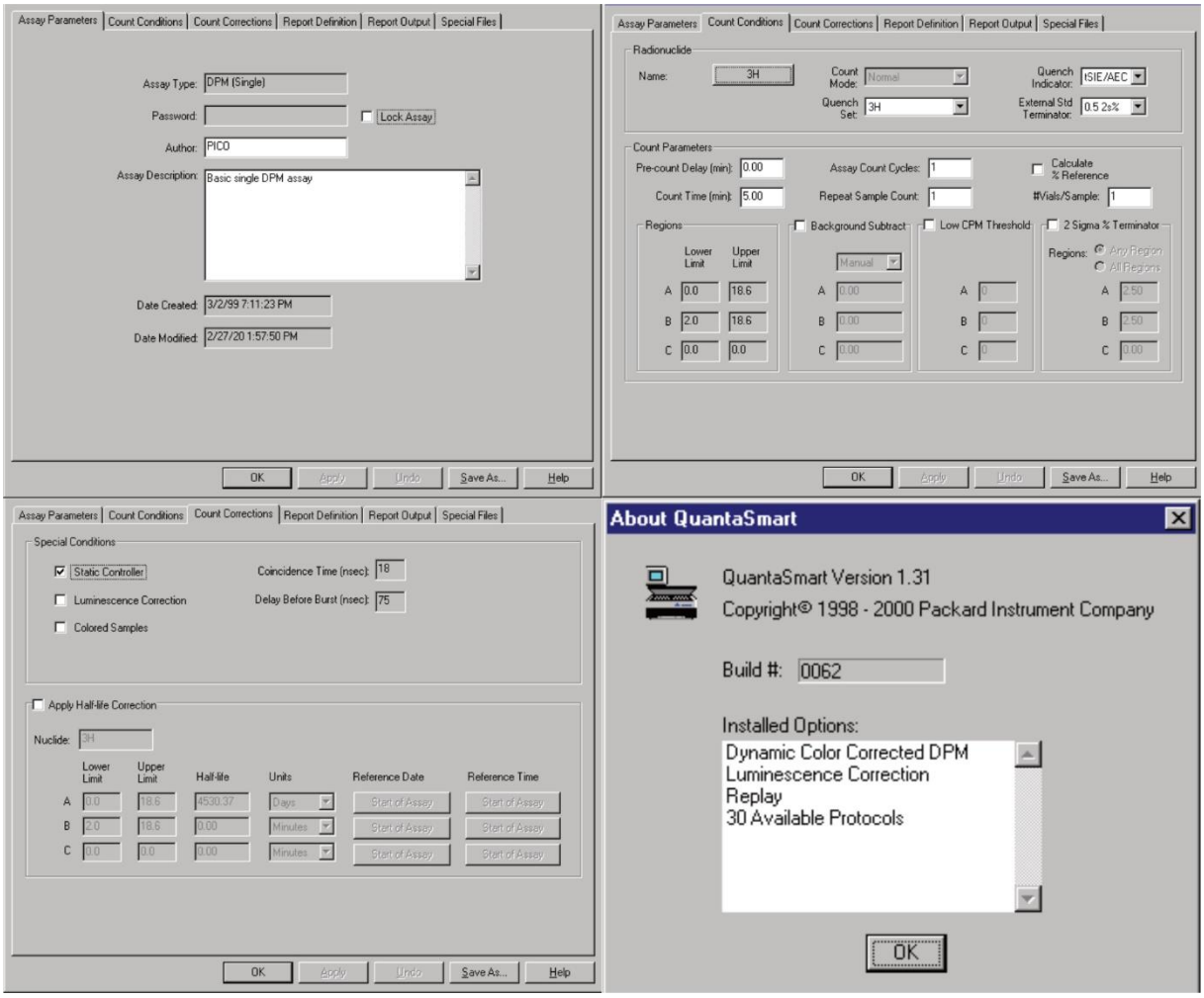

Supplemental Figure 1: Software settings for liquid scintillation counting using a light scintillation counter.

Screenshots showing the software version, as well as settings used for scintillation counting of [^{3}H] samples performed with this protocol are depicted.

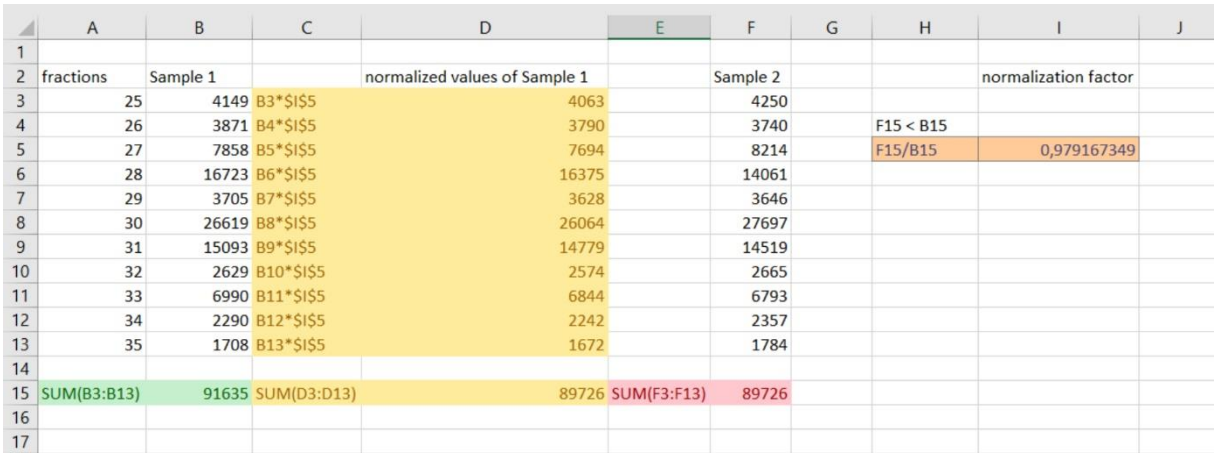

	A	B	C	D	E	F	G	H	I	J
1										
2	fractions	Sample 1		normalized values of Sample 1		Sample 2			normalization factor	
3	25	4149	B3*I5	4063		4250				
4	26	3871	B4*I5	3790		3740		F15 < B15		
5	27	7858	B5*I5	7694		8214		F15/B15	0,979167349	
6	28	16723	B6*I5	16375		14061				
7	29	3705	B7*I5	3628		3646				
8	30	26619	B8*I5	26064		27697				
9	31	15093	B9*I5	14779		14519				
10	32	2629	B10*I5	2574		2665				
11	33	6990	B11*I5	6844		6793				
12	34	2290	B12*I5	2242		2357				
13	35	1708	B13*I5	1672		1784				
14										
15	SUM(B3:B13)	91635	SUM(D3:D13)	89726	SUM(F3:F13)	89726				
16										
17										

Supplemental Figure 2: Representative example of data normalization.
A screenshot of a worksheet shows all steps and formulas used to normalize SAX-HPLC runs to each other. For simplification, only fractions 25–35 of samples are shown.

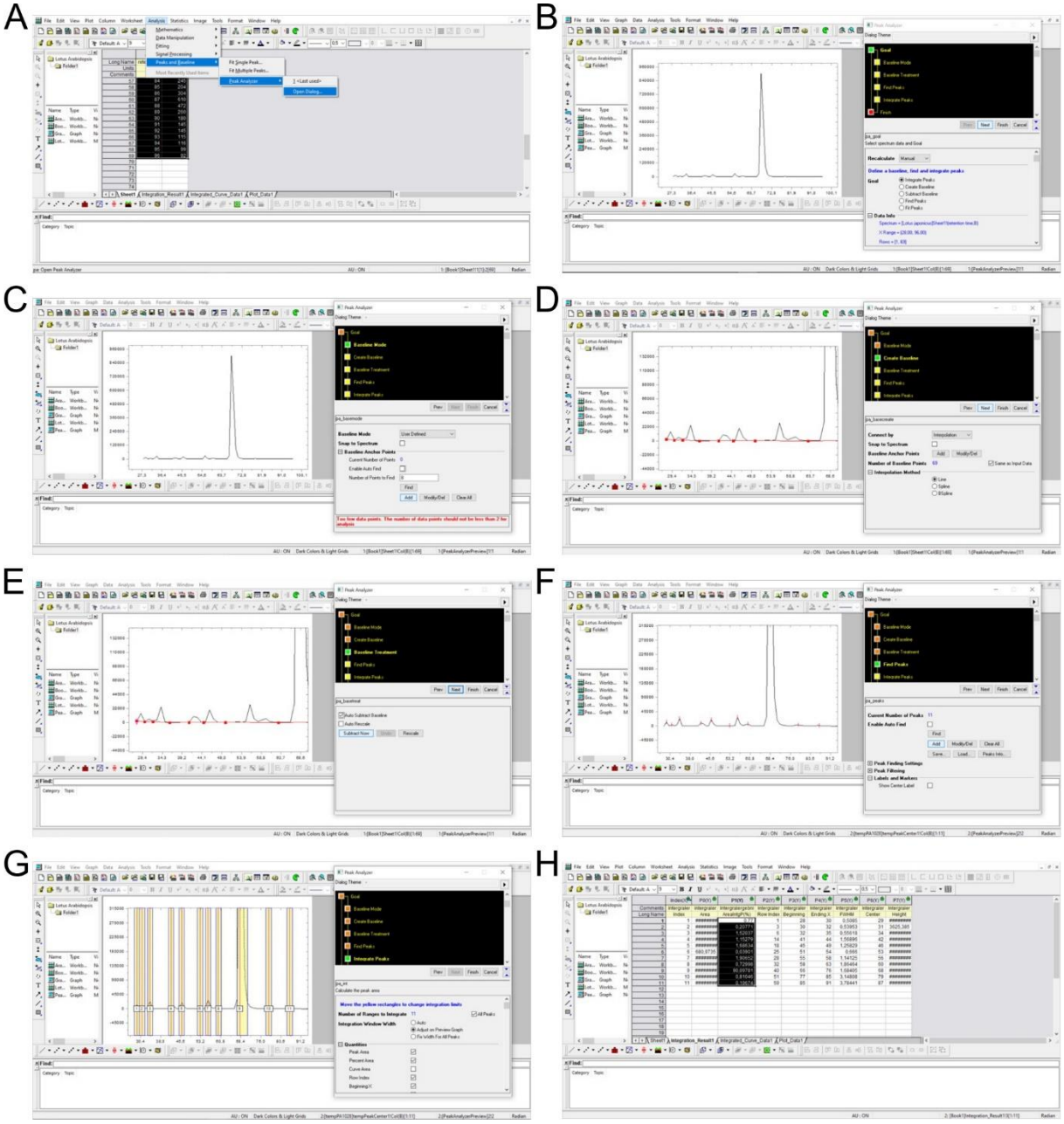

Supplemental Figure 3: Peak determination, background subtraction and integration using analysis software.

(A) Data from SAX-HPLC analysis is loaded into the software (minutes 28–96) and the peak analyzer tool is selected. (B–E) The baseline is defined manually by setting points between individual peaks and the background is subtracted. (F) Peaks are determined manually based on appearance and published chromatographic mobilities5,7. (G) Peak ranges are defined manually by cpm values. (H) Peaks are integrated and calculated as % of all peaks.

Arabidopsis PFA-DSP-Type Phosphohydrolases Target Specific Inositol Pyrophosphate Messengers

Gaugler, P., Schneider, R., Liu, G., Qiu, D., Weber, J., Schmid, J., Jork, N., Häner, M., Ritter, K., Fernández-Rebollo, N., Giehl, R.F.H., Trung, M.N., Yadav, R., Fiedler, D., Gaugler, V., Jessen, H.J., Schaaf, G., Laha, D.

Biochemistry. **2022 Jun 21;61(12):1213-1227 https://doi.org/10.1021/acs.biochem.2c00145**

Highlights:

- *Arabidopsis* PFA-DSPs are evolutionary conserved PP-InsP phosphohydrolases with high specificity for the 5-β-phosphate
- They can fully complement Siw14 in regards of $InsP_7$ homeostasis and wortmannin tolerance
- Wortmannin sensitivity of *siw14*Δ yeast is linked to Kcs1-derived PP-InsPs
- The *Arabidopsis* homologs appear to be redundant
- Ectopic expression of *PFA-DSP1* in *Arabidopsis* and heterologous expression in *N. benthamiana* causes a specific decrease of $InsP_7$, respectively 5-$InsP_7$

Graphical abstract:

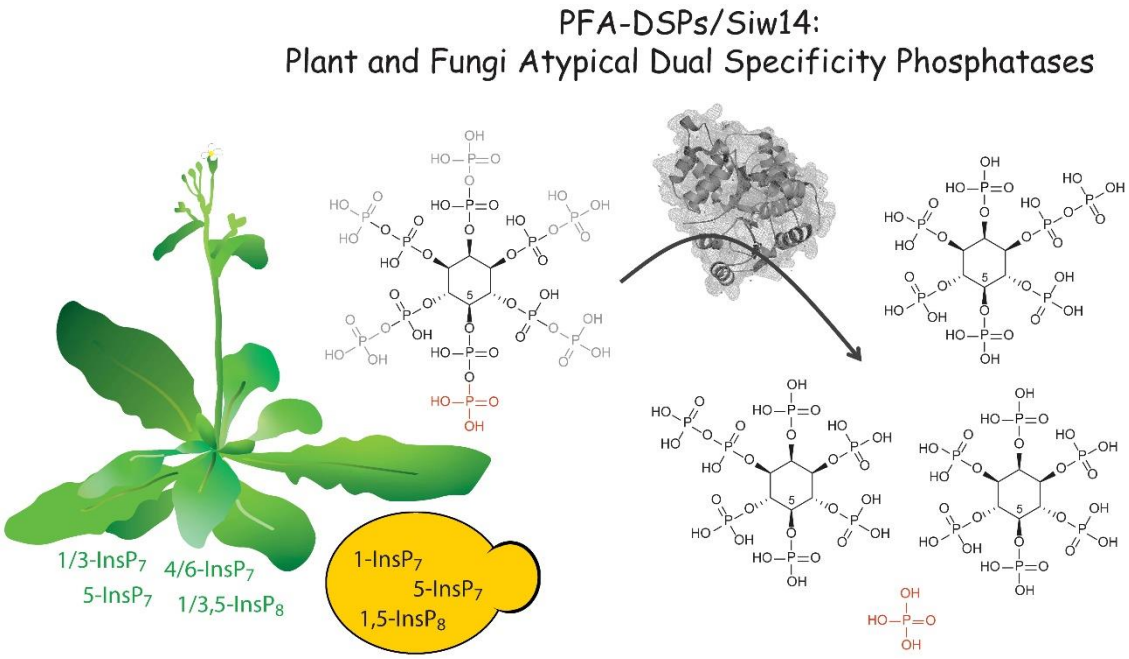

Biochemistry

pubs.acs.org/biochemistry Article

Arabidopsis PFA-DSP-Type Phosphohydrolases Target Specific Inositol Pyrophosphate Messengers

Philipp Gaugler,◆ Robin Schneider,◆ Guizhen Liu, Danye Qiu, Jonathan Weber, Jochen Schmid, Nikolaus Jork, Markus Häner, Kevin Ritter, Nicolás Fernández-Rebollo, Ricardo F. H. Giehl, Minh Nguyen Trung, Ranjana Yadav, Dorothea Fiedler, Verena Gaugler, Henning J. Jessen, Gabriel Schaaf,* and Debabrata Laha*

Cite This: *Biochemistry* 2022, 61, 1213−1227 Read Online

ACCESS | Metrics & More | Article Recommendations | Supporting Information

ABSTRACT: Inositol pyrophosphates are signaling molecules containing at least one phosphoanhydride bond that regulate a wide range of cellular processes in eukaryotes. With a cyclic array of phosphate esters and diphosphate groups around *myo*-inositol, these molecular messengers possess the highest charge density found in nature. Recent work deciphering inositol pyrophosphate biosynthesis in *Arabidopsis* revealed important functions of these messengers in nutrient sensing, hormone signaling, and plant immunity. However, despite the rapid hydrolysis of these molecules in plant extracts, very little is known about the molecular identity of the phosphohydrolases that convert these messengers back to their inositol polyphosphate precursors. Here, we investigate whether *Arabidopsis* Plant and Fungi Atypical Dual Specificity Phosphatases (PFA-DSP1-5) catalyze inositol pyrophosphate phosphohydrolase activity. We find that recombinant proteins of all five *Arabidopsis* PFA-DSP homologues display phosphohydrolase activity with a high specificity for the 5-β-phosphate of inositol pyrophosphates and only minor activity against the β-phosphates of 4-InsP$_7$ and 6-InsP$_7$. We further show that heterologous expression of *Arabidopsis* PFA-DSP1-5 rescues wortmannin sensitivity and deranged inositol pyrophosphate homeostasis caused by the deficiency of the PFA-DSP-type inositol pyrophosphate phosphohydrolase Siw14 in yeast. Heterologous expression in *Nicotiana benthamiana* leaves provided evidence that *Arabidopsis* PFA-DSP1 also displays 5-β-phosphate-specific inositol pyrophosphate phosphohydrolase activity *in planta*. Our findings lay the biochemical basis and provide the genetic tools to uncover the roles of inositol pyrophosphates in plant physiology and plant development.

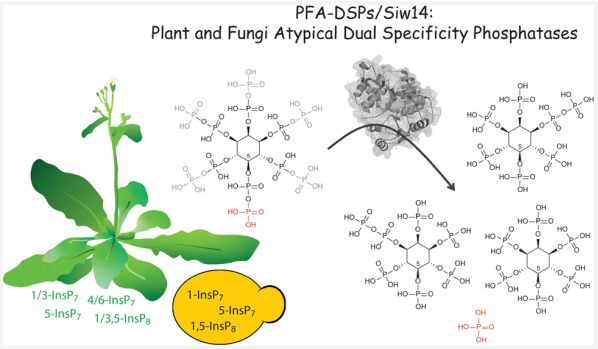

INTRODUCTION

Inositol pyrophosphates (PP-InsPs), such as InsP$_7$ and InsP$_8$, are molecules derived from *myo*-inositol (Ins) esterified with unique patterns of monophosphates (P) and diphosphates (PP) and have been described as versatile messengers in yeast, amoeba, and animal cells.[1−4] With recent discoveries that PP-InsPs regulate nutrient sensing and immunity in plants, these molecules are a novel focus of research in plant physiology.[5−13] The synthesis of PP-InsPs is partially conserved in eukaryotes, with some important distinctions in plants. In baker's yeast and mammals, 5-InsP$_7$ is synthesized by Kcs1/IP6K-type proteins, whereas Vip1/PPIP5K-type kinases phosphorylate the C1 position of both InsP$_6$ (also termed phytic acid) and 5-InsP$_7$, generating 1-InsP$_7$ and 1,5-InsP$_8$, respectively.[14−17] In plants, detection, quantification, and characterization of PP-InsPs have been challenging due to the low abundance of these molecules and their susceptibility to hydrolytic activities during extraction.[18,19] Employing [^{3}H] *myo*-inositol labeling and subsequent analysis of plant extracts by strong-anion exchange high-performance liquid chromatography (SAX-HPLC) allowed the detection of PP-InsPs in different plant species.[5,20−22] The recent development of capillary electrophoresis (CE) coupled to electrospray ionization mass spectrometry (ESI-MS), has enabled the detection and quantification of many InsP and PP-InsP isomers in various cell extracts including all InsP$_7$ isomers, except enantiomers (labeled, e.g., as 1/3 or 4/6-InsP$_7$).[23] Similar to yeast and mammals, the *Arabidopsis* PPIP5K isoforms VIH1 and VIH2 catalyze the synthesis of InsP$_8$[5,10] and are likely involved in the synthesis of 1/3-InsP$_7$.[11] However, Kcs1/IP6K-type proteins are absent in

Received: March 14, 2022
Revised: May 2, 2022
Published: May 31, 2022

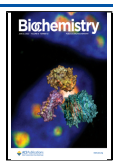

land plants. The question of how plants synthesize 5-InsP$_7$ has been partially solved by work on *Arabidopsis* inositol (1,3,4) triphosphate 5/6 kinases ITPK1 and ITPK2. Notably, ITPK1 and ITPK2 were reported to catalyze the synthesis of 5-InsP$_7$ from InsP$_6$ *in vitro*[24−26] and consequently *itpk*1 mutant plants display reduced 5-InsP$_7$ levels.[11,13]

In *Arabidopsis*, disturbances in the synthesis of InsP$_7$ and/or InsP$_8$ result in defective signaling of the plant hormones jasmonate[5,6] and auxin,[13] as well as defects in salicylic acid-dependent plant immunity[12] and impaired phosphate (P$_i$) homeostasis.[9−11,27] In the case of auxin and jasmonate perception, 5-InsP$_7$ and InsP$_8$, respectively, are proposed to function as co-ligands of the respective receptor complexes.[5,6,13] The role of PP-InsPs in P$_i$ signaling is related to their ability to bind to SPX proteins, which act as receptors for these messenger molecules.[7,9,10,28−30] InsP$_8$ has been found as the preferred ligand for stand-alone SPX proteins *in vivo*.[9,10,28] InsP$_8$-bound SPX receptors inactivate the MYB-type transcription factors PHR1 and PHL1, which control the expression of a majority of P$_i$ starvation-induced (PSI) genes to regulate various metabolic and developmental adaptations induced by P$_i$ deficiency.[28,31−33] The tissue levels of various PP-InsPs, including 5-InsP$_7$ and InsP$_8$, respond sensitively to the plant's P$_i$ status,[9,11] suggesting that their synthesis and degradation are tightly regulated. While the steps involved in the synthesis of PP-InsPs in plants are now better understood, still little is known about how these molecules are degraded.

Vip1/PPIP5Ks are bifunctional enzymes that harbor an N-terminal ATP-grasp kinase domain and a C-terminal phosphatase domain conserved in yeast, animals, and plants.[5,10,15,17,34] *In vitro*, the phosphatase domain of *Arabidopsis* PPIP5K VIH2 hydrolyzes PP-InsPs to InsP$_6$,[10] similar to the respective C-terminal domains of fission yeast and mammalian PPIP5Ks.[35,36] Although *Arabidopsis* ITPK1 harbors no phosphatase domain, under conditions of low adenylate charge, it can shift its activity *in vitro* from kinase to ADP phosphotransferase activity using 5-InsP$_7$ but no other InsP$_7$ isomer.[11,26] Apart from relying on the reversible activities of ITPK1 and Vip1/PPIP5Ks, the degradation of PP-InsPs may also be controlled by specialized phosphohydrolases.

In mammalian cells, diphosphoinositol polyphosphate phosphohydrolases (DIPPs), members of the nudix hydrolase family, have been shown to catalyze the hydrolysis of the diphosphate groups of InsP$_7$ and InsP$_8$ at the C1 and C5 position.[4,37,38] The baker's yeast genome encodes a single homologue of mammalian DIPP1, named diadenosine and diphosphoinositol polyphosphate phosphohydrolase (DDP1), which hydrolyzes various substrates including diadenosine polyphosphates, 5-InsP$_7$ and InsP$_8$, but has a preference for inorganic polyphosphates (poly-P) and for the β-phosphate of 1-InsP$_7$.[39−41] In addition, baker's yeast has an unrelated PP-InsP phosphohydrolase, Siw14 (also named Oca3) with a high specificity for the β-phosphate at position C5 of 5-InsP$_7$.[42,43] This enzyme is a member of the Plant and Fungi Atypical Dual Specificity Phosphatases (PFA-DSPs) that belong to a large family of protein tyrosine phosphatases (PTPs).[43−45]

Blast search analyses revealed that the *Arabidopsis thaliana* genome encodes five PFA-DSPs, with AtPFA-DSP1 sharing 61% identity and 76% similarity with yeast Siw14.[44,45] X-ray crystallography revealed that the protein adopts an α/β-fold typical for cysteine phosphatases, with the predicted catalytic cysteine (Cys150) residing at the bottom of a positively charged pocket.[44,46] Of a number of putative phosphatase substrates tested, recombinant AtPFA-DSP1 displayed the highest activity against inorganic polyphosphate, as well as against deoxyribo- and ribonucleoside triphosphates, and less activity against phosphotyrosine-containing peptides and phosphoinositides.[46] Here, we investigated whether *Arabidopsis* PFA-DSPs might function as PP-InsP phosphohydrolases.

METHODS

Plant Materials and Growth Conditions. Seeds of *A. thaliana* T-DNA insertion lines *pfa-dsp*1-3 (WiscDsLox_473_B10, Col-0), *pfa-dsp*1-4 (CSHL_GT1415, Ler-0), *pfa-dsp*1-6 (SAIL_116_C12, Col-0) and *mrp*5 (GK-068B10) were obtained from The European Arabidopsis Stock Centre (http://arabidopsis.info/). To identify homozygous lines, F2 and F3 plants were genotyped by PCR using the primers indicated in Table S2.

For sterile cultures, *Arabidopsis* seeds were surface sterilized in 1.2% (v/v) $NaHClO_4$ and 0.05% (v/v) Triton X-100 for 3 min, in 70% (v/v) ethanol and 0.05% (v/v) Triton X-100 for 3 min and in 100% (v/v) ethanol before transferring onto sterile filter paper. Sterilized seeds were sown onto half-strength Murashige and Skoog (MS) medium[59] containing 1% sucrose, pH 5.7 and solidified with 0.7% (w/v) Phytagel (Sigma-Aldrich). After 2 days of stratification at 4 °C, the plates were transferred to a growth incubator and the seedlings were grown under short-day conditions with the following regime: 8/16 h light/dark; light intensity 120 μmol m^{-2} s^{-1}; temperature 22 °C/20 °C.

Constructs. The following full-length ORFs were amplified by PCR from an *Arabidopsis* whole seedling cDNA preparation: *PFA-DSP*1 (At1g05000), *PFA-DSP*2 (At2g32960), *PFA-DSP*3 (At3g02800) *PFA-DSP*4 (At4g03960), and *PFA-DSP*5 (At5g16480). Likewise, the *SIW*14 ORF sequence was amplified from yeast genomic DNA. Primers used for amplification are listed in Table S2. The reverse primers contained a *V*5 sequence (underlined) allowing a translational fusion of the resulting gene products with a C-terminal V5 epitope tag. Amplification products were cloned into pDONR221 (Invitrogen) via BP clonase II (Invitrogen) reaction following the manufacturer's instructions. The ORFs were then swapped into the episomal yeast expression vector pDRf1-GW[60] by the LR clonase II (Invitrogen) reaction following the manufacturer's instructions. For expression of *SIW*14 under control of the endogenous promoter from a *CEN*-based plasmid, the *SIW*14 gDNA was amplified from purified yeast gDNA using the primers listed in Table S2. The *SIW*14 gDNA was inserted into YCplac33 (ATCC #87586) using the restriction enzymes *Pst*I and *Eco*RI.

For protein expression, *PFA-DSP*1−5 were amplified as described before but with a reverse primer containing a stop codon. Amplified products were cloned into pDONR221 (Invitrogen), then swapped by LR clonase II (Invitrogen) into the bacterial expression vector pDEST566 (Addgene plasmid # 11517), which contains a sequence encoding an N-terminal His$_6$-maltose-binding protein (MBP) epitope tag. Free His-tagged MBP protein was expressed from a modified pET28 vector carrying an N-terminal sequence encoding a His$_8$-maltose-binding protein (MBP) epitope tag.[5]

For transient expression in *Nicotiana benthamiana*, the ORF of *PFA-DSP*1 (wild-type sequence and with a mutated sequence encoding the C150S substitution) was swapped by LR clonase II (Invitrogen) from pDONR221 into the plant

https://doi.org/10.1021/acs.biochem.2c00145
Biochemistry 2022, 61, 1213−1227

expression vector pGWB641,[61] which harbors a viral CaMV 35S promoter to allow gene expression and a sequence encoding a C-terminal EYFP tag. Site-directed mutagenesis was performed on the respective plasmids with the primers listed in Table S2.

***N. benthamiana* Infiltration.** A single colony of transformed *Agrobacteria* was inoculated in 2 mL of LB media containing the appropriate antibiotics and cultivated overnight at 26 °C in a spinning wheel. On the next morning, 1 mL of overnight culture was added to 5 mL of fresh LB with antibiotics and grown for another 4 h at 26 °C. Afterward, the cultures were harvested by centrifugation at 4 °C with 3000*g* for 20 min. The pellet was then resuspended in 3 mL of infiltration solution containing 10 mM $MgCl_2$, 10 mM MES-KOH (pH 5.6), and 150 μM acetosyringone. OD_{600} was determined using a 1:10 dilution and adjusted to 0.8 in infiltration solution. Then, the working solution was prepared by pooling equal amounts of cultures (e.g., *P*19 + *PFA-DSP*1), which were then co-infiltrated in the abaxial surface of the leaf using a 1 mL syringe without a needle. Afterward, the plants were placed in a dark incubator at 26 °C for ∼1 day before keeping them for another 4 days on the workbench. The leaves were then harvested and frozen in liquid nitrogen before continuing with the extraction of inositol phosphates.

Yeast Strains. Different strains of the budding yeast *Saccharomyces cerevisiae* were used. The BY4741 wild-type (MATa *his*3Δ *leu*2Δ *met*15Δ *ura*3Δ), *siw*14Δ (*YNL032w::kanMX4*), *vip*1Δ (*YLR410w::kanMX4*),[5] *kcs*1Δ (*YDR017c::kanMX4*), and *ipk*2Δ (*YDR173c::kanMX4*) were obtained from Euroscarf. *vip*1Δ *siw*14Δ, *kcs*1Δ *siw*14Δ, *ipk*2Δ *siw*14Δ were generated using *loxP*/Cre gene disruption and the *ble* resistance marker, which confers phleomycine/Zeocin (Invitrogen) resistance[62] using the primers listed in Table S2. In addition, the following mutants in the DDY1810 background (MATa; *leu*2Δ *ura*3-52 *trp*1Δ; *prb*1-1122 *pep*4-3 *pre*1-451)[63] were used: *kcs*1Δ and *kcs*1Δ *ddp*1Δ. *kcs*1Δ *siw*14Δ, *kcs*1Δ *ddp*1Δ *siw*14Δ, and *siw*14Δ were generated in this background as described before. For all assays, the yeast cells were transformed by the Li-acetate method[64] and cultured in either 2 × YPD + CSM medium or selective synthetic deficiency (SD) medium.

Yeast Growth Complementation Assay. Yeast transformants were inoculated in selective synthetic deficiency (SD) medium and grown overnight at 28 °C while shaking (200 rpm). Then, OD_{600} was measured, adjusted to 1.0, and an 8-fold dilution series was prepared in a 96-well plate. Subsequently, 10 μL of each dilution were spotted on selective solid media as described earlier[65] and incubated at 26 °C for 2−4 days. To prepare selective solid media supplemented with wortmannin, autoclaved media was cooled down to 60 °C, wortmannin was added from a 10 mM stock in DMSO (Sigma-Aldrich) to a final concentration of 1−3 μM. Since the activity of wortmannin changed by age and by the number of freezing/thawing cycles, aliquots were kept at −20 °C and were not thawed more than five times. In addition, several concentrations were employed for the spotting assays to be able to identify the activity at which growth differences between *siw*14Δ, *kcs*1Δ, and their isogenic wild-type transformants became most obvious. Pictures were taken with a Bio-Rad ChemiDoc MP imager using white backlight.

Protein Preparation. His_6-MBP-PFA-DSP protein fusions or free His_8-MBP were expressed in *Escherichia coli* BL21 CodonPlus (DE3)-RIL cells (Stratagene). Overnight bacterial cultures were inoculated 1:1000 into fresh 2YT medium (1.6% tryptone, 1% yeast extract, 0.5% NaCl) with 100 mg/L ampicillin (pDEST566) or 50 mg/L kanamycin (pET28) and 25 mg/L chloramphenicol. Cells were grown at 37 °C while shaking (200 rpm) for 4 h (∼0.6 OD_{600}), and protein expression was induced at 16 °C overnight with 0.1 mM isopropyl-D-1-thiogalactopyranoside. The cells were lysed as described[66] using the following lysis buffer: 50 mM Tris-Cl, pH 7.5, 100 mM NaCl, 25 mM imidazole, 10% (v/v) glycerol, 0.1% (v/v) Tween 20, 5 mM β-mercaptoethanol, and EDTA-free complete ULTRA protease inhibitor cocktail (Roche). Proteins were batch-purified using Ni-NTA agarose resin (Macherey-Nagel) and eluted using the above-mentioned lysis buffer with increased imidazole concentration (250 mM). Three elutions were combined and dialyzed using Slide-A-Lyzer Dialysis Cassettes (Thermo Scientific) following the manufacturer's instructions and a buffer containing 50 mM Tris-Cl, pH 7.5 and 100 mM NaCl. The concentrated protein preparations were then stored at −20 °C. Purified proteins were analyzed using SDS-PAGE followed by Coomassie blue staining. Proteins were compared with PageRuler plus prestained protein ladder (Thermo Fisher) and with designated amounts of a BSA standard to estimate target protein concentrations.

***In Vitro* PP-InsP Phosphohydrolase Assay.** The phosphohydrolase assay was carried out in a 15 μL reaction mixture containing 0.35−2 μM recombinant PFA-DSP or Siw14 protein, 50 mM HEPES (pH 7.0), 10 mM NaCl, 5% (v/v) glycerol, 0.1% (v/v) β-mercaptoethanol, and 0.33 mM of various $InsP_7$ and $InsP_8$ isomers as indicated, and was incubated for 1, 2, or 24 h at 22 °C. The PP-InsP isomers were synthesized as described previously.[67,68] Reactions were separated by 33% PAGE and visualized by toluidine blue or DAPI staining.

Titanium Dioxide Bead Extraction and PAGE/CE-ESI-MS. Purification of inositol polyphosphates using TiO_2 beads and analysis via PAGE was performed as described previously.[11] CE-ESI-MS analyses of *in vitro*, yeast and plant samples were performed as described previously.[11,23]

Inositol Polyphosphate Extraction from Yeast Cells and Seedlings and HPLC Analyses. For inositol polyphosphate analyses from yeast, transformants were inoculated into a selective synthetic deficiency (SD) medium and grown overnight at 28 °C while shaking (200 rpm). They were then diluted 1:200 in 2 mL of fresh medium supplemented with 6 μCi mL^{-1} [^{3}H]-*myo*-inositol (30−80 Ci $mmol^{-1}$; Biotrend; ART-0261-5) and grown overnight at 28 °C in a spinning wheel. After centrifugation and washing of the cell pellet, inositol polyphosphates were extracted and analyzed as described before.[5,69,70]

Extraction of [^{3}H]-*myo*-inositol polyphosphates from *Arabidopsis* seedlings and subsequent SAX-HPLC analyses were performed as described previously.[70]

RNA Isolation and Quantitative Real-Time PCR. Fifteen-day-old seedlings were transferred from solid half-strength MS plates to liquid half-strength MS media (supplemented with 1% sucrose) for 5 days before harvest and immediately frozen in liquid N_2. Total RNA was extracted with NucleoSpin RNA Plant and Fungi kit (Macherey-Nagel). cDNA was synthesized using RevertAid RT reverse transcription kit (Thermo Fisher). Quantitative PCR reactions were conducted with the CFX384 real-time system (Bio-Rad) and the SsoAdvanced Universal SYBR Green Supermix (Bio-

https://doi.org/10.1021/acs.biochem.2c00145
Biochemistry 2022, 61, 1213−1227

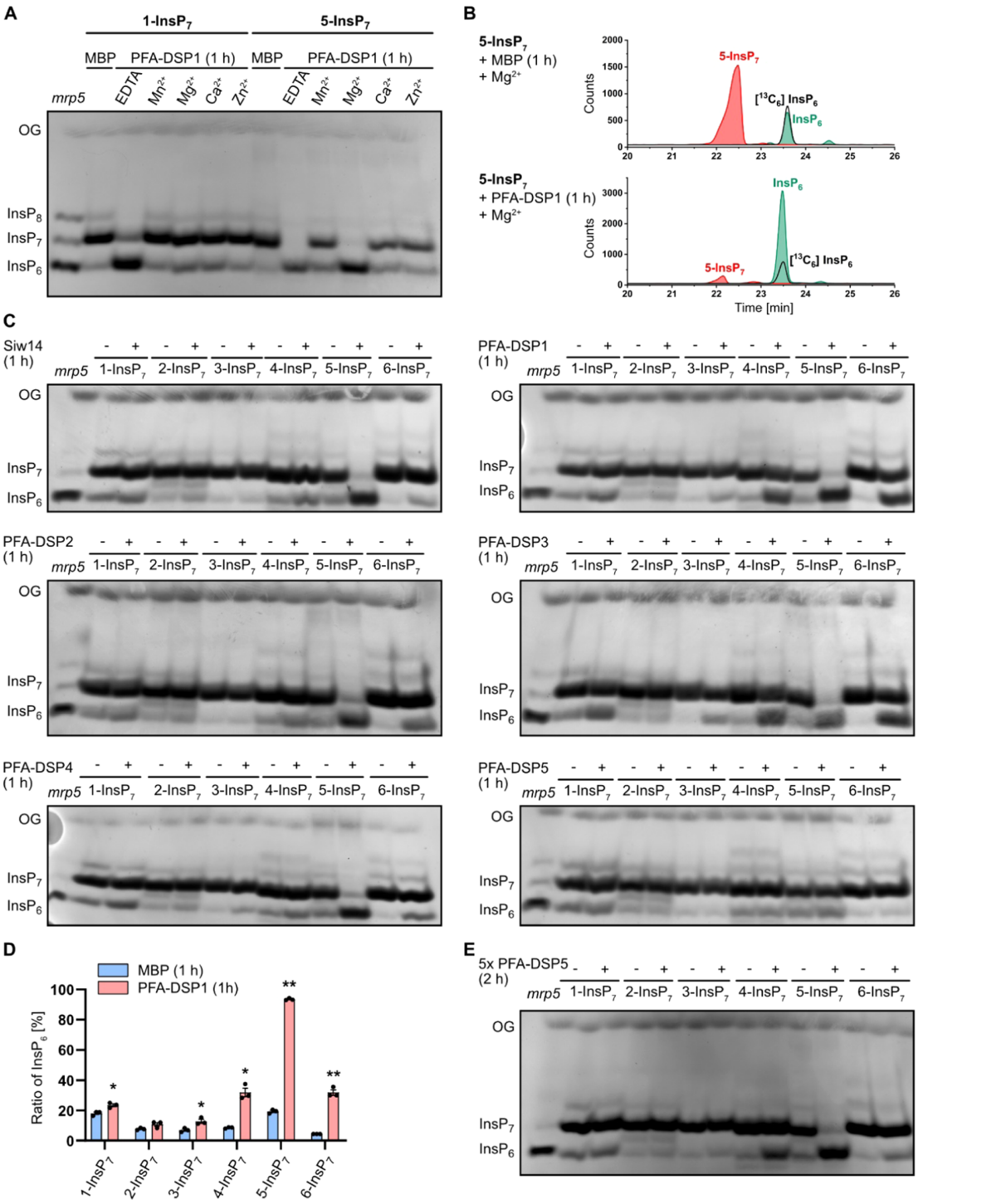

Figure 1. *In vitro*, *Arabidopsis* PFA-DSPs display Mg^{2+}-dependent PP-InsP phosphohydrolase activity with high specificity for 5-$InsP_7$. Recombinant His-MBP-PFA-DSPs and His-MBP-Siw14 (indicated with the plus symbol in (C) and (E)) were incubated with 0.33 mM $InsP_7$ at 22 °C. His-MBP served as a negative control (as indicated with the minus symbol in (C) and (E)). (A) 0.4 μM His-MBP-PFA-DSP1 was incubated for 1 h with 1-$InsP_7$ or 5-$InsP_7$, and 1 mM EDTA, $MnCl_2$, $MgCl_2$, $CaCl_2$, or $ZnCl_2$ as indicated. The reaction products were then separated by 33% PAGE and visualized by toluidine blue. (B–D) The $InsP_7$ phosphohydrolase activity of ~0.4 μM His-MBP-PFA-DSPs and His-MBP-Siw14 was analyzed in the presence of 1 mM $MgCl_2$. After 1 h, the reaction products were then (B, D) spiked with isotopic standards mixture ([$^{13}C_6$] 1,5-$InsP_8$, [$^{13}C_6$] 5-$InsP_7$, [$^{13}C_6$] 1-$InsP_7$, [$^{13}C_6$] $InsP_6$, [$^{13}C_6$] 2-OH $InsP_5$) and subjected to CE-ESI-MS analyses or (C) separated by 33% PAGE and visualized by toluidine blue/DAPI staining. (D) Data represent mean ± SEM (n = 3). Representative extracted-ion electropherograms are shown in Figure S2. Asterisks indicate values that are significantly different from the MBP control reactions (according to Student's t test, $P < 0.05$ (*); $P < 0.01$ (**)). (E) Recombinant His-MBP-PFA-DSP5 (2 μM) was incubated with 0.33 mM $InsP_7$ isomers for 2 h. The reaction product was separated by 33% PAGE and visualized with toluidine blue. (A, C, E) Identity of bands was determined by migration compared to TiO_2-purified *mrp5* seed extract.

https://doi.org/10.1021/acs.biochem.2c00145
Biochemistry 2022, 61, 1213–1227

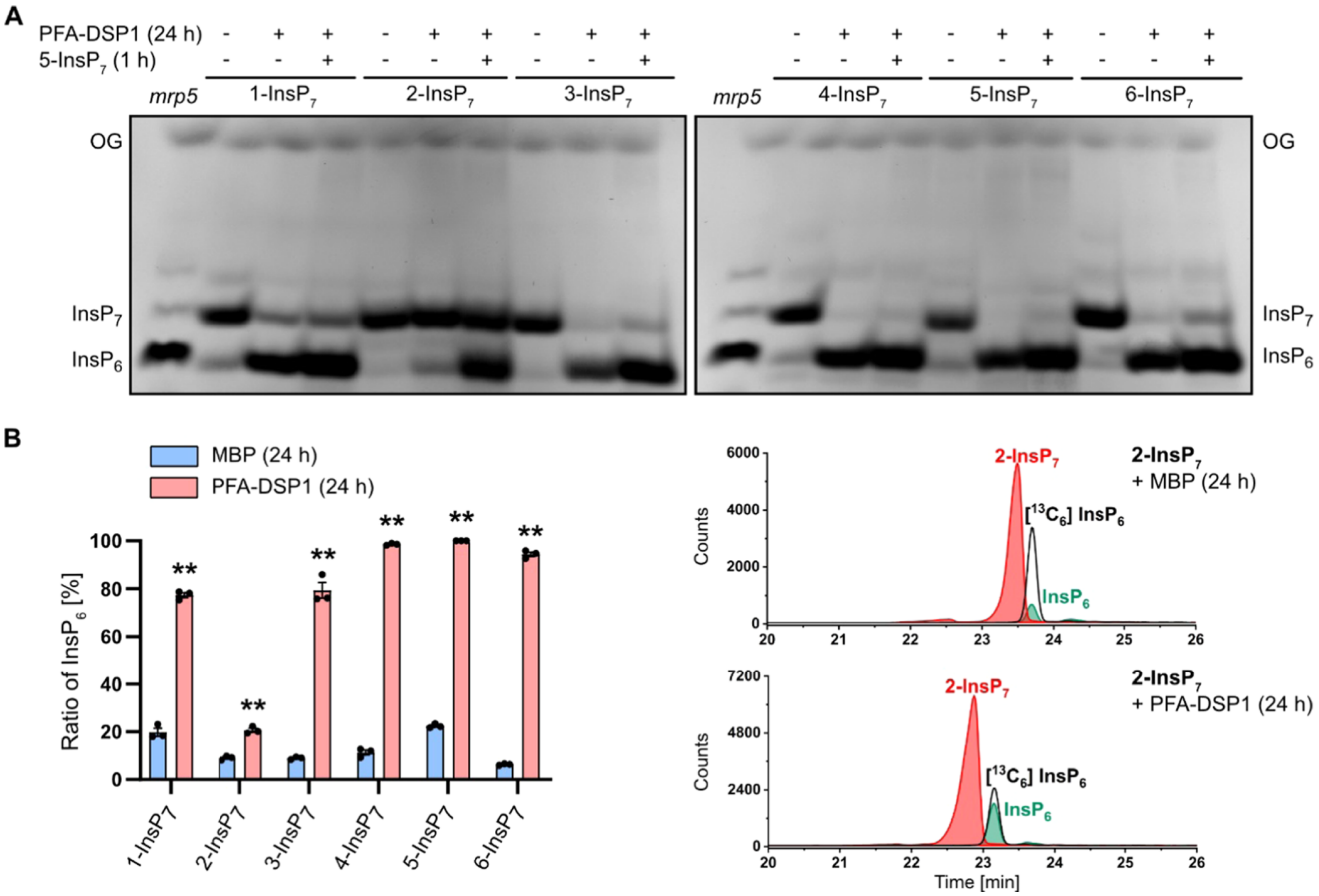

Figure 2. Under prolonged incubation time *Arabidopsis* PFA-DSP1 hydrolyzes various $InsP_7$ isomers *in vitro*, except for 2-$InsP_7$. Recombinant His-MBP-PFA-DSP1 (0.4 μM) (indicated with the plus symbol in the first line of (A)) was incubated with 0.33 mM $InsP_7$ and 1 mM $MgCl_2$ for 24 h at 22 °C. To ensure that PFA-DSP1 is active during the whole incubation time, after 23 h, 0.33 mM 5-$InsP_7$ was added to a replicate and incubated for another 1 h (indicated with the plus symbol in the second line of (A)). His-MBP served as a negative control (as indicated with the minus symbol in (A)). (A) An aliquot of the reaction product was separated by 33% PAGE and visualized with toluidine blue. The identity of bands was determined by migration compared to TiO_2-purified *mrp5* seed extract. (B) Another reaction was spiked with an isotopic standards mixture ([$^{13}C_6$] 1,5-$InsP_8$, [$^{13}C_6$] 5-$InsP_7$, [$^{13}C_6$] 1-$InsP_7$, [$^{13}C_6$] $InsP_6$, [$^{13}C_6$] 2-OH $InsP_5$) and subjected to CE-ESI-MS analyses. Data represent mean ± SEM (n = 3). Asterisks indicate values that are significantly different from the MBP control reactions (according to Student's t test, $P < 0.05$ (*); $P < 0.01$ (**)). Representative extracted-ion electropherograms are shown in Figure S5.

Rad) using the primers listed in Table S2. *TIP41-like* and *PP2AA3* were used as reference genes to normalize relative expression levels of all tested genes. Relative expression was calculated using the CFX Maestro software (Bio-Rad).

Yeast Protein Extraction and Immunodetection. Multiple transformants were inoculated into 4 mL of YPD (with 3% glucose) or selective SD-media and grown for up to 24 h at 28 °C. On the following day, the yeast was reinoculated into 4 mL of fresh media and grown for another day. Afterward, the cells were harvested and resuspended in 500 μL of extraction buffer (300 mM sorbitol, 150 mM NaCl, 50 mM Na_2HPO_4, 1 mM EDTA, pH 7.5), supplemented with 100 mM β-mercaptoethanol and a 1:50 dilution of protease inhibitor cocktail for fungal extracts (Sigma-Aldrich). The cells were lysed with bead beating using 150−200 μL of glass beads (ø 0.5 mm). The lysate was spun down and the supernatant boiled for 10 min after the addition of sample buffer. The protein extracts were then resolved by SDS-PAGE. Target proteins were detected by immunoblot. As the primary antibody, a mouse anti-V5 (Invitrogen, R960-25, 1:2000 dilution) antibody was used, followed by either an Alexa fluor plus 800 goat anti-mouse antibody (Invitrogen, 1:20 000 dilution) or a goat anti-mouse HRP antibody (Bio-Rad, 1:10 000 dilution). As a loading control, Gal4 was detected using a rabbit polyclonal anti-Gal4 antibody (Santa Cruz, 1:1000 dilution), followed by a goat anti-rabbit StarBright Blue 700 antibody (Bio-Rad, 1:2500 dilution). The signal was detected using the multi-plex function of the ChemiDoc MP imager (Bio-Rad). Alternatively, for blots where a secondary antibody coupled to HRP was used, the chemiluminescence signal of the ECL reagent was detected, followed by Ponceau staining as loading control.

RESULTS AND DISCUSSION

***Arabidopsis* PFA-DSP Proteins Display *In Vitro* PP-InsP Phosphohydrolase Activity with High Specificity for 5-$InsP_7$.** To explore the potential role of *Arabidopsis* PFA-DSP proteins in PP-InsP hydrolysis, we first generated translational fusions of PFA-DSPs with an N-terminal hexahistidine tag followed by a maltose-binding protein (MBP) and expressed recombinant proteins in bacteria. Corresponding His-MBP-Siw14 and free His-MBP constructs were generated as controls. All constructs allowed the purification of soluble recombinant proteins (Figure S1). We

https://doi.org/10.1021/acs.biochem.2c00145
Biochemistry 2022, 61, 1213−1227

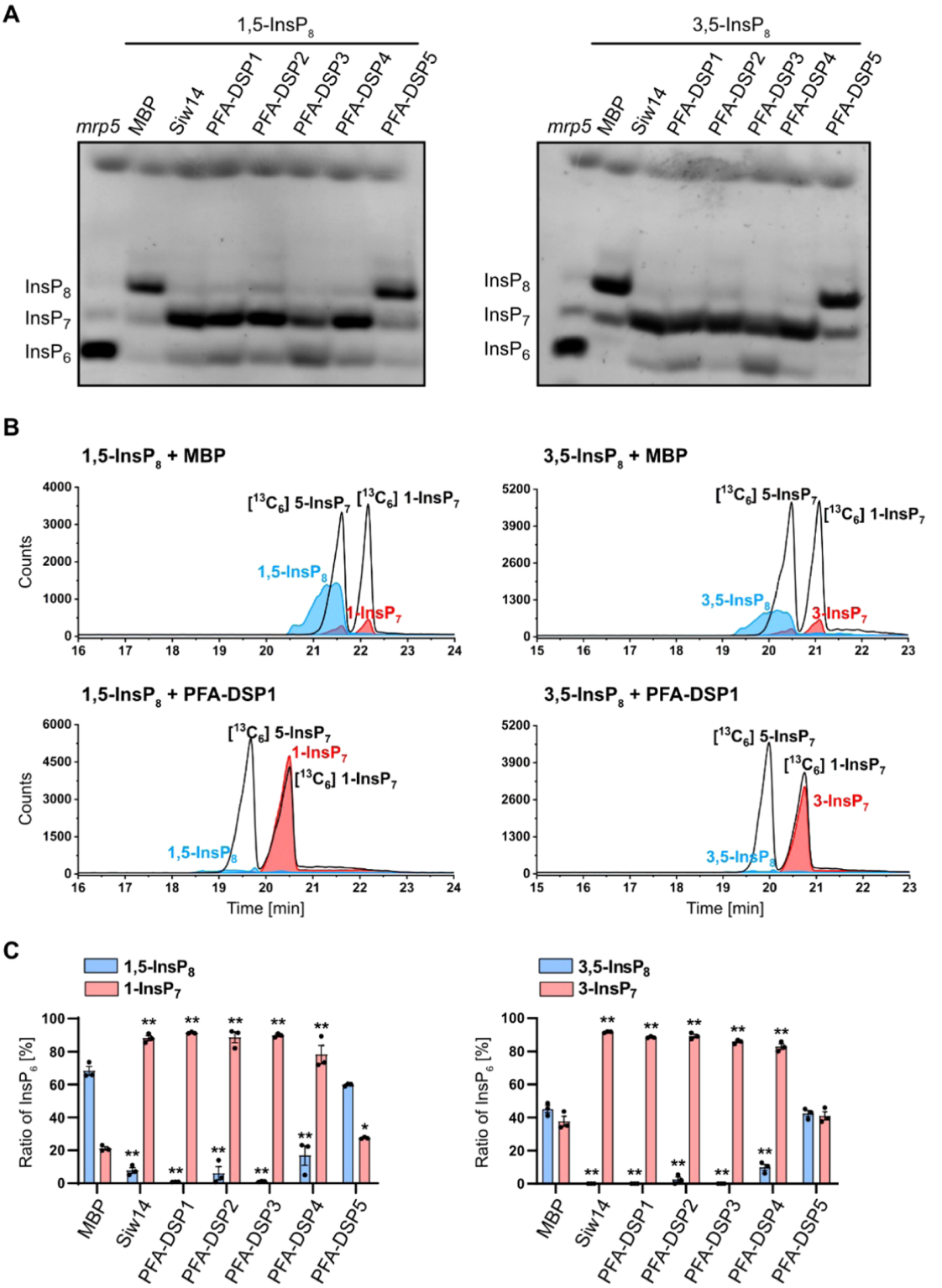

Figure 3. *Arabidopsis* PFA-DSPs display robust 1/3,5-$InsP_8$ phosphohydrolase activity *in vitro*. (A) Approximately 0.4 μM His-MBP-PFA-DSPs and His-MBP-Siw14 were incubated with 0.33 mM 1,5-$InsP_8$ or 3,5-$InsP_8$ for 1 h, in the presence of 1 mM $MgCl_2$, and analyzed by PAGE and subsequent toluidine blue staining. The identity of bands was determined by migration compared to TiO_2-purified *mrp*5 seed extract. (B, C) Second and third reactions were spiked with isotopic standards mixture ([$^{13}C_6$] 1,5-$InsP_8$, [$^{13}C_6$] 5-$InsP_7$, [$^{13}C_6$] 1-$InsP_7$, [$^{13}C_6$] $InsP_6$, [$^{13}C_6$] 2-OH $InsP_5$) and subjected to CE-ESI-MS analyses. (C) Data represent mean ± SEM (n = 3). Asterisks indicate values that are significantly different from the MBP control reactions (according to Student's t test, $P < 0.05$ (*); $P < 0.01$ (**)). Representative extracted-ion electropherograms are shown in Figure S7.

then tested potential PP-InsP phosphohydrolase activities of PFA-DSP1 with 1-$InsP_7$ or 5-$InsP_7$ in the presence of various divalent cations. Notably, PFA-DSP1 failed to catalyze the hydrolysis of 1-$InsP_7$ or 5-$InsP_7$ in the presence of Mn^{2+}, Ca^{2+},

https://doi.org/10.1021/acs.biochem.2c00145
Biochemistry 2022, 61, 1213−1227

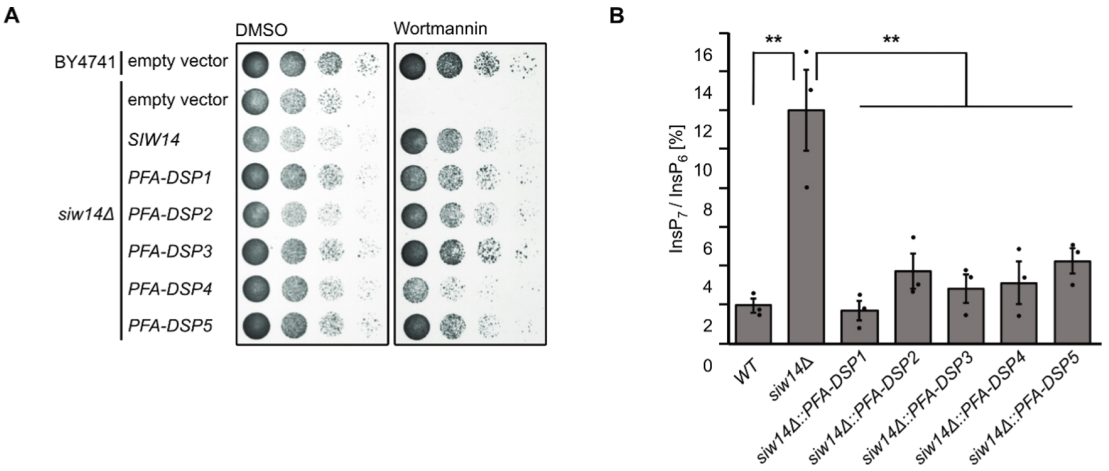

Figure 4. Heterologous expression of *Arabidopsis* PFA-DSPs complements *siw*14Δ-associated wortmannin sensitivity in yeast. (A) Growth complementation assays of an *siw*14Δ yeast strain. Wild-type yeast (BY4741) and an isogenic *siw*14Δ yeast mutant were transformed with either the empty episomal pDRf1-GW plasmid or different pDRf1-GW plasmids carrying the respective *PFA-DSP* gene or *SIW*14. Yeast transformants were then spotted in 8-fold serial dilutions (starting from OD_{600} 1.0) onto selective media supplemented with either wortmannin or DMSO as control. Plates were incubated at 26 °C for 2 days before photographing. The yeast growth assay was repeated twice ($n = 3$) with similar results. (B) Relative amounts of $InsP_7$ of wild-type yeast, *siw*14Δ and *siw*14Δ transformed with pDRf1-GW carrying the *PFA-DSP* genes are shown as $InsP_7$/$InsP_6$ ratios. $InsP_6$ and $InsP_7$ levels were determined by analysis of SAX-HPLC profiles using OriginPro 8. Data represent mean ± SEM ($n = 3$). Asterisks indicate values that are significantly different from *siw*14Δ (according to Student's *t* test, $P < 0.05$ (*); $P < 0.01$ (**)).

or Zn^{2+}. However, in the presence of the cytoplasmic prevalent cation Mg^{2+}, PFA-DSP1 displayed a robust hydrolytic activity against 5-$InsP_7$, likely resulting in the generation of $InsP_6$, as deduced from the mobility of the reaction product compared to TiO_2-purified *mrp*5 (multidrug resistance-associated protein 5) seed extract separated by polyacrylamide gel electrophoresis (PAGE) and visualized by toluidine blue staining (Figure 1A). Seeds of *Arabidopsis mrp*5 mutants that have a defective ABC-transporter involved in vacuolar loading of $InsP_6$[47] display reduced $InsP_6$ levels and simultaneously increased $InsP_7$ and $InsP_8$ levels.[20,24] Therefore, TiO_2-purified *mrp*5 seed extract serves as a marker to visualize $InsP_6$, $InsP_7$, and $InsP_8$ on PAGE. CE-ESI-MS analysis of the reaction product spiked with a [$^{13}C_6$] $InsP_6$ standard confirmed that the resulting product indeed had the migration behavior and the mass of phytic acid (Figure 1B). In contrast, 1-$InsP_7$ was largely resistant to PFA-DSP1 also in the presence of Mg^{2+} (Figure 1A). In the absence of divalent cations (i.e., in buffer not supplemented with divalent cations but instead supplemented with EDTA, a condition unlikely to represent any cellular condition), both $InsP_7$ isomers were hydrolyzed to $InsP_6$, as deduced from the mobility of the reaction product by PAGE (Figure 1A).

We then tested the hydrolytic activities of the *Arabidopsis* PFA-DSP homologues with all six "simple," synthetic $InsP_7$ isomers and with the two enantiomeric $InsP_8$ isomers 1,5-$InsP_8$ and 3,5-$InsP_8$ in the presence of Mg^{2+}. Of note, *myo*-inositol is a meso compound with a mirror plane dissecting the C2 and C5 positions. Derivatives differentially (pyro)phosphorylated at the C1 and C3 positions, as well as at the C4 and C6 positions are enantiomeric forms that can only be distinguished in the presence of appropriate chiral selectors.[48,49] Yeast Siw14 and all *Arabidopsis* PFA-DSPs with the exception of PFA-DSP5, displayed robust activity with a high specificity toward 5-$InsP_7$ (Figure 1C), confirming earlier reports that 5-$InsP_7$ is a preferred substrate for yeast Siw14 compared to 1-$InsP_7$.[42,43] PFA-DSP1−4 and Siw14 also displayed partial hydrolytic activities against the enantiomers 4-$InsP_7$ and 6-$InsP_7$, as well as very weak hydrolytic activities against enantiomeric 1-$InsP_7$ and 3-$InsP_7$ (Figure 1C). The latter activities were more pronounced in PFA-DSP1 and PFA-DSP3 compared to Siw14 and PFA-DSP2. As for 5-$InsP_7$, the reaction products with the other $InsP_7$ isomers had the mass and the migration behavior of the $InsP_6$ isomer phytic acid, as deduced from CE-ESI-MS analyses (Figures 1D and S2). Notably, PFA-DSP5 only showed very weak activities at the 0.4 μM concentration tested in our assay. However, when the reaction time was extended from 1 h to 2 h and the enzyme concentration was increased to 2 μM, PFA-DSP5 displayed robust activity with a substrate specificity similar to PFA-DSP1-4 and yeast Siw14, with a high selectivity for 5-$InsP_7$ and only weak hydrolytic activities against 4-$InsP_7$ and 6-$InsP_7$ (Figure 1E).

Notably, the meso $InsP_7$ isomer 2-$InsP_7$ was completely resistant to Siw14 or any of the *Arabidopsis* PFA-DSP proteins under the assay conditions. This was also the case in the absence of divalent cations (i.e., in buffer not supplemented with divalent cations but instead supplemented with EDTA), where Siw14 and *Arabidopsis* PFA-DSP1-4 failed to hydrolyze 2-$InsP_7$ to a significant extent while all other $InsP_7$ isomers were at least partially converted to an InsP isomer with the mobility of phytic acid (Figures S3 and S4). Even after a 24 h-long incubation with *Arabidopsis* PFA-DSP1, 2-$InsP_7$ remained largely resistant to hydrolysis. In contrast, all other PP-$InsP_7$ isomers were hydrolyzed to $InsP_6$ under these conditions, as revealed by PAGE and CE-ESI-MS analyses (Figures 2A,B and S5). Corresponding control reactions that were supplemented with 5-$InsP_7$ after 23 h validated the activity of *Arabidopsis* PFA-DSP1 after such long incubation times (Figures 2A and S6). These spiking experiments also rule out the possibility that 2-$InsP_7$ contained a contaminant that inhibits PFA-DSP-dependent hydrolysis, as 5-$InsP_7$ was still efficiently hydrolyzed in the presence of 2-$InsP_7$.

Finally, we tested whether the enantiomeric $InsP_8$ isomers 1,5-$InsP_8$ and 3,5-$InsP_8$ serve as substrates for PFA-DSPs. As reported earlier for Siw14,[43] PFA-DSP1−4 hydrolyzed 1,5-

https://doi.org/10.1021/acs.biochem.2c00145
Biochemistry 2022, 61, 1213−1227

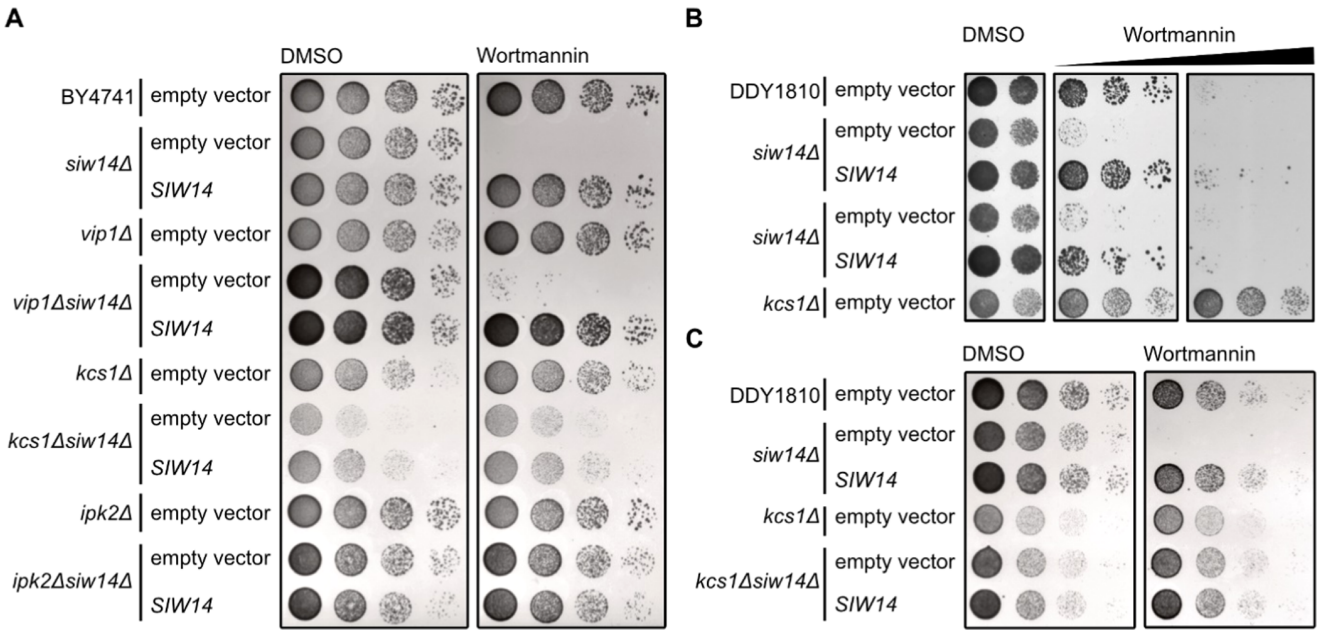

Figure 5. Yeast *siw*14Δ-associated wortmannin sensitivity requires Kcs1-dependent 5-InsP$_7$. (A) Wild-type yeast (BY4741), *siw*14Δ, *vip*1Δ, *kcs*1Δ, *ipk*2Δ, *vip*1Δ *siw*14Δ, *kcs*1Δ *siw*14Δ, and *ipk*2Δ *siw*14Δ double-mutant yeast strains were transformed with either an empty (*CEN*-based) YCplac33 vector or a YCplac33 vector carrying a genomic fragment of *SIW*14 including a 653 bp promoter and 5′UTR and a 289 bp terminator region. Yeast transformants were then spotted in 8-fold serial dilutions (starting from OD_{600} 1.0) onto selective media supplemented with either wortmannin or DMSO as control. Plates were incubated at 26 °C for 2 days before photographing. (B, C) Wild-type yeast (DDY1810), *siw*14Δ, *kcs*1Δ, and (C) *kcs*1Δ *siw*14Δ double-mutant yeast strains were transformed with either an empty YCplac33 vector or a YCplac33 vector carrying the genomic fragment of *SIW*14. The growth assay was performed as described for (A). All yeast growth assays (A–C) were repeated twice (n = 3) with similar results.

InsP$_8$ to an InsP$_7$ isomer based on the mobility of the reaction product in PAGE analyses (Figure 3A). Also the enantiomeric 3,5-InsP$_8$ was efficiently hydrolyzed by Siw14 and PFA-DSP1–4 (Figure 3A), and CE-ESI-MS analysis of the reaction products showed the migration behavior and the mass of 1/3-InsP$_7$ (Figures 3B,C and S7).

Altogether, these findings reveal that *Arabidopsis* PFA-DSP proteins and yeast Siw14 have a high specificity for the 5-β-phosphate of 5-InsP$_7$, 1,5-InsP$_8$, and 3,5-InsP$_8$, and a weak activity against the β-phosphates of 4-InsP$_7$ and 6-InsP$_7$, respectively. In contrast, InsP$_6$ and 2-InsP$_7$ are resistant to PFA-DSP-catalyzed hydrolysis (summarized in Table S1).

Heterologous Expression of *Arabidopsis* PFA-DSP Homologues Complement Yeast *siw*14Δ Defects. To investigate the physiological consequences of *Arabidopsis* PFA-DSP activities *in vivo*, we carried out heterologous expression experiments in baker's yeast. To this end, we investigated the sensitivity of our *siw*14Δ yeast strain under conditions where phenotypes for *siw*14Δ strains and other yeast mutants defective in PP-InsP homeostasis have been reported previously[5,24,50−52] and selected the fungal toxin wortmannin[53] that caused a severe *siw*14Δ-associated growth defect. Previous observations that *kcs*1Δ yeast cells are resistant to wortmannin[54] suggest that wortmannin sensitivity of *siw*14Δ yeast might be related to Kcs1-dependent PP-InsPs. The *siw*14Δ-associated growth defect was fully complemented by heterologous expression of either of the five *Arabidopsis PFA-DSP* homologues or of yeast *SIW*14 from episomal plasmids under control of a *PMA*1 promoter fragment (Figure 4A). Immunoblot analyses taking advantage of a C-terminal V5-tag revealed that all PFA-DSP homologues were expressed in yeast with PFA-DSP1 and PFA-DSP4 showing the highest protein abundance (Figure S8). Reduced growth of *siw*14Δ transformants expressing PFA-DSP4 on media supplemented with wortmannin is therefore likely not caused by inefficient expression of this homologue in yeast but might rather be a consequence of excess protein activity in this heterologous expression system. To investigate the contribution of PFA-DSPs in InsP metabolism, we monitored InsP profiles using SAX-HPLC analyses of various [^{3}H]-*myo*-inositol labeled yeast transformants. Of note, conventional SAX-HPLC analyses as employed here do not allow the discrimination of different InsP$_7$ or InsP$_8$ isomers.[11,49] Heterologous expression of PFA-DSPs in *siw*14Δ restored InsP$_7$/InsP$_6$ ratios to wild-type levels, indicating that *Arabidopsis* PFA-DSP proteins are functionally similar to Siw14 (Figure 4B).

Notably, the InsP$_7$ signal was the only one consistently affected by the loss of *SIW*14 and heterologous expression of any *PFA-DSP* gene (Figure S9). We generated variants of Siw14 or PFA-DSP1, in which the catalytic cysteine was replaced by a serine resulting in a C214S and a C150S substitution in Siw14 and PFA-DSP1, respectively, and observed that complementation of *siw*14Δ-associated growth defects of respective transformants requires the catalytic activity of these proteins (Figure S10A,B). The inability of catalytic dead mutants to complement *siw*14Δ-associated growth defects was not caused by compromised expression or protein stability of these variants, as confirmed by immunoblot analyses (Figure S10C). In agreement with the growth complementation assays, the catalytically inactive versions of Siw14 and PFA-DSP1 also failed to restore wild-type InsP$_7$ levels in *siw*14Δ transformants (Figure S10D,E). These experiments suggest that *Arabidopsis* PFA-DSPs can substitute for endogenous Siw14 in yeast with respect to

https://doi.org/10.1021/acs.biochem.2c00145
Biochemistry 2022, 61, 1213−1227

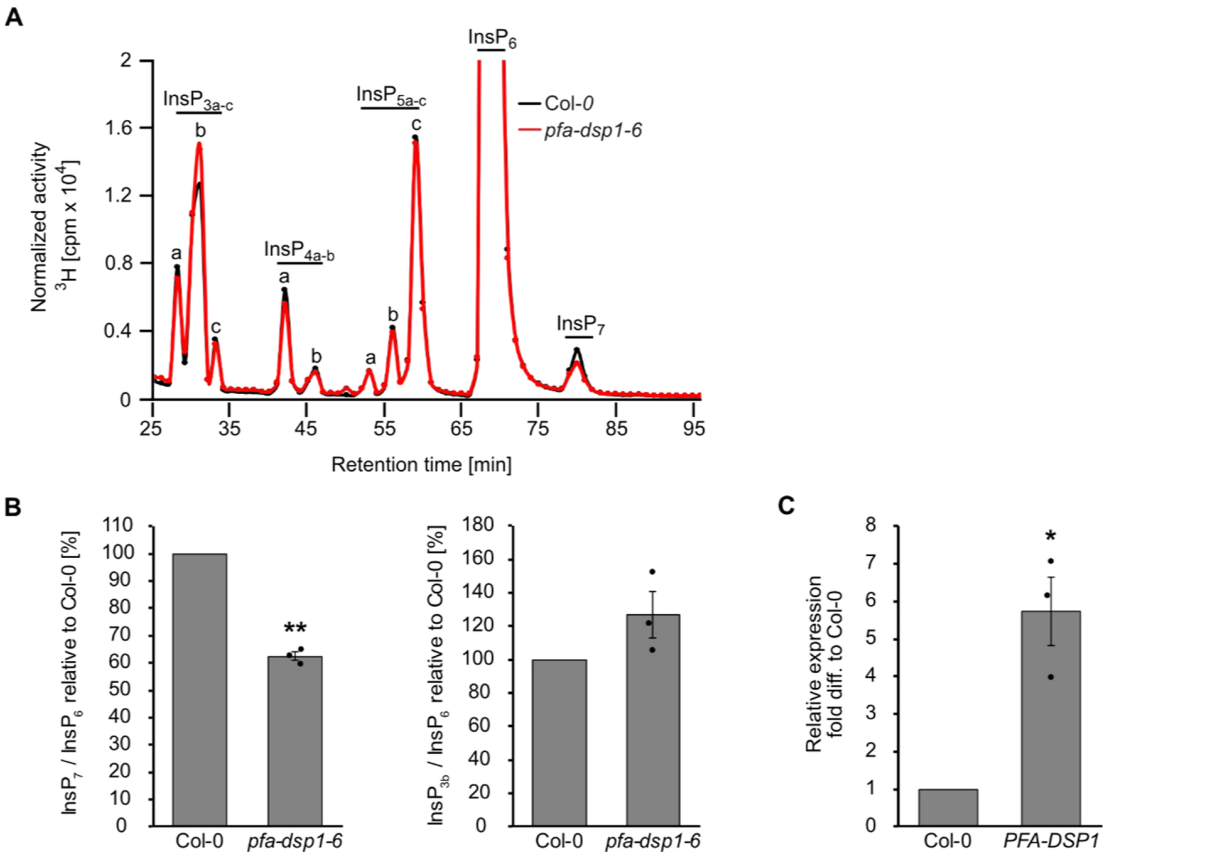

Figure 6. Increased expression of *PFA-DSP*1 in *Arabidopsis* decreases $InsP_7$ levels. (A) Representative SAX-HPLC profile of 20-day-old wild-type (Col-0) and *pfa-dsp*1-6 *Arabidopsis* seedlings radiolabeled with [^{3}H]-*myo*-inositol. All visible peaks are highlighted and assigned to the corresponding InsP species. Based on published chromatographic mobilities,[56,57] $InsP_{4a}$ likely represents Ins(1,4,5,6)P_4 or Ins(3,4,5,6)P_4, $InsP_{5a}$ likely represents $InsP_5$ [2-OH], $InsP_{5b}$ likely represents $InsP_5$ [4-OH] or its enantiomeric form $InsP_5$ [6-OH], and $InsP_{5c}$ likely represents $InsP_5$ [1-OH] or its enantiomeric form $InsP_5$ [3-OH]. The isomeric natures of $InsP_{3a-c}$, $InsP_{4b}$, $InsP_7$, and $InsP_8$ are unknown. (B) $InsP_7$/$InsP_6$ and $InsP_{3b}$/$InsP_6$ ratio of *pfa-dsp*1-6 relative to Col-0 determined by the analysis of SAX-HPLC profiles using OriginPro 8. (C) Relative expression of *PFA-DSP*1 in plants grown under identical conditions as for SAX-HPLC analyses, presented as fold difference compared to Col-0. (B, C) Data represent mean ± SEM (n = 3). Asterisks indicate values that are significantly different from the Col-0 control (according to Student's t test, $P < 0.05$ (*); $P < 0.01$ (**)).

wortmannin tolerance and $InsP_7$ homeostasis and that complementation of the *siw*14Δ-associated defects depends on the catalytic activity of these proteins.

Growth Defects of *siw*14Δ Yeast on Wortmannin Require Kcs1-Dependent 5-$InsP_7$ Synthesis. For a deeper understanding of the wortmannin phenotype of *siw*14Δ yeast, we investigated genetic interactions between Siw14 and different InsP kinases. We generated different double mutants with defects in Siw14 and the PP-InsP synthases Kcs1 and Vip1, and tested their performance on wortmannin-containing media (Figure 5A). Again, *siw*14Δ cells did not survive on media supplemented with 3 μM wortmannin, a defect that was fully complemented by the expression of *SIW*14 under control of the endogenous promoter from a *CEN*-based single-copy plasmid (Figure 5A). The growth of *vip*1Δ cells was comparable to wild-type yeast. In contrast, the *vip*1Δ *siw*14Δ double mutant showed a severe growth defect on media supplemented with wortmannin similar to single *siw*14Δ cells (Figure 5A). Like the *vip*1Δ yeast strain, a *kcs*1Δ strain did not show growth defects on media supplemented with wortmannin compared to control media. In contrast, at increased concentrations, we observed *kcs*1Δ-associated wortmannin resistance (Figure 5B), as reported earlier.[54] Importantly, deletion of *KCS*1 in *siw*14Δ cells rescued *siw*14Δ-associated wortmannin sensitivity since the resulting *kcs*1Δ *siw*14Δ double-mutant yeast strain, despite growing overall weaker than the *kcs*1Δ single-mutant strain, showed no increased sensitivity to wortmannin (Figure 5A). These findings indicate that the presence of Kcs1 is critical for the growth defects displayed by *siw*14Δ single-mutant cells on wortmannin. We then investigated whether the presence of Kcs1 itself or of Kcs1-dependent PP-InsPs such as 5-$InsP_7$ are relevant for *siw*14Δ-associated wortmannin sensitivity. To this end, we examined the phenotypes of *ipk*2Δ and of *ipk*2Δ *siw*14Δ yeast transformants. Both mutants lack IPK2, an inositol polyphosphate multikinase that sequentially phosphorylates Ins(1,4,5)P_3 to Ins(1,3,4,5,6)P_5 and is hence required for $InsP_6$ and subsequent Kcs1-dependent 5-$InsP_7$ or PP-$InsP_4$ synthesis.[54,55] Neither of the strains showed growth defects on media supplemented with wortmannin compared to the isogenic wild-type yeast strain, suggesting that also the loss of *IPK*2 rescues *siw*14Δ-associated wortmannin sensitivity (Figure 5A). We further tested wortmannin sensitivity of *kcs*1Δ and *kcs*1Δ *siw*14Δ yeast transformants in a different genetic background and observed similar results (Figure 5B,C). Taken together, these results provide a causal link

https://doi.org/10.1021/acs.biochem.2c00145
Biochemistry 2022, 61, 1213−1227

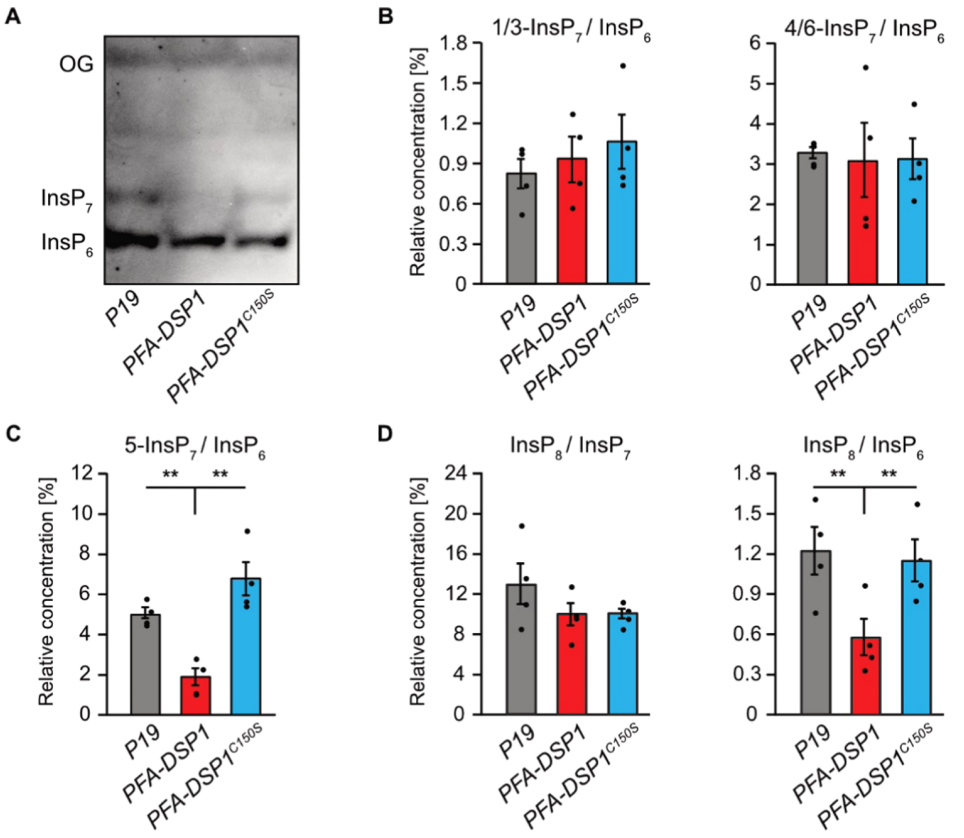

Figure 7. Transient expression of *PFA-DSP*1 in *N. benthamiana* leaves specifically decreases 5-$InsP_7$ and $InsP_8$. InsPs from infiltrated *N. benthamiana* leaves, transiently expressing the silencing inhibitor *P*19 alone or together with *PFA-DSP*1-*EYFP* or *PFA-DSP*1^{C150S}-*EFYP*, were purified with TiO_2 pulldown and analyzed using CE-ESI-MS. Detected peaks were assigned to specific InsP isomers and quantified by comparing them with ^{13}C InsP standards that were spiked into the purified samples. (A) Representative PAGE gel of a sample set used for CE-ESI-MS analysis. (B−D) Relative amounts of PP-InsPs compared to $InsP_6$ or of $InsP_8$ compared to all $InsP_7$ isomers as indicated. Data represent mean ± SEM (n = 4). Asterisks indicate values that are significantly different from wild-type (according to Student's t test, $P < 0.05$ (*); $P < 0.01$ (**)). Note that 4- or 6-$InsP_7$, as well as 1- or 3-$InsP_7$ represent enantiomeric forms that cannot be distinguished by CE-ESI-MS analyses.

between Kcs1 (but not Vip1)-dependent PP-InsPs and *siw*14Δ-associated wortmannin sensitivity with Kcs1 and Siw14/PFA-DSPs playing antagonistic roles in regulating this sensitivity.

Increased *PFA-DSP1* Expression Coincides with Decreased $InsP_7$ Levels *In Planta*. To gain insight into PFA-DSP functions *in planta*, we searched for *Arabidopsis* T-DNA insertion lines of *PFA-DSP*1 and were able to identify three lines, *pfa-dsp*1-3 and *pfa-dsp*1-6 in the Col-0 background and *pfa-dsp*1-4 in the Ler-0 background, for which homozygous progeny could be obtained. None of these lines displayed an obvious growth phenotype under our standard growth conditions. SAX-HPLC profiles of extracts of 20-day-old [^3H]-*myo*-inositol labeled *pfa-dsp*1-3 and *pfa-dsp*1-4 seedlings did not reveal a significant difference compared to the respective wild-types (Figure S11A,B). However, SAX-HPLC analyses of the *pfa-dsp*1-6 line revealed a significant average reduction (around 36%) of the $InsP_7/InsP_6$ ratio compared to Col-0 (Figure 6B). The levels of other InsP species remained largely unaffected (Figure 6A,B). The available sequencing data for this line, as well as our analysis, indicated that the insertion of the T-DNA is 18 bp upstream of the start codon, suggesting that the full-length transcript and PFA-DSP1 protein might be expressed in this line. We therefore conducted qPCR analyses of *pfa-dsp*1-6 seedlings that were grown under identical conditions as the seedlings for SAX-HPLC analyses and detected ca. 6-fold increased expression of *PFA-DSP*1 in *pfa-dsp*1-6 in comparison to Col-0 seedlings (Figure 6C).

Since the analyses of the *pfa-dsp*1-6 line indicated that the T-DNA insertion causes an overexpression of *PFA-DSP*1, resulting in decreased $InsP_7$ levels, we investigated whether PP-InsP phosphohydrolase activity is also observed in a heterologous plant expression system. To this end, we transiently expressed a translational fusion of PFA-DSP1 with a C-terminal EYFP under control of the strong viral CaMV 35*S* promoter in *N. benthamiana* using agrobacterium-mediated transfection. The respective catalytically inactive PFA-DSP1^{C150S}-EYFP fusion protein was also expressed and InsPs were then extracted from *N. benthamiana* leaves and purified by TiO_2 pulldown 5 days after infiltration. PAGE analyses showed that transient expression of PFA-DSP1 or expression of its catalytic inactive version did not alter $InsP_6$ levels (Figure 7A). In contrast, $InsP_7$ levels were reduced by the transient expression of PFA-DSP1 but not by the expression of its catalytic inactive version (Figure 7A). These findings were strengthened by subsequent CE-ESI-MS analyses that revealed no changes in the ratios of 1/3-$InsP_7/InsP_6$ or 4/6-$InsP_7/InsP_6$ compared to control leaves infiltrated with agrobacteria carrying the silencing inhibitor *P*19 alone (Figure 7B). In contrast, the 5-$InsP_7/InsP_6$ ratio was significantly reduced in plants expressing *PFA-DSP*1 compared to plants expressing the

https://doi.org/10.1021/acs.biochem.2c00145
Biochemistry 2022, 61, 1213−1227

inactive version of *PFA-DSP*1 or *P*19 alone (Figure 7C). The $InsP_8/InsP_6$ ratio, in turn, was strongly reduced by the expression of *PFA-DSP*1 (Figure 7D) in agreement with a partial hydrolytic activity of PFA-DSP proteins against $InsP_8$ isomers (Figures 3 and S7) and in agreement with the finding that 5-$InsP_7$, a substrate hydrolyzed by PFA-DSP1, represents the major precursor for $InsP_8$ synthesis.[11] In summary, these results demonstrate that ectopic expression of *Arabidopsis PFA-DSP*1 results in a specific decrease of 5-$InsP_7$ and $InsP_8$ *in planta*.

CONCLUSIONS

Recent studies elucidating the identity and substrate specificity of $InsP_6$/PP-InsP kinases have allowed us to establish important functions of PP-InsPs in nutrient sensing, hormone signaling, and plant immunity.[5−13,20,28] In contrast, information on enzymatic activities removing PP-InsPs to switch off their signaling functions in plants is sparse. Intriguingly, the first robust detection of PP-InsP messengers in mammalian cells was made possible by blocking mammalian PP-InsP phosphohydrolases with fluoride.[1] While substantial progress in elucidating the role of various PP-InsP phosphohydrolases in regulating these messengers in yeast and mammalian cells has been made,[37,41,42,58] we are unaware of any study about PP-InsP degrading enzymes in plants at the onset of this study. Here, we provide evidence that the *Arabidopsis* PFA-DSP proteins are functional homologues of yeast Siw14 with high phosphohydrolase specificity for the 5-β-phosphate of various PP-InsPs.

The striking biochemical similarities between *Arabidopsis PFA-DSPs* as deduced from *in vitro* assays and heterologous expressions analyses in yeast might well explain redundancies of these enzymes and consequently a lack of obvious phenotypes in single *pfa-dsp* loss-of-function lines in *Arabidopsis*. A search in transcriptome studies revealed that *PFA-DSP*1, 2, and 4 are strongly induced by P_i deficiency (Figure S12). Such P_i-dependent regulation is in line with the disappearance of PP-InsPs in tissues of P_i-starved plants[9,11] but future studies are required to establish the involvement of PFA-DSPs in the removal of messengers controlling P_i signaling. The high specificity of PFA-DSPs observed in this study establishes these enzymes as ideal tools to investigate the physiological roles of 5-β-phosphate containing PP-InsPs in plant development, plant immunity, nutrient perception, and abiotic stress tolerance. This is particularly important because of potentially confounding effects caused by the recently discovered plant 4/6-$InsP_7$[11] and also because higher-order mutants involved in the synthesis of 5-β-phosphate containing PP-InsPs such as *itpk*1 *itpk*2 and *vih*1 *vih*2 display severe developmental defects or die at the young seedling stage.[10,11] With the availability of a variety of promoters with tight spatial and temporal regulation, ectopic expression of *PFA-DSPs* in a tissue and developmentally controlled manner will provide helpful insights to unravel the roles of 5-$InsP_7$ and 1/3, 5-$InsP_8$ in plant development and plant physiology.

ASSOCIATED CONTENT

Supporting Information

The Supporting Information is available free of charge at https://pubs.acs.org/doi/10.1021/acs.biochem.2c00145.

Purification of PFA-DSP proteins (Figure S1); *in vitro*, *Arabidopsis* PFA-DSP1 displays robust PP-InsP phosphohydrolase activity against 5-$InsP_7$ and partial phosphohydrolase activity against 4-$InsP_7$ and 6-$InsP_7$, respectively (Figure S2); in the absence of divalent cations, all $InsP_7$ isomers with the exception of 2-$InsP_7$ become substrates for selected *Arabidopsis* PFA-DSPs *in vitro* (Figure S3); in the presence of Mg^{2+}, PFA-DSP1 and PFA-DSP3 display robust *in vitro* $InsP_7$ phosphohydrolase activity with high specificity for the 5-β-phosphate (Figure S4); under prolonged incubation time, *Arabidopsis* PFA-DSP1 efficiently hydrolyzes 5-$InsP_7$, 4-$InsP_7$, and 6-$InsP_7$ but only displays partial activities against 1-$InsP_7$ and 3-$InsP_7$, and a very weak activity against 2-$InsP_7$ (Figure S5); *Arabidopsis* PFA-DSP1 maintains 5-$InsP_7$ phosphohydrolase activity during prolonged incubation times *in vitro* (Figure S6); *in vitro*, *Arabidopsis* PFA-DSPs display robust 1/3,5-$InsP_8$ phosphohydrolase activity (Figure S7); all five PFA-DSP homologues are stably expressed in the *siw*14Δ yeast strain (Figure S8); heterologous expression of *Arabidopsis* PFA-DSPs complements *siw*14Δ-associated defects in $InsP_7/InsP_6$ ratios in yeast (Figure S9); complementation of *siw*14Δ-associated growth defects depends on catalytic activity (Figure S10); single-mutant *Arabidopsis pfa-dsp*1 loss-of-function lines do not display InsP/PP-InsP defects (Figure S11); *Arabidopsis PFA-DSP*1, 2, and 4 are strongly induced by P_i deficiency (Figure S12); overview of *Arabidopsis* PFA-DSP substrate specificities in the presence of Mg^{2+} showing a robust PP-InsP phosphohydrolase activity against 5-$InsP_7$, 1,5-$InsP_8$, and 3,5-$InsP_8$, *in vitro* (Table S1); and oligonucleotide sequences (Table S2) (PDF)

Accession Codes

DNA and Protein Sequences can be obtained from the Saccharomyces Genome database (https://www.yeastgenome.org/), TAIR (https://www.arabidopsis.org), and UniProt (https://www.uniprot.org/) under the following accession numbers: *SIW*14 (YNL032W, NC_001146.8), *Arabidopsis PFA-DSP*1 (At1g05000, NM_100379.3), *Arabidopsis PFA-DSP*2 (At2g32960, NM_128856.5), *Arabidopsis PFA-DSP*3 (At3g02800, NM_111148.3), *Arabidopsis PFA-DSP*4 (At4g03960, NM_116634.4), *Arabidopsis PFA-DSP*5 (At5g16480, NM_121653.4), *Arabidopsis PP2AA*3 (At1g13320, NM_101203), and *Arabidopsis TIP*41*-like* (At3g54000, NM_115260). PDB ID: 1XRI.

AUTHOR INFORMATION

Corresponding Authors

Gabriel Schaaf − *Department of Plant Nutrition, Institute of Crop Science and Resource Conservation, Rheinische Friedrich-Wilhelms-Universität Bonn, 53115 Bonn, Germany*; orcid.org/0000-0001-9022-4515; Email: gabriel.schaaf@uni-bonn.de

Debabrata Laha − *Department of Biochemistry, Indian Institute of Science (IISc), Bengaluru 560012, India*; Email: dlaha@iisc.ac.in

Authors

Philipp Gaugler − *Department of Plant Nutrition, Institute of Crop Science and Resource Conservation, Rheinische Friedrich-Wilhelms-Universität Bonn, 53115 Bonn, Germany*

Robin Schneider − *Department of Plant Nutrition, Institute of Crop Science and Resource Conservation, Rheinische Friedrich-Wilhelms-Universität Bonn, 53115 Bonn, Germany*

Guizhen Liu − *Department of Chemistry and Pharmacy and CIBSS-Centre for Integrative Biological Signalling Studies, Albert-Ludwigs University Freiburg, 79104 Freiburg, Germany*
Danye Qiu − *Department of Chemistry and Pharmacy and CIBSS-Centre for Integrative Biological Signalling Studies, Albert-Ludwigs University Freiburg, 79104 Freiburg, Germany*
Jonathan Weber − *Department of Plant Nutrition, Institute of Crop Science and Resource Conservation, Rheinische Friedrich-Wilhelms-Universität Bonn, 53115 Bonn, Germany*
Jochen Schmid − *Center for Plant Molecular Biology, Department of Plant Physiology, Eberhard Karls University Tübingen, 72076 Tübingen, Germany;* Present Address: Department of Biomedicine, University of Basel, 4058 Basel, Switzerland
Nikolaus Jork − *Department of Chemistry and Pharmacy and CIBSS-Centre for Integrative Biological Signalling Studies, Albert-Ludwigs University Freiburg, 79104 Freiburg, Germany; Spemann Graduate School of Biology and Medicine (SGBM), University of Freiburg, 79104 Freiburg, Germany*
Markus Häner − *Department of Chemistry and Pharmacy and CIBSS-Centre for Integrative Biological Signalling Studies, Albert-Ludwigs University Freiburg, 79104 Freiburg, Germany*
Kevin Ritter − *Department of Chemistry and Pharmacy and CIBSS-Centre for Integrative Biological Signalling Studies, Albert-Ludwigs University Freiburg, 79104 Freiburg, Germany*
Nicolás Fernández-Rebollo − *Center for Plant Molecular Biology, Department of Plant Physiology, Eberhard Karls University Tübingen, 72076 Tübingen, Germany*
Ricardo F. H. Giehl − *Department of Physiology & Cell Biology, Leibniz-Institute of Plant Genetics and Crop Plant Research, 06466 Gatersleben, Germany*
Minh Nguyen Trung − *Leibniz-Forschungsinstitut für Molekulare Pharmakologie, 13125 Berlin, Germany; Department of Chemistry, Humboldt Universität zu Berlin, 12489 Berlin, Germany*
Ranjana Yadav − *Department of Biochemistry, Indian Institute of Science (IISc), Bengaluru 560012, India*
Dorothea Fiedler − *Leibniz-Forschungsinstitut für Molekulare Pharmakologie, 13125 Berlin, Germany; Department of Chemistry, Humboldt Universität zu Berlin, 12489 Berlin, Germany;* orcid.org/0000-0002-0798-946X
Verena Gaugler − *Department of Plant Nutrition, Institute of Crop Science and Resource Conservation, Rheinische Friedrich-Wilhelms-Universität Bonn, 53115 Bonn, Germany*
Henning J. Jessen − *Department of Chemistry and Pharmacy and CIBSS-Centre for Integrative Biological Signalling Studies, Albert-Ludwigs University Freiburg, 79104 Freiburg, Germany;* orcid.org/0000-0002-1025-9484

Complete contact information is available at: https://pubs.acs.org/10.1021/acs.biochem.2c00145

Author Contributions

◆P.G. and R.S. contributed equally to this manuscript. D.L., G.S., and P.G. conceived the study. P.G., D.L., G.S., H.J.J., and R.F.H.G. designed experiments. P.G., R.S., D.L., G.L. D.Q., J.W., M.H., N.J., K.R., J.S., N.F.-R., and R.F.H.G. performed experiments. P.G. generated yeast mutants and performed all yeast experiments, generated constructs, isolated T-DNA insertion lines, performed HPLC analyses of plants, performed qPCR analyses, performed plant infiltration and TiO_2 pull-downs, and analyzed most of the experiments. R.S. purified recombinant proteins and carried out and analyzed *in vitro* kinase assays. G.L. and D.Q. performed CE-ESI-MS/MS analysis and isomer identification. J.W. and J.S. generated constructs and established the expression and purification of recombinant proteins. N.J., M.H., and K.R. synthesized $InsP_7$ and $InsP_8$ isomers. N.F.-R. isolated T-DNA insertion lines, performed HPLC analyses of plants, generated constructs, and performed qPCR analyses. R.F.H.G. generated plant samples for CE-ESI-MS analysis and did transcriptome analysis. M.N.T. synthesized ^{13}C-InsP standards. V.G. analyzed and quantified HPLC analyses. P.G., G.S., D.L., H.J.J., and D.F. supervised the experimental work. P.G., G.S., R.S., D.L., and R.Y. wrote the manuscript with input from all authors.

Funding

This work was funded by grants from the Deutsche Forschungsgemeinschaft (SCHA 1274/4-1, SCHA 1274/5-1, Research Training Group GRK 2064 and under Germany's Excellence Strategy, EXC-2070-390732324, PhenoRob to G.S.; JE 572/4-1 and under Germany's Excellence Strategy, CIBSS-EXC-2189−Project ID 390939984 to H.J.J.; and HE 8362/1-1, DFG Eigene Stelle, to R.F.H.G.). D.L. acknowledges the Department of Biotechnology (DBT) for HGK-IYBA award (BT/13/IYBA/2020/04) and a DBT Indian Institute of Science Partnership Program. H.J.J. acknowledges funding from the Volkswagen Foundation (Momentum Grant 2021).

Notes

The authors declare no competing financial interest.
During the revision of this manuscript, a study by Wang and colleagues[71] reported high-resolution crystal structures of *Arabidopsis* PFA-DSP1 in complex with 5-$InsP_7$, 6-$InsP_7$, and 5-$InsP_7$ analogues and provided evidence for efficient *in vitro* phosphatase activity of this enzyme against 5-$InsP_7$ as well as weaker *in vitro* activities against 4-$InsP_7$ and 6-$InsP_7$ in agreement with our findings.

■ ACKNOWLEDGMENTS

The authors thank Li Schlüter and Brigitte Ueberbach (Department of Plant Nutrition, Institute of Crop Science and Resource Conservation, University of Bonn) for excellent technical assistance and Marília Kamleitner (Department of Plant Nutrition, Institute of Crop Science and Resource Conservation, University of Bonn) for critically reading this manuscript. They also thank Priyanshi Rana (Department of Biochemistry, Indian Institute of Science) for her inputs during the revision of the manuscript.

■ REFERENCES

(1) Menniti, F. S.; Miller, R. N.; Putney, J. W., Jr.; Shears, S. B. Turnover of inositol polyphosphate pyrophosphates in pancreatoma cells. *J. Biol. Chem.* **1993**, *268*, 3850−3856.
(2) Stephens, L.; Radenberg, T.; Thiel, U.; Vogel, G.; Khoo, K. H.; Dell, A.; Jackson, T. R.; Hawkins, P. T.; Mayr, G. W. The detection, purification, structural characterization, and metabolism of diphosphoinositol pentakisphosphate(s) and bisdiphosphoinositol tetrakisphosphate(s). *J. Biol. Chem.* **1993**, *268*, 4009−4015.
(3) Thota, S. G.; Bhandari, R. The emerging roles of inositol pyrophosphates in eukaryotic cell physiology. *J Biosci.* **2015**, *40*, 593−605.

(4) Shears, S. B. Intimate connections: Inositol pyrophosphates at the interface of metabolic regulation and cell signaling. *J. Cell. Physiol.* **2018**, *233*, 1897−1912.
(5) Laha, D.; Johnen, P.; Azevedo, C.; Dynowski, M.; Weiss, M.; Capolicchio, S.; Mao, H.; Iven, T.; Steenbergen, M.; Freyer, M.; Gaugler, P.; de Campos, M. K.; Zheng, N.; Feussner, I.; Jessen, H. J.; Van Wees, S. C.; Saiardi, A.; Schaaf, G. VIH2 Regulates the Synthesis of Inositol Pyrophosphate InsP8 and Jasmonate-Dependent Defenses in Arabidopsis. *Plant Cell* **2015**, *27*, 1082−1097.
(6) Laha, D.; Parvin, N.; Dynowski, M.; Johnen, P.; Mao, H.; Bitters, S. T.; Zheng, N.; Schaaf, G. Inositol Polyphosphate Binding Specificity of the Jasmonate Receptor Complex. *Plant Physiol.* **2016**, *171*, 2364−2370.
(7) Wild, R.; Gerasimaite, R.; Jung, J. Y.; Truffault, V.; Pavlovic, I.; Schmidt, A.; Saiardi, A.; Jessen, H. J.; Poirier, Y.; Hothorn, M.; Mayer, A. Control of eukaryotic phosphate homeostasis by inositol polyphosphate sensor domains. *Science* **2016**, *352*, 986−990.
(8) Couso, I.; Evans, B.; Li, J.; Liu, Y.; Ma, F.; Diamond, S.; Allen, D. K.; Umen, J. G. Synergism between inositol polyphosphates and TOR kinase signaling in nutrient sensing, growth control and lipid metabolism in Chlamydomonas. *Plant Cell* **2016**, *28*, 2026−2042.
(9) Dong, J.; Ma, G.; Sui, L.; Wei, M.; Satheesh, V.; Zhang, R.; Ge, S.; Li, J.; Zhang, T. E.; Wittwer, C.; Jessen, H. J.; Zhang, H.; An, G. Y.; Chao, D. Y.; Liu, D.; Lei, M. Inositol Pyrophosphate InsP8 Acts as an Intracellular Phosphate Signal in Arabidopsis. *Mol. Plant* **2019**, *12*, 1463−1473.
(10) Zhu, J.; Lau, K.; Puschmann, R.; Harmel, R. K.; Zhang, Y.; Pries, V.; Gaugler, P.; Broger, L.; Dutta, A. K.; Jessen, H. J.; Schaaf, G.; Fernie, A. R.; Hothorn, L. A.; Fiedler, D.; Hothorn, M. Two bifunctional inositol pyrophosphate kinases/phosphatases control plant phosphate homeostasis. *eLife* **2019**, *8*, No. e43582.
(11) Riemer, E.; Qiu, D.; Laha, D.; Harmel, R. K.; Gaugler, P.; Gaugler, V.; Frei, M.; Hajirezaei, M. R.; Laha, N. P.; Krusenbaum, L.; Schneider, R.; Saiardi, A.; Fiedler, D.; Jessen, H. J.; Schaaf, G.; Giehl, R. F. H. ITPK1 is an InsP6/ADP phosphotransferase that controls phosphate signaling in Arabidopsis. *Mol. Plant* **2021**, *14*, 1864−1880.
(12) Gulabani, H.; Goswami, K.; Walia, Y.; Roy, A.; Noor, J. J.; Ingole, K. D.; Kasera, M.; Laha, D.; Giehl, R. F. H.; Schaaf, G.; Bhattacharjee, S. Arabidopsis inositol polyphosphate kinases IPK1 and ITPK1 modulate crosstalk between SA-dependent immunity and phosphate-starvation responses. *Plant Cell Rep.* **2021**, *41*, 347−363.
(13) Laha, N. P.; Dhir, Y. W.; Giehl, R. F. H.; Schäfer, E. M.; Gaugler, P.; Shishavan, Z. H.; Gulabani, H.; Mao, H.; Zheng, N.; von Wirén, N.; Jessen, H. J.; Saiardi, A.; Bhattacharjee, S.; Laha, D.; Schaaf, G. ITPK1-Dependent Inositol Polyphosphates Regulate Auxin Responses in Arabidopsis thaliana, 2020. DOI: 10.1101/2020.04.23.058487.
(14) Lin, H.; Fridy, P. C.; Ribeiro, A. A.; Choi, J. H.; Barma, D. K.; Vogel, G.; Falck, J. R.; Shears, S. B.; York, J. D.; Mayr, G. W. Structural analysis and detection of biological inositol pyrophosphates reveal that the family of VIP/diphosphoinositol pentakisphosphate kinases are 1/3-kinases. *J. Biol. Chem.* **2009**, *284*, 1863−1872.
(15) Mulugu, S.; Bai, W.; Fridy, P. C.; Bastidas, R. J.; Otto, J. C.; Dollins, D. E.; Haystead, T. A.; Ribeiro, A. A.; York, J. D. A conserved family of enzymes that phosphorylate inositol hexakisphosphate. *Science* **2007**, *316*, 106−109.
(16) Saiardi, A.; Erdjument-Bromage, H.; Snowman, A. M.; Tempst, P.; Snyder, S. H. Synthesis of diphosphoinositol pentakisphosphate by a newly identified family of higher inositol polyphosphate kinases. *Curr. Biol.* **1999**, *9*, 1323−1326.
(17) Wang, H.; Falck, J. R.; Hall, T. M.; Shears, S. B. Structural basis for an inositol pyrophosphate kinase surmounting phosphate crowding. *Nat. Chem. Biol.* **2012**, *8*, 111−116.
(18) Laha, D.; Kamleitner, M.; Johnen, P.; Schaaf, G. Analyses of Inositol Phosphates and Phosphoinositides by Strong Anion Exchange (SAX)-HPLC. *Methods Mol. Biol.* **2021**, *2295*, 365−378.
(19) Qiu, D. Y.; Eisenbeis, V. B.; Saiardi, A.; Jessen, H. J. Absolute Quantitation of Inositol Pyrophosphates by Capillary Electrophoresis Electrospray Ionization Mass Spectrometry. *J. Vis. Exp.* **2021**, *174*, No. e62847.
(20) Desai, M.; Rangarajan, P.; Donahue, J. L.; Williams, S. P.; Land, E. S.; Mandal, M. K.; Phillippy, B. Q.; Perera, I. Y.; Raboy, V.; Gillaspy, G. E. Two inositol hexakisphosphate kinases drive inositol pyrophosphate synthesis in plants. *Plant J.* **2014**, *80*, 642−653.
(21) Flores, S.; Smart, C. C. Abscisic acid-induced changes in inositol metabolism in Spirodela polyrrhiza. *Planta* **2000**, *211*, 823−832.
(22) Lemtiri-Chlieh, F.; MacRobbie, E. A.; Brearley, C. A. Inositol hexakisphosphate is a physiological signal regulating the K+-inward rectifying conductance in guard cells. *Proc. Natl. Acad. Sci. U.S.A.* **2000**, *97*, 8687−8692.
(23) Qiu, D. Y.; Wilson, M. S.; Eisenbeis, V. B.; Harmel, R. K.; Riemer, E.; Haas, T. M.; Wittwer, C.; Jork, N.; Gu, C. F.; Shears, S. B.; Schaaf, G.; Kammerer, B.; Fiedler, D.; Saiardi, A.; Jessen, H. J. Analysis of inositol phosphate metabolism by capillary electrophoresis electrospray ionization mass spectrometry. *Nat. Commun.* **2020**, *11*, No. 6035.
(24) Laha, D.; Parvin, N.; Hofer, A.; Giehl, R. F. H.; Fernandez-Rebollo, N.; von Wiren, N.; Saiardi, A.; Jessen, H. J.; Schaaf, G. Arabidopsis ITPK1 and ITPK2 Have an Evolutionarily Conserved Phytic Acid Kinase Activity. *ACS Chem. Biol.* **2019**, *14*, 2127−2133.
(25) Adepoju, O.; Williams, S. P.; Craige, B.; Cridland, C. A.; Sharpe, A. K.; Brown, A. M.; Land, E.; Perera, I. Y.; Mena, D.; Sobrado, P.; Gillaspy, G. E. Inositol Trisphosphate Kinase and Diphosphoinositol Pentakisphosphate Kinase Enzymes Constitute the Inositol Pyrophosphate Synthesis Pathway in Plants, 2019. DOI: 10.1101/724914.
(26) Whitfield, H.; White, G.; Sprigg, C.; Riley, A. M.; Potter, B. V. L.; Hemmings, A. M.; Brearley, C. A. An ATP-responsive metabolic cassette comprised of inositol tris/tetrakisphosphate kinase 1 (ITPK1) and inositol pentakisphosphate 2-kinase (IPK1) buffers diphosphosphoinositol phosphate levels. *Biochem. J.* **2020**, *477*, 2621−2638.
(27) Wang, Z. R.; Kuo, H. F.; Chiou, T. J. Intracellular phosphate sensing and regulation of phosphate transport systems in plants. *Plant Physiol.* **2021**, *187*, 2043−2055.
(28) Ried, M. K.; Wild, R.; Zhu, J. S.; Pipercevic, J.; Sturm, K.; Broger, L.; Harmel, R. K.; Abriata, L. A.; Hothorn, L. A.; Fiedler, D.; Hiller, S.; Hothorn, M. Inositol pyrophosphates promote the interaction of SPX domains with the coiled-coil motif of PHR transcription factors to regulate plant phosphate homeostasis. *Nat. Commun.* **2021**, *12*, No. 384.
(29) Gerasimaite, R.; Pavlovic, I.; Capolicchio, S.; Hofer, A.; Schmidt, A.; Jessen, H. J.; Mayer, A. Inositol Pyrophosphate Specificity of the SPX-Dependent Polyphosphate Polymerase VTC. *ACS Chem. Biol.* **2017**, *12*, 648−653.
(30) Zhou, J.; Hu, Q.; Xiao, X.; Yao, D.; Ge, S.; Ye, J.; Li, H.; Cai, R.; Liu, R.; Meng, F.; Wang, C.; Zhu, J. K.; Lei, M.; Xing, W. Mechanism of phosphate sensing and signaling revealed by rice SPX1-PHR2 complex structure. *Nat. Commun.* **2021**, *12*, No. 7040.
(31) Rubio, V.; Linhares, F.; Solano, R.; Martin, A. C.; Iglesias, J.; Leyva, A.; Paz-Ares, J. A conserved MYB transcription factor involved in phosphate starvation signaling both in vascular plants and in unicellular algae. *Genes Dev.* **2001**, *15*, 2122−2133.
(32) Bustos, R.; Castrillo, G.; Linhares, F.; Puga, M. I.; Rubio, V.; Perez-Perez, J.; Solano, R.; Leyva, A.; Paz-Ares, J. A Central Regulatory System Largely Controls Transcriptional Activation and Repression Responses to Phosphate Starvation in Arabidopsis. *PLoS Genet.* **2010**, *6*, No. e1001102.
(33) Puga, M. I.; Mateos, I.; Charukesi, R.; Wang, Z.; Franco-Zorrilla, J. M.; de Lorenzo, L.; Irigoye, M. L.; Masiero, S.; Bustos, R.; Rodriguez, J.; Leyva, A.; Rubio, V.; Sommer, H.; Paz-Ares, J. SPX1 is a phosphate-dependent inhibitor of PHOSPHATE STARVATION RESPONSE 1 in Arabidopsis. *Proc. Natl. Acad. Sci. U.S.A.* **2014**, *111*, 14947−14952.
(34) Fridy, P. C.; Otto, J. C.; Dollins, D. E.; York, J. D. Cloning and characterization of two human VIP1-like inositol hexakisphosphate

and diphosphoinositol pentakisphosphate kinases. *J. Biol. Chem.* **2007**, *282*, 30754−30762.
(35) Wang, H.; Nair, V. S.; Holland, A. A.; Capolicchio, S.; Jessen, H. J.; Johnson, M. K.; Shears, S. B. Asp1 from Schizosaccharomyces pombe binds a [2Fe-2S](2+) cluster which inhibits inositol pyrophosphate 1-phosphatase activity. *Biochemistry* **2015**, *54*, 6462−6474.
(36) Pascual-Ortiz, M.; Saiardi, A.; Walla, E.; Jakopec, V.; Kunzel, N. A.; Span, I.; Vangala, A.; Fleig, U. Asp1 Bifunctional Activity Modulates Spindle Function via Controlling Cellular Inositol Pyrophosphate Levels in Schizosaccharomyces pombe. *Mol. Cell. Biol.* **2018**, *38*, No. e00047-18.
(37) Kilari, R. S.; Weaver, J. D.; Shears, S. B.; Safrany, S. T. Understanding inositol pyrophosphate metabolism and function: Kinetic characterization of the DIPPs. *FEBS Lett.* **2013**, *587*, 3464−3470.
(38) Caffrey, J. J.; Hidaka, K.; Matsuda, M.; Hirata, M.; Shears, S. B. The human and rat forms of multiple inositol polyphosphate phosphatase: functional homology with a histidine acid phosphatase up-regulated during endochondral ossification. *FEBS Lett.* **1999**, *442*, 99−104.
(39) Safrany, S. T.; Ingram, S. W.; Cartwright, J. L.; Falck, J. R.; McLennan, A. G.; Barnes, L. D.; Shears, S. B. The diadenosine hexaphosphate hydrolases from Schizosaccharomyces pombe and Saccharomyces cerevisiae are homologues of the human diphosphoinositol polyphosphate phosphohydrolase - Overlapping substrate specificities in a MutT-type protein. *J. Biol. Chem.* **1999**, *274*, 21735−21740.
(40) Andreeva, N.; Ledova, L.; Ryazanova, L.; Tomashevsky, A.; Kulakovskaya, T.; Eldarov, M. Ppn2 endopolyphosphatase overexpressed in Saccharomyces cerevisiae: Comparison with Ppn1, Ppx1, and Ddp1 polyphosphatases. *Biochimie* **2019**, *163*, 101−107.
(41) Lonetti, A.; Szijgyarto, Z.; Bosch, D.; Loss, O.; Azevedo, C.; Saiardi, A. Identification of an Evolutionarily Conserved Family of Inorganic Polyphosphate Endopolyphosphatases. *J. Biol. Chem.* **2011**, *286*, 31966−31974.
(42) Steidle, E. A.; Chong, L. S.; Wu, M.; Crooke, E.; Fiedler, D.; Resnick, A. C.; Rolfes, R. J. A Novel Inositol Pyrophosphate Phosphatase in Saccharomyces cerevisiae: Siw14 PROTEIN SELECTIVELY CLEAVES THE beta-PHOSPHATE FROM 5-DIPHOSPHOINOSITOL PENTAKISPHOSPHATE (5PP-IP5). *J. Biol. Chem.* **2016**, *291*, 6772−6783.
(43) Wang, H.; Gu, C.; Rolfes, R. J.; Jessen, H. J.; Shears, S. B. Structural and biochemical characterization of Siw14: A protein-tyrosine phosphatase fold that metabolizes inositol pyrophosphates. *J. Biol. Chem.* **2018**, *293*, 6905−6914.
(44) Romá-Mateo, C.; Sacristan-Reviriego, A.; Beresford, N. J.; Caparros-Martin, J. A.; Culianez-Macia, F. A.; Martin, H.; Molina, M.; Tabernero, L.; Pulido, R. Phylogenetic and genetic linkage between novel atypical dual-specificity phosphatases from non-metazoan organisms. *Mol. Genet. Genomics* **2011**, *285*, 341−354.
(45) Romá-Mateo, C.; Rios, P.; Tabernero, L.; Attwood, T. K.; Pulido, R. A novel phosphatase family, structurally related to dual-specificity phosphatases, that displays unique amino acid sequence and substrate specificity. *J. Mol. Biol.* **2007**, *374*, 899−909.
(46) Aceti, D. J.; Bitto, E.; Yakunin, A. F.; Proudfoot, M.; Bingman, C. A.; Frederick, R. O.; Sreenath, H. K.; Vojtik, F. C.; Wrobel, R. L.; Fox, B. G.; Markley, J. L.; Phillips, G. N. Structural and functional characterization of a novel phosphatase from the Arabidopsis thaliana gene locus At1g05000. *Proteins* **2008**, *73*, 241−253.
(47) Nagy, R.; Grob, H.; Weder, B.; Green, P.; Klein, M.; Frelet-Barrand, A.; Schjoerring, J. K.; Brearley, C.; Martinoia, E. The Arabidopsis ATP-binding cassette protein AtMRP5/AtABCC5 is a high affinity inositol hexakisphosphate transporter involved in guard cell signaling and phytate storage. *J. Biol. Chem.* **2009**, *284*, 33614−33622.
(48) Irvine, R. F.; Schell, M. J. Back in the water: the return of the inositol phosphates. *Nat. Rev. Mol. Cell Biol.* **2001**, *2*, 327−338.
(49) Blüher, D.; Laha, D.; Thieme, S.; Hofer, A.; Eschen-Lippold, L.; Masch, A.; Balcke, G.; Pavlovic, I.; Nagel, O.; Schonsky, A.; Hinkelmann, R.; Wörner, J.; Parvin, N.; Greiner, R.; Weber, S.; Tissier, A.; Schutkowski, M.; Lee, J.; Jessen, H.; Schaaf, G.; Bonas, U. A 1-phytase type III effector interferes with plant hormone signaling. *Nat. Commun.* **2017**, *8*, No. 2159.
(50) Osada, S.; Kageyama, K.; Ohnishi, Y.; Nishikawa, J.; Nishihara, T.; Imagawa, M. Inositol phosphate kinase Vip1p interacts with histone chaperone Asf1p in Saccharomyces cerevisiae. *Mol. Biol. Rep.* **2012**, *39*, 4989−4996.
(51) Steidle, E. A.; Morrissette, V. A.; Fujimaki, K.; Chong, L.; Resnick, A. C.; Capaldi, A. P.; Rolfes, R. J. The InsP7 phosphatase Siw14 regulates inositol pyrophosphate levels to control localization of the general stress response transcription factor Msn2. *J. Biol. Chem.* **2020**, *295*, 2043−2056.
(52) Brown, J. A.; Sherlock, G.; Myers, C. L.; Burrows, N. M.; Deng, C.; Wu, H. I.; McCann, K. E.; Troyanskaya, O. G.; Brown, J. M. Global analysis of gene function in yeast by quantitative phenotypic profiling. *Mol. Syst. Biol.* **2006**, *2*, No. 2006.0001.
(53) Arcaro, A.; Wymann, M. P. Wortmannin is a potent phosphatidylinositol 3-kinase inhibitor: the role of phosphatidylinositol 3,4,5-trisphosphate in neutrophil responses. *Biochem. J.* **1993**, *296*, 297−301.
(54) Saiardi, A.; Resnick, A. C.; Snowman, A. M.; Wendland, B.; Snyder, S. H. Inositol pyrophosphates regulate cell death and telomere length through phosphoinositide 3-kinase-related protein kinases. *Proc. Natl. Acad. Sci. U.S.A.* **2005**, *102*, 1911−1914.
(55) Estevez, F.; Pulford, D.; Stark, M. J.; Carter, A. N.; Downes, C. P. Inositol trisphosphate metabolism in Saccharomyces cerevisiae: identification, purification and properties of inositol 1,4,5-trisphosphate 6-kinase. *Biochem. J.* **1994**, *302*, 709−716.
(56) Kuo, H. F.; Hsu, Y. Y.; Lin, W. C.; Chen, K. Y.; Munnik, T.; Brearley, C. A.; Chiou, T. J. Arabidopsis inositol phosphate kinases IPK1 and ITPK1 constitute a metabolic pathway in maintaining phosphate homeostasis. *Plant J.* **2018**, *95*, 613−630.
(57) Stevenson-Paulik, J.; Bastidas, R. J.; Chiou, S. T.; Frye, R. A.; York, J. D. Generation of phytate-free seeds in Arabidopsis through disruption of inositol polyphosphate kinases. *Proc. Natl. Acad. Sci. U.S.A.* **2005**, *102*, 12612−12617.
(58) Safrany, S. T.; Caffrey, J. J.; Yang, X.; Bembenek, M. E.; Moyer, M. B.; Burkhart, W. A.; Shears, S. B. A novel context for the 'MutT' module, a guardian of cell integrity, in a diphosphoinositol polyphosphate phosphohydrolase. *EMBO J.* **1998**, *17*, 6599−6607.
(59) Gruber, B. D.; Giehl, R. F.; Friedel, S.; von Wiren, N. Plasticity of the Arabidopsis root system under nutrient deficiencies. *Plant Physiol.* **2013**, *163*, 161−179.
(60) Loqué, D.; Lalonde, S.; Looger, L. L.; von Wiren, N.; Frommer, W. B. A cytosolic trans-activation domain essential for ammonium uptake. *Nature* **2007**, *446*, 195−198.
(61) Nakamura, S.; Mano, S.; Tanaka, Y.; Ohnishi, M.; Nakamori, C.; Araki, M.; Niwa, T.; Nishimura, M.; Kaminaka, H.; Nakagawa, T.; Sato, Y.; Ishiguro, S. Gateway Binary Vectors with the Bialaphos Resistance Gene, as a Selection Marker for Plant Transformation. *Biosci., Biotechnol., Biochem.* **2010**, *74*, 1315−1319.
(62) Gueldener, U.; Heinisch, J.; Koehler, G. J.; Voss, D.; Hegemann, J. H. A second set of loxP marker cassettes for Cre-mediated multiple gene knockouts in budding yeast. *Nucleic Acids Res.* **2002**, *30*, No. e23.
(63) Onnebo, S. M.; Saiardi, A. Inositol pyrophosphates modulate hydrogen peroxide signalling. *Biochem. J.* **2009**, *423*, 109−118.
(64) Gietz, R. D.; Schiestl, R. H.; Willems, A. R.; Woods, R. A. Studies on the transformation of intact yeast cells by the LiAc/SS-DNA/PEG procedure. *Yeast* **1995**, *11*, 355−360.
(65) Zonneveld, B. J. M. B.J.M. Zonneveld. 1986. Cheap and simple yeast media. *J. Microb. Methods* **1986**, *4*, 287−291.
(66) Schaaf, G.; Betts, L.; Garrett, T. A.; Raetz, C. R.; Bankaitis, V. A. Crystallization and preliminary X-ray diffraction analysis of phospholipid-bound Sfh1p, a member of the *Saccharomyces cerevisiae*

Sec. 14p-like phosphatidylinositol transfer protein family. *Acta Crystallogr., Sect. F* **2006**, *62*, 1156−1160.
(67) Capolicchio, S.; Thakor, D. T.; Linden, A.; Jessen, H. J. Synthesis of unsymmetric diphospho-inositol polyphosphates. *Angew. Chem., Int. Ed.* **2013**, *52*, 6912−6916.
(68) Capolicchio, S.; Wang, H.; Thakor, D. T.; Shears, S. B.; Jessen, H. J. Synthesis of Densely Phosphorylated Bis-1,5-Diphospho-myo-Inositol Tetrakisphosphate and its Enantiomer by Bidirectional P-Anhydride Formation. *Angew. Chem., Int. Ed.* **2014**, *53*, 9508−9511.
(69) Azevedo, C.; Saiardi, A. Extraction and analysis of soluble inositol polyphosphates from yeast. *Nat. Protoc.* **2006**, *1*, 2416−2422.
(70) Gaugler, P.; Gaugler, V.; Kamleitner, M.; Schaaf, G. Extraction and Quantification of Soluble, Radiolabeled Inositol Polyphosphates from Different Plant Species using SAX-HPLC. *J. Vis. Exp.* **2020**, *160*, No. e61495.
(71) Wang, H.; Perera, L.; Jork, N.; Zong, G.; Riley, A. M.; Potter, B. V. L.; Jessen, H. J.; Shears, S. B. A structural expose of noncanonical molecular reactivity within the protein tyrosine phosphatase WPD loop. *Nat. Commun.* **2022**, *13*, No. 2231.

https://doi.org/10.1021/acs.biochem.2c00145
Biochemistry 2022, 61, 1213−1227

Supporting Information

Short title

A. thaliana **inositol pyrophosphate phosphohydrolases**

Article title

Arabidopsis PFA-DSP-type phosphohydrolases target specific inositol pyrophosphate messengers

Philipp Gaugler[1§], Robin Schneider[1§], Guizhen Liu[2], Danye Qiu[2], Jonathan Weber[1], Jochen Schmid[3&], Nikolaus Jork[2,4], Markus Häner[2], Kevin Ritter[2], Nicolás Fernández-Rebollo[3], Ricardo F.H. Giehl[5], Minh Nguyen Trung[6], Ranjana Yadav[7], Dorothea Fiedler[6], Verena Gaugler[1], Henning J. Jessen[2], Gabriel Schaaf[1]*, Debabrata Laha[7]*

[1]Department of Plant Nutrition, Institute of Crop Science and Resource Conservation, Rheinische Friedrich-Wilhelms-Universität Bonn, 53115 Bonn, Germany

[2]Department of Chemistry and Pharmacy and CIBSS-Centre for Integrative Biological Signalling Studies, Albert-Ludwigs University Freiburg, 79104 Freiburg, Germany

[3]Center for Plant Molecular Biology, Department of Plant Physiology, Eberhard Karls University Tübingen, 72076 Tübingen, Germany

[4]Spemann Graduate School of Biology and Medicine (SGBM), University of Freiburg, 79104 Freiburg, Germany

[5]Department of Physiology & Cell Biology, Leibniz-Institute of Plant Genetics and Crop Plant Research, 06466 Gatersleben, Germany

[6]Leibniz-Forschungsinstitut für Molekulare Pharmakologie, 13125 Berlin, Germany; Department of Chemistry, Humboldt Universität zu Berlin, 12489 Berlin, Germany.

[7]Department of Biochemistry, Indian Institute of Science (IISc), Bengaluru-560012, India

[§]P.G. and R.S. contributed equally to this manuscript

*E-mail: gabriel.schaaf@uni-bonn.de, dlaha@iisc.ac.in

ORCID IDs: P.G.: 0000-0002-9187-404X, R.S. 0000-0002-9657-4548, G.L. 0000-0003-1748-6687, DQ: 0000-0003-2197-3218, J.S.: 0000-0001-7527-7088, N.J.: 0000-0002-3717-443X, M.H.: 0000-0003-3313-4868, K.R.: 0000-0001-7900-1855, N.F.R.: 0000-0003-3556-8766, R.F.H.G: 0000-0003-1006-3163, M.N.T.: 0000-0003-3100-9609, R.Y.: 0000-0003-4956-5638, D.F.: 0000-0002-0798-946X, V.G.: 0000-0002-3249-2922, H.J.J: 0000-0002-1025-9484, GS: 0000-0001-9022-4515, D.L.: 0000-0002-7823-5489

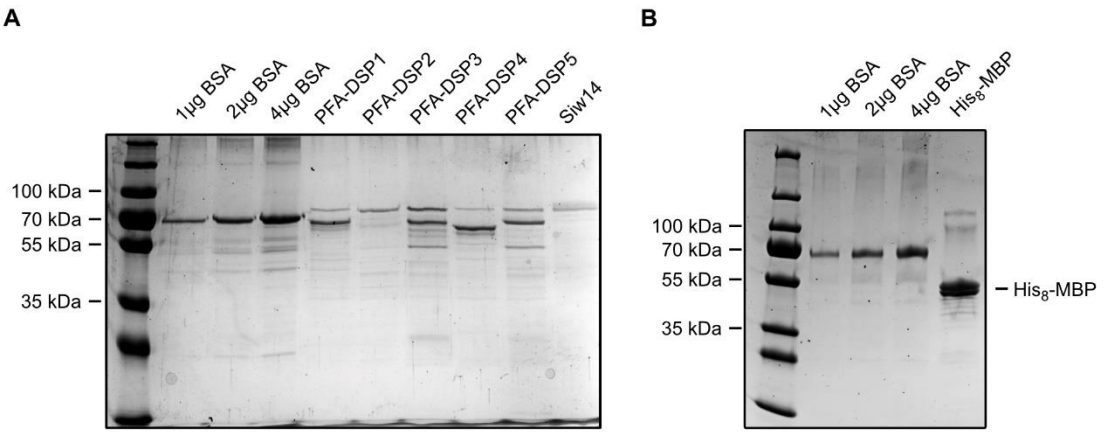

Figure S1: Purification of PFA-DSP proteins. (A, B) Recombinant His-MBP-PFA-DSPs or His-MBP-Siw14 were expressed in *E. coli* and purified with Ni-NTA resin as described in methods. Dialyzed proteins were denatured and separated by SDS-PAGE in parallel with BSA standards to determine protein concentrations by staining with Coomassie blue.

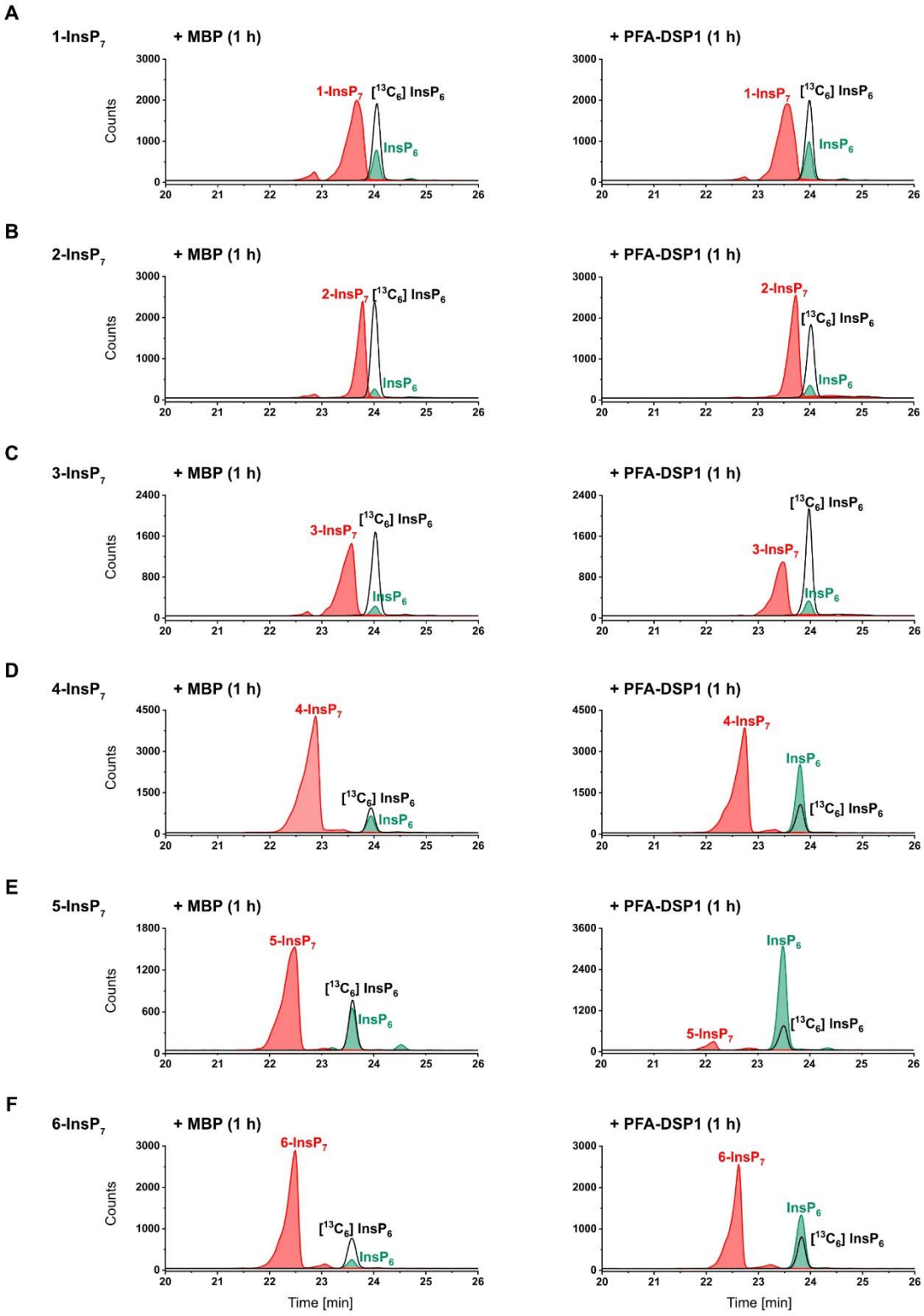

Figure S2: *In vitro*, *Arabidopsis* PFA-DSP1 displays robust PP-InsP phosphohydrolase activity against 5-InsP$_7$ and partial phosphohydrolase activity against 4-InsP$_7$ and 6-InsP$_7$, respectively. (A – F) 0.4 µM PFA-DSP1 was incubated with 0.33 mM InsP$_7$ and 1 mM $MgCl_2$ for 1 h. The reaction product was spiked with an isotopic standards mixture ([$^{13}C_6$]1,5-InsP$_8$, [$^{13}C_6$]5-InsP$_7$, [$^{13}C_6$]1-InsP$_7$, [$^{13}C_6$] InsP$_6$, [$^{13}C_6$]2-OH InsP$_5$) and subjected to CE-ESI-MS analyses. Representative extracted-ion electropherograms of samples shown in Figure 1.

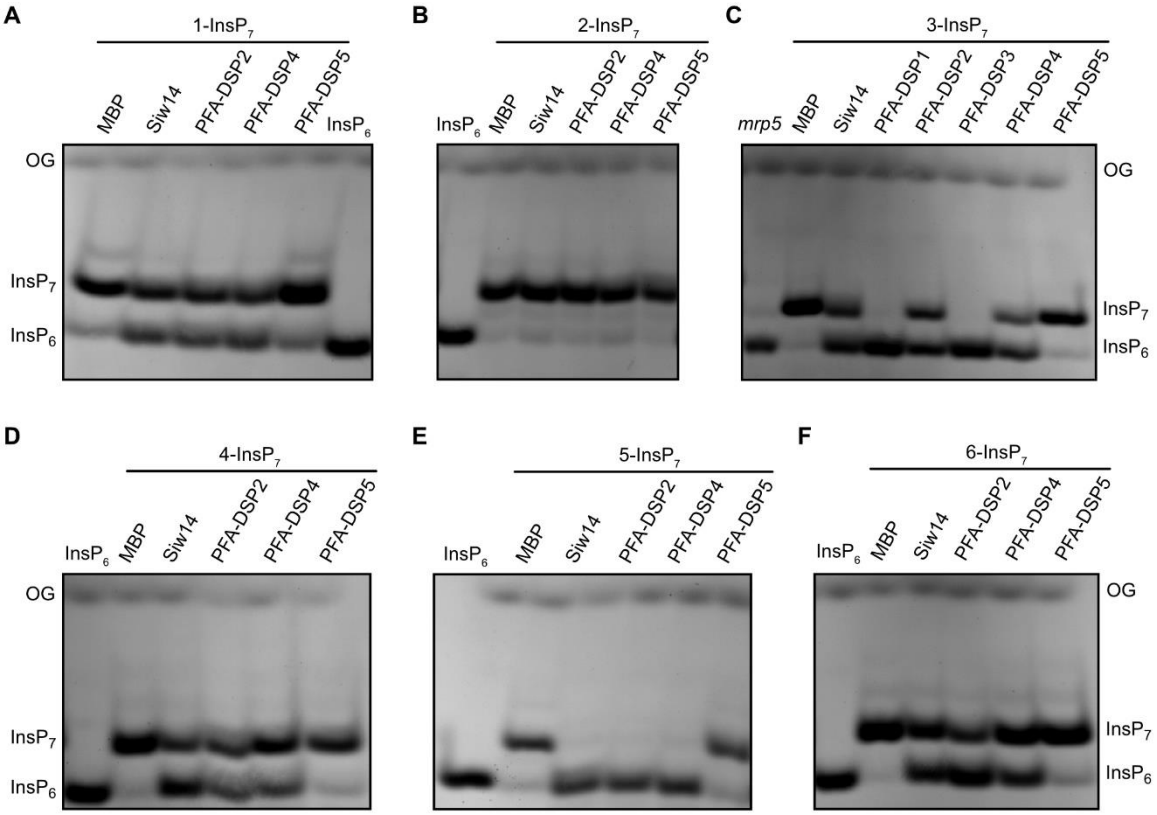

Figure S3: In the absence of divalent cations, all $InsP_7$ isomers with the exception of 2-$InsP_7$ become substrates for selected *Arabidopsis* PFA-DSPs *in vitro*. (A – F) Approximately 0.4 µM His-MBP-PFA-DSPs and His-MBP were incubated with 1 mM EDTA and 0.33 mM $InsP_7$ for 1 h at 22°C. His-MBP served as a negative control. The reaction products were separated by 33 % PAGE and visualized with toluidine blue. The identity of bands was determined by migration compared to $InsP_6$ or (C) compared to TiO_2-purified *mrp5* seed extract.

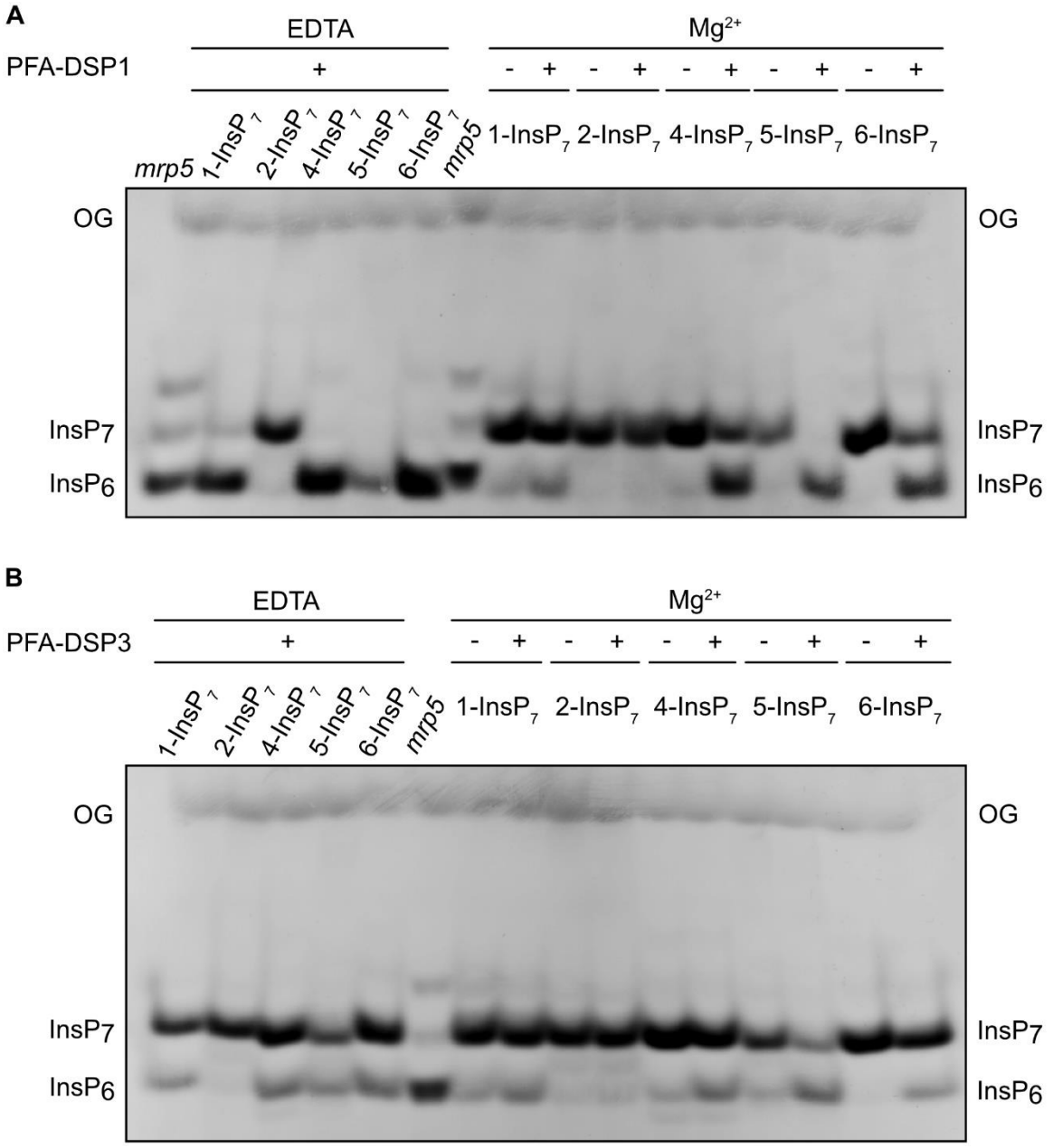

Figure S4: In the presence of Mg^{2+}, PFA-DSP1 and PFA-DSP3 display robust *in vitro* $InsP_7$ phosphohydrolase activity with high specificity for the 5-β-phosphate. (A – B) Approximately 0.4 µM His-MBP-PFA-DSP1 and His-MBP-PFA-DSP3 were incubated with 0.33 mM $InsP_7$ and 1 mM EDTA or 1 mM $MgCl_2$ for 1 h at 22°C. His-MBP served as a negative control. The reaction products were separated by 33 % PAGE and visualized with toluidine blue. The identity of bands was determined by migration compared to TiO_2-purified *mrp5* seed extract.

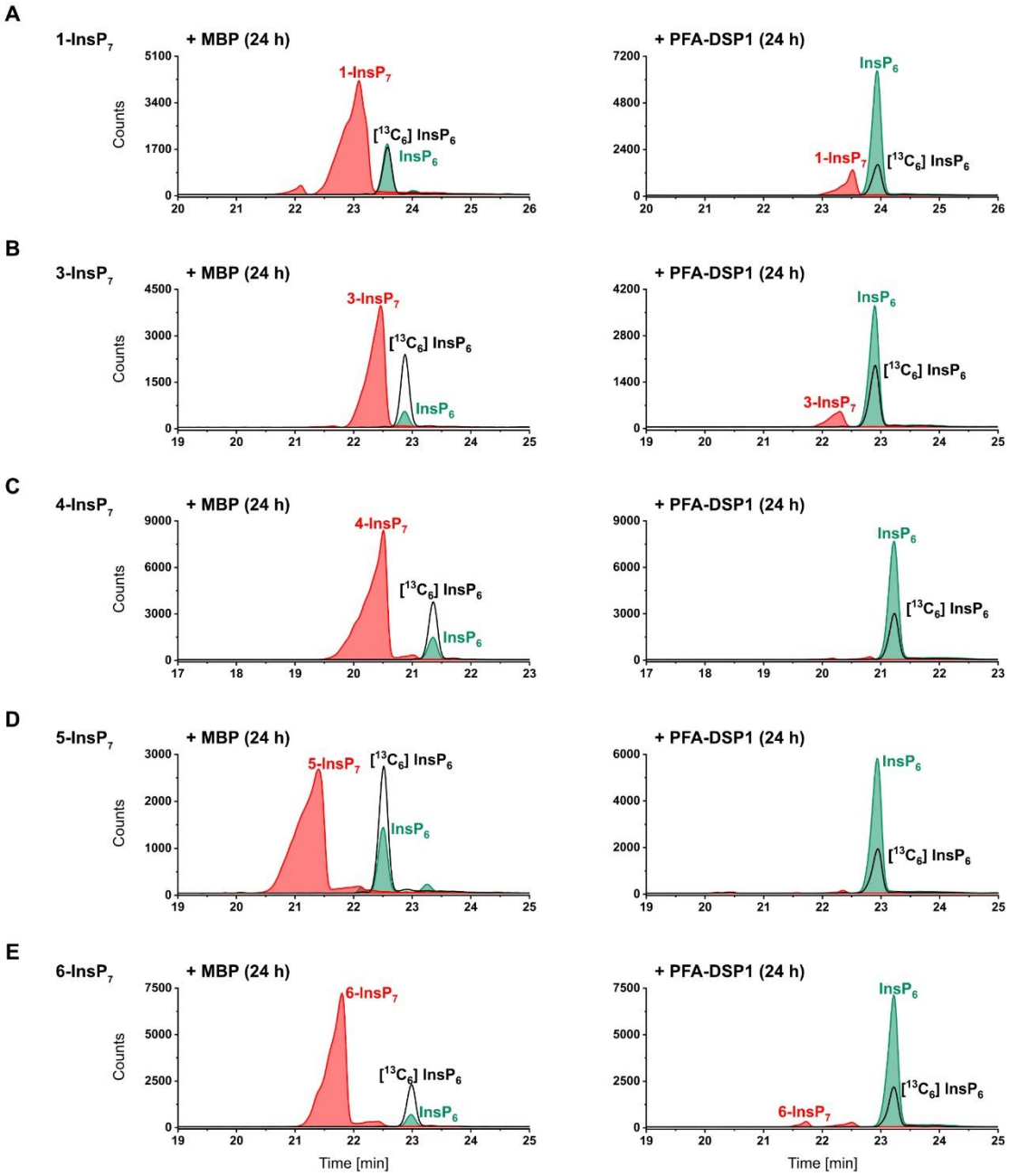

Figure S5: Under prolonged incubation time, *Arabidopsis* PFA-DSP1 efficiently hydrolyzes 5-InsP$_7$, 4-InsP$_7$ and 6-InsP$_7$ but only displays partial activities against 1-InsP$_7$ and 3-InsP$_7$. (A – E) 0.4 µM PFA-DSP1 was incubated with 0.33 mM InsP$_7$ and 1 mM $MgCl_2$ for 24 h. The reaction product was spiked with an isotopic standards mixture ([$^{13}C_6$]1,5-InsP$_8$, [$^{13}C_6$]5-InsP$_7$, [$^{13}C_6$]1-InsP$_7$, [$^{13}C_6$] InsP$_6$, [$^{13}C_6$]2-OH InsP$_5$) and subjected to CE-ESI-MS analyses. Representative extracted-ion electropherograms of samples shown in Figure 2.

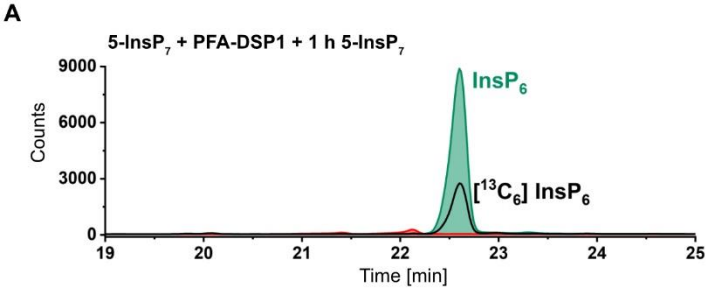

Figure S6: *Arabidopsis* PFA-DSP1 maintains 5-InsP$_7$ phosphohydrolase activity during prolonged incubation time *in vitro*. (A) 0.4 µM PFA-DSP1 was incubated with 0.33 mM 5-InsP$_7$ and 1 mM $MgCl_2$ for 24 h. To ensure that PFA-DSP1 is active during the whole incubation time, 0.33 mM 5-InsP$_7$ was added after 23 h and incubated for another 1 h. The reaction product was spiked with an isotopic standards mixture ([$^{13}C_6$]1,5-InsP$_8$, [$^{13}C_6$]5-InsP$_7$, [$^{13}C_6$]1-InsP$_7$, [$^{13}C_6$] InsP$_6$, [$^{13}C_6$]2-OH InsP$_5$) and subjected to CE-ESI-MS analyses.

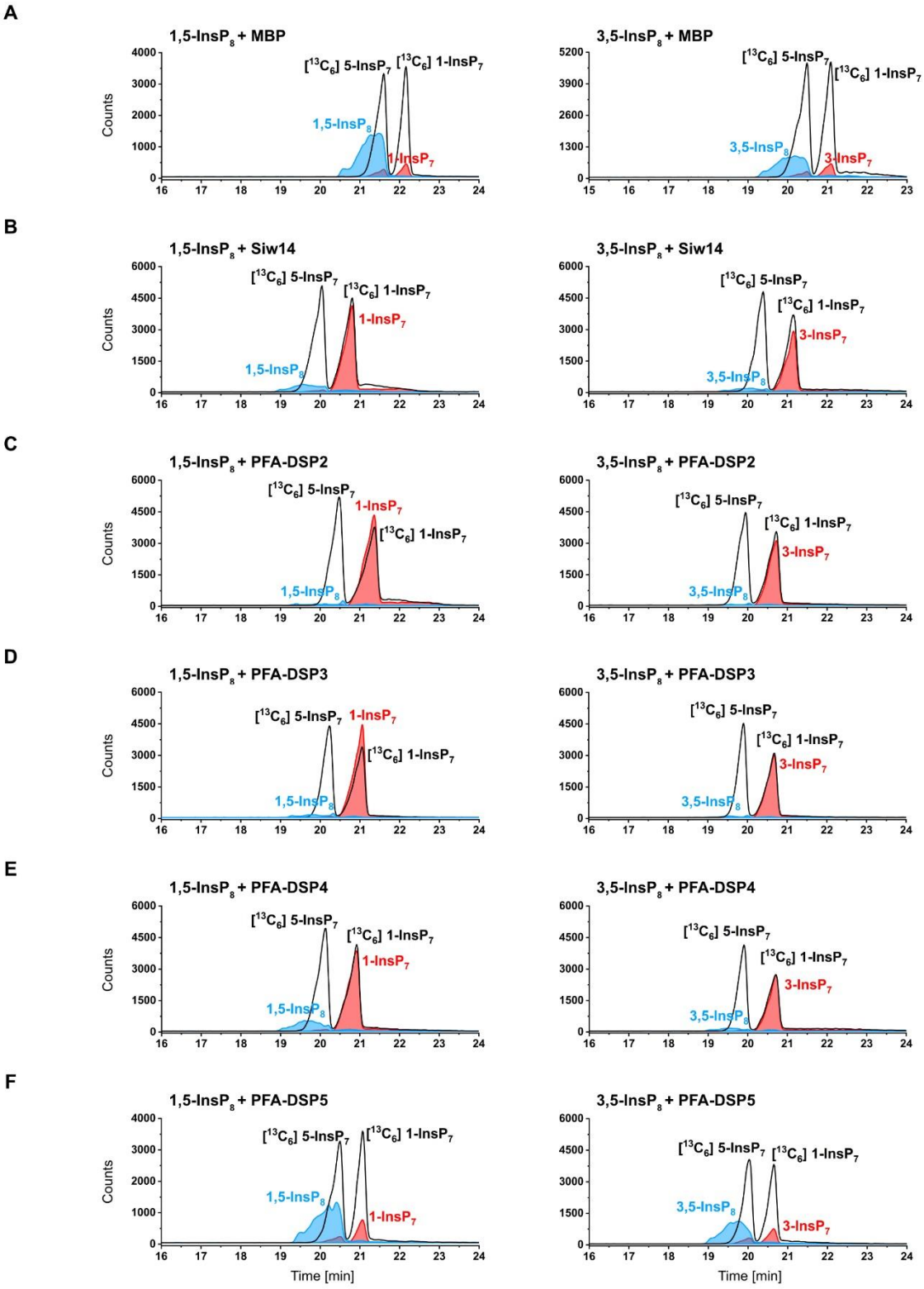

Figure S7: *In vitro*, *Arabidopsis* PFA-DSPs display robust 1/3,5-InsP$_8$ phosphohydrolase activity. (A – F) Approximately 0.4 µM His-MBP-PFA-DSPs and His-MBP-Siw14 were incubated with 0.33 mM 1,5-InsP$_8$ or 3,5-InsP$_8$ and 1 mM $MgCl_2$ for 1 h. The reaction products were spiked with isotopic standards mixture ([$^{13}C_6$]1,5-InsP$_8$, [$^{13}C_6$]5-InsP$_7$, [$^{13}C_6$]1-InsP$_7$, [$^{13}C_6$] InsP$_6$, [$^{13}C_6$]2-OH InsP$_5$) and subjected to CE-ESI-MS analyses. Representative extracted-ion electropherograms of samples shown in Figure 3C.

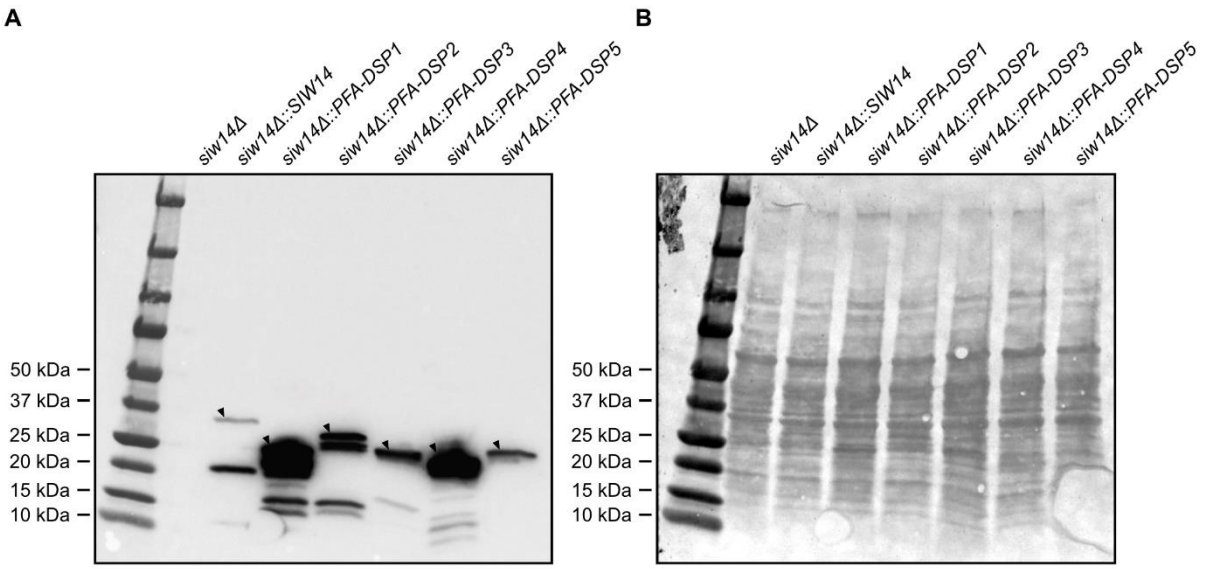

Figure S8: All five PFA-DSP homologs are stably expressed in the *siw14Δ* yeast strain. Immunoblot analyses of protein extracts from *siw14Δ* yeast transformed with either empty pDRf1-GW plasmid or pDRf1-GW carrying *SIW14* or *PFA-DSP1–5* encoding translational fusions with a C-terminal V5-tag. (A) For detection of V5-tagged proteins, an anti-V5 tag primary antibody (Invitrogen; 1:2000 dilution) and an anti-mouse secondary antibody coupled with HRP (Bio-Rad; goat; 1:10000 dilution) were used. The chemiluminescence signal of the ECL substrate (Bio-Rad) was detected using the ChemiDoc MP imager (Bio-Rad). Black arrows indicate the specific protein bands based on the calculated molecular weight. (B) Ponceau staining of the same blot.

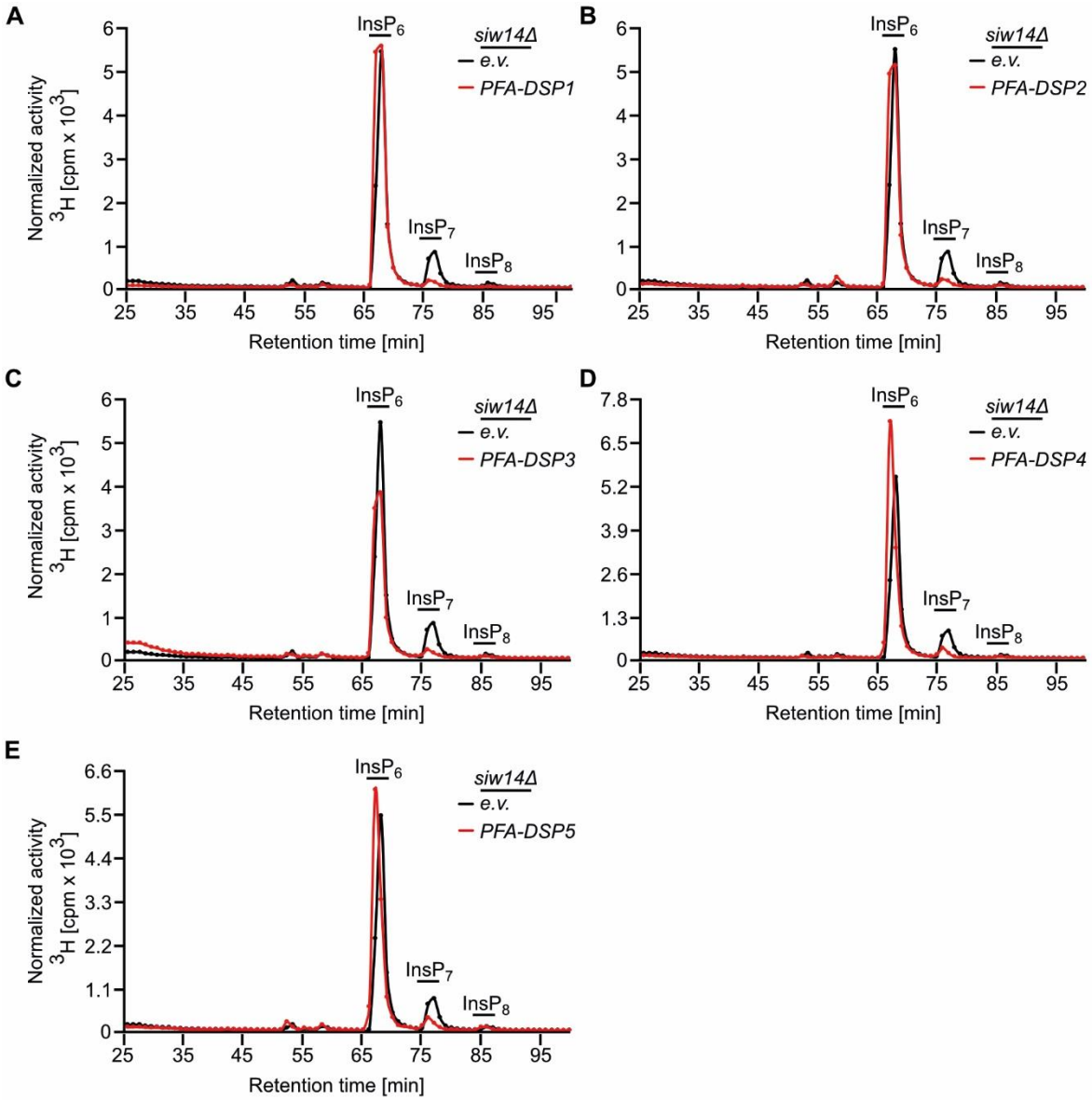

Figure S9: Heterologous expression of *Arabidopsis* PFA-DSPs complements *siw14Δ*-associated defects in $InsP_7/InsP_6$ ratios in yeast. (A - E) SAX-HPLC profiles of radiolabeled *siw14Δ* yeast transformed with either empty pDRf1-GW plasmid (e.v.) or pDRf1-GW carrying *PFA-DSP1 - 5*. Depicted is a representative analysis of each *PFA-DSP* transformant, with the same analysis of a representative empty vector transformant shown in the same profile in each graph. The experiment was repeated twice (n = 3) with similar results (combined data shown in Figure 4B).

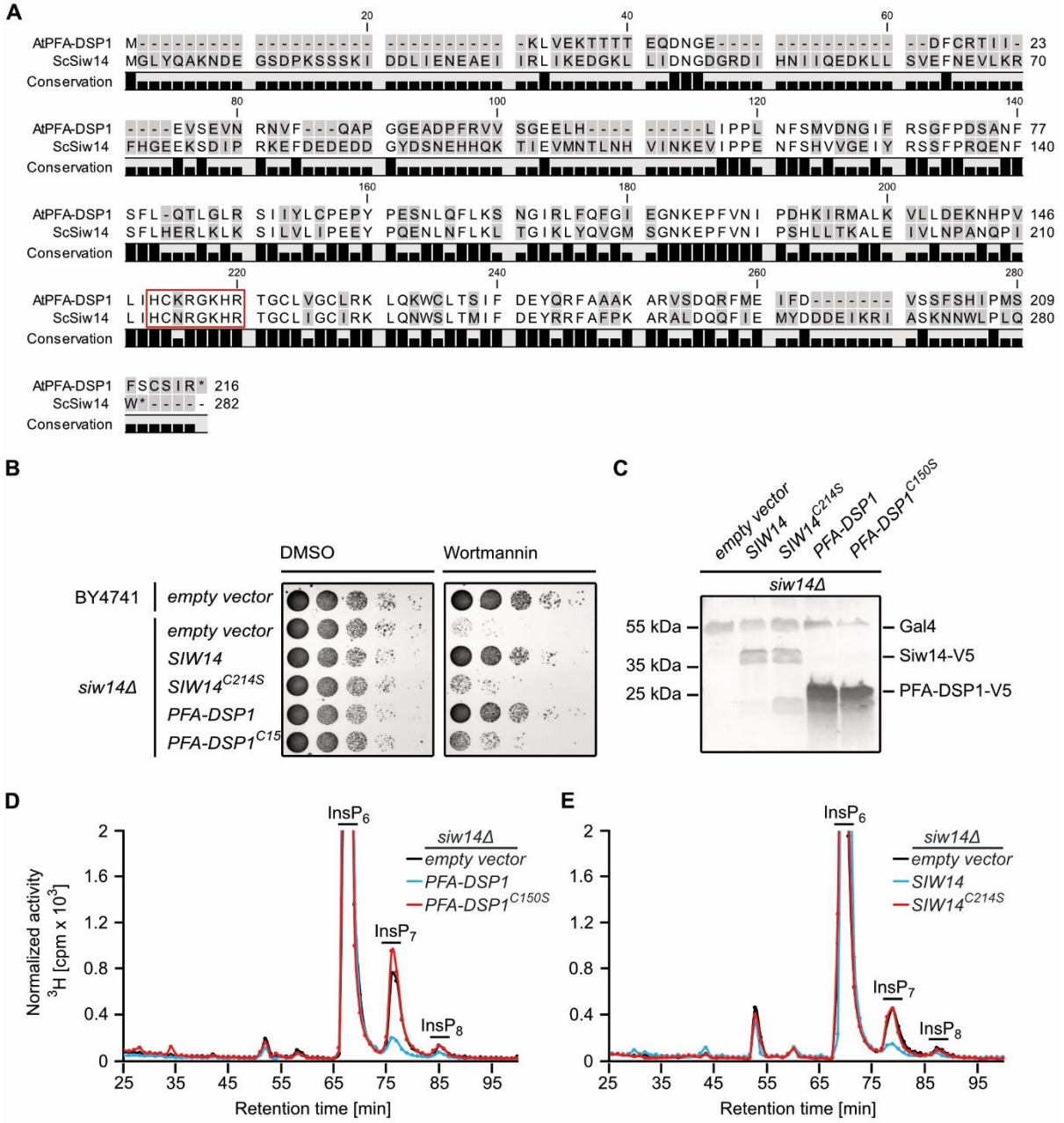

Figure S10: Complementation of *siw14Δ*-associated growth defects depends on catalytic activity. (A) Protein alignment of Siw14 from yeast and its homolog PFA-DSP1 from *Arabidopsis thaliana*. Identical amino acids are shown in black, different residues are highlighted with grey boxes. The conserved PTP (Protein Tyrosine Phosphatase) signature motif HC(X)5R is highlighted with the red box. The alignment was generated via the Multiple Alignments function of CLC Main Workbench 8 (QIAGEN). (B) Growth complementation assay with *siw14Δ*. Wild-type yeast (BY4741) and the *siw14Δ* yeast mutant were transformed with pDRf1-GW plasmids carrying either *SIW14* or its catalytic mutant C214S or carrying *PFA-DSP1* or its catalytic mutant C150S. Yeast strains transformed with empty pDRf1-GW vector as indicated served as controls. Transformants were then spotted in 8-fold serial dilutions (starting from OD 1.0) onto selective media containing wortmannin solved in DMSO or DMSO alone as control. Plates were incubated at 26 °C for 2 days before photographing. (C) Immunoblotting of Siw14, Siw14^{C214S}, PFA-DSP1 and PFA-DSP1^{C150S}. For detection of V5-tagged proteins an anti-V5 tag primary antibody

(Invitrogen; 1:2000 dilution) and an anti-mouse secondary antibody coupled with Alexa Fluor plus 800 (Invitrogen; goat; 1:20000 dilution) were used. As loading control, Gal4 protein levels were detected simultaneously using a polyclonal anti-Gal4 antibody (Santa Cruz; 1:1000 dilution) and an anti-rabbit StarBright Blue 700 antibody (Bio-Rad, goat; 1:2500 dilution). The signal was detected using the multiplex function of the ChemiDoc MP imager (Bio-Rad). (D) SAX-HPLC profiles of extracts of radiolabeled *siw14Δ* yeast transformed with either empty pDRf1-GW plasmid (empty vector) or pDRf1-GW carrying either *SIW14* or *SIW14*^{C214S}. (E) SAX-HPLC profiles of radiolabeled *siw14Δ* yeast transformed with either empty pDRf1-GW plasmid (e.v.) or pDRf1-GW carrying either *PFA-DSP1* or *PFA-DSP1*^{C150S}. (B – E) The experiments were repeated independently with similar results.

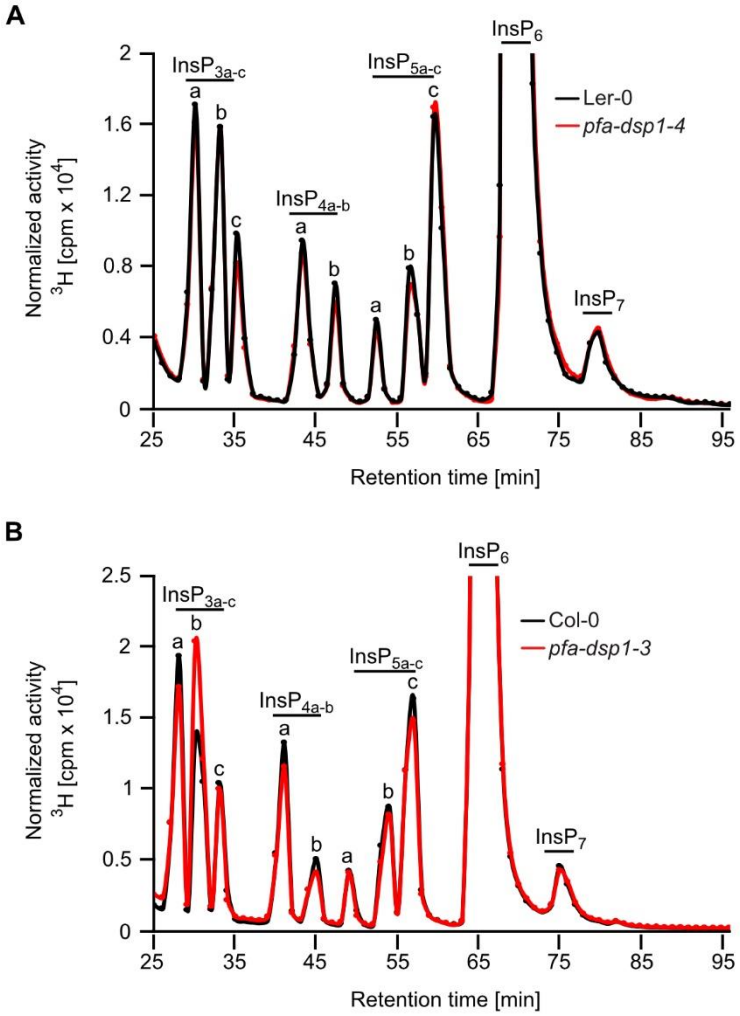

Figure S11: Single mutant *Arabidopsis pfa-dsp1* loss-of-function lines do not display InsP/PP-InsP defects. Representative SAX-HPLC profiles of 20-days-old wild-type Ler-0 and *pfa-dsp1-4 Arabidopsis* seedlings (A) and of Col-0 and *pfa-dsp1-3 Arabidopsis* seedlings (B) radiolabeled with [^{3}H]-*myo*-inositol. All visible peaks are highlighted and assigned to the corresponding InsP species. Based on published chromatographic mobilities [1, 2], $InsP_{4a}$ likely represents Ins(1,4,5,6)P_4 or Ins(3,4,5,6)P_4, $InsP_{5a}$ likely represents $InsP_5$ [2-OH], $InsP_{5b}$ likely represents $InsP_5$ [4-OH] or its enantiomeric form $InsP_5$ [6-OH], and $InsP_{5c}$ likely represents $InsP_5$ [1-OH] or its enantiomeric form $InsP_5$ [3-OH]. The isomeric natures of $InsP_{3a-c}$, $InsP_{4b}$, $InsP_7$, and $InsP_8$ are unknown.

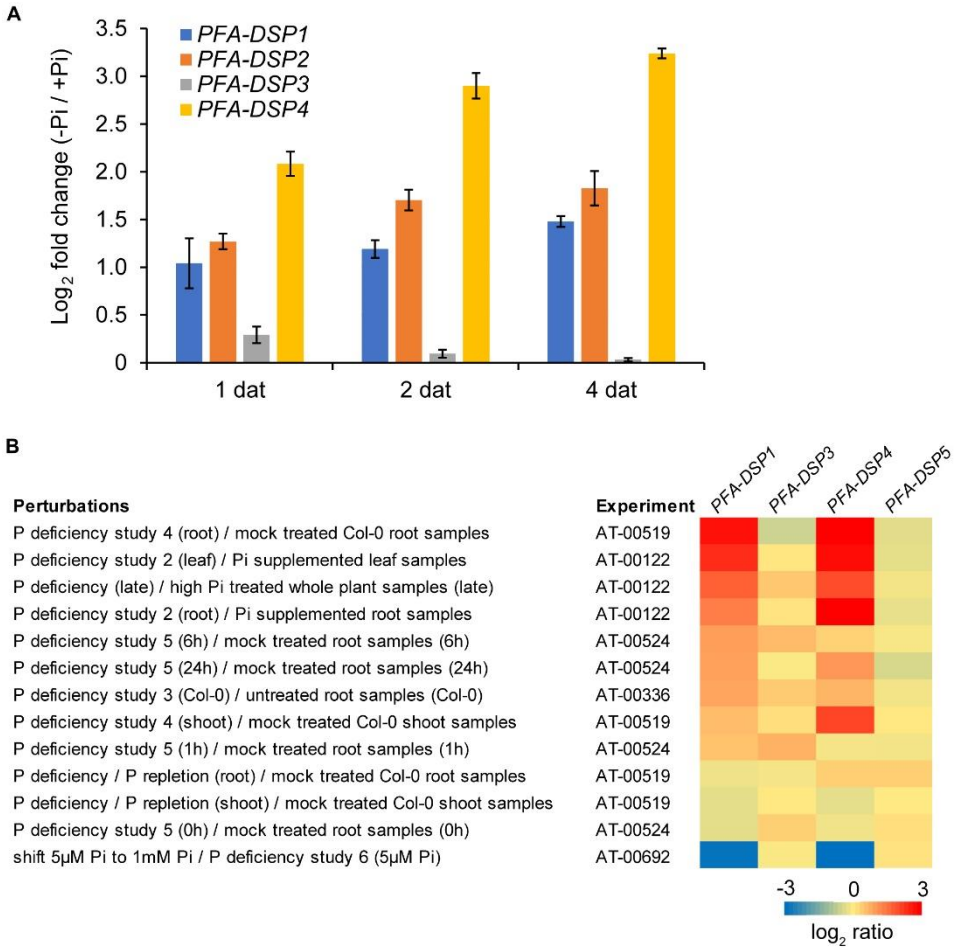

Figure S12: *Arabidopsis PFA-DSP1*, *2* and *4* are strongly induced by P_i deficiency. (A) Expression of the indicated *PFA-DSP*s in roots of *Aradidopsis thaliana* (accession Col-0) plants according to a transcriptome experiment with Agilent microarrays [3]; data deposited on e!DAL repository under the accession code https://doi.org/10.5447/IPK/2018/4. No probe for *PFA-DSP5* was present in the microarray chips. Seven-day-old plants pre-cultured on sufficient P_i supply were transferred to fresh solid media containing 625 µM P_i (+Pi) or 100 µM P_i (-Pi). Whole roots were collected at the indicated time points after transfer. Data represent means ± SD (n = 3). (B) Heatmap analysis of *PFA-DSP*s genes in response to the indicated P_i treatmens. No data are presented for *PFA-DSP2* as no probe for this gene is present in Affimetrix chips. Transcriptional data were retrieved and analyzed with Genevestigator (http://www.genevestigator.ethz.ch).

Table S1: Overview of *Arabidopsis* PFA-DSP substrate specificities in presence of Mg^{2+} showing a robust PP-InsP phosphohydrolase activity against 5-InsP$_7$, 1,5-InsP$_8$ and 3,5-InsP$_8$, *in vitro*. The table summarizes the *in vitro* results of Figure 1, 3, S2 and S7. (-) indicates no substrate, (+) poor substrate, (++) good substrate and n.d. no data.

Mg^{2+}	1-InsP$_7$	2-InsP$_7$	3-InsP$_7$	4-InsP$_7$	5-InsP$_7$	6-InsP$_7$	1,5-InsP$_8$	3,5-InsP$_8$
Siw14	(-)	(-)	(-)	(+)	(++)	(+)	(++)	(++)
PFA-DSP1	(+)	(-)	(+)	(+)	(++)	(+)	(++)	(++)
PFA-DSP2	(-)	(-)	(-)	(+)	(++)	(+)	(++)	(++)
PFA-DSP3	(+)	(-)	(+)	(+)	(++)	(+)	(++)	(++)
PFA-DSP4	(+)	(-)	(+)	(+)	(++)	(+)	(++)	(++)
PFA-DSP5	(-)	(-)	(-)	(-)	(-)	(-)	(-)	(-)
PFA-DSP5 *	(-)	(-)	(-)	(+)	(++)	(+)	n.d.	n.d.

* tested with a higher PFA-DSP5 concentration and increased incubation time

Table S2: Oligonucleotide sequences.

Primer name	Sequence
attB1 adapter	GGGGACAAGTTTGTACAAAAAAGCAGGCTTC
attB2 adapter	GGGGACCACTTTGTACAAGAAAGCTGGGTC
attB2+V5 adapter	GGGGACCACTTTGTACAAGAAAGCTGGGTCTTACGTAGAATCGAGACCGAGGAGAGGG TTAGGGATAGGCTTACCTCCTCCAGATCC
attB1_ScSIW14	AAAAAGCAGGCTTCATGGGTTTATATCAAGCAAAG
attB2_ScSIW14s	AAAAAGCAGGCTTCATGGGTTTATATCAAGCAAAG
attB2_ScSIW14V5	CTTACCTCCTCCAGATCCCCATTGTAGAGGCAACCAG
attB1_AtPFA-DSP1	AAAAAGCAGGCTTCATGAAGCTTGTGGAGAAGAC
attB2_AtPFA-DSP1ns	AGAAAGCTGGGTCCCTGATGGAACAAGAGAATG
attB2_AtPFA-DSP1s	AGAAAGCTGGGTCTTACCTGATGGAACAAGAG
attB2_AtPFA-DSP1V5	ACCTCCTCCAGATCCCCTGATGGAACAAGAGAATG
attB1_AtPFA-DSP2	AAAAAGCAGGCTTCATGAAACTGATTGAGAAGACG
attB2_AtPFA-DSP2s	AGAAAGCTGGGTCTTACCTATTGGAGCAAGAAAAAG
attB2_AtPFA-DSP2V5	ACCTCCTCCAGATCCCCTATTGGAGCAAGAAAAAGAC
attB1_AtPFA-DSP3	AAAAAGCAGGCTTCATGTGTTTGATTATGGAAACGG
attB2_AtPFA-DSP3s	AGAAAGCTGGGTCTTAAACTCTAGCAGCCTGCG
attB2_AtPFA-DSP3V5	ACCTCCTCCAGATCCAACTCTAGCAGCCTGCGG
attB1_AtPFA-DSP4	AAAAAGCAGGCTTCATGACGTTAGAGAGTTACGCCG
attB2_AtPFA-DSP4s	AGAAAGCTGGGTCTCAGTAATCAATAGTATTAGTATACCTCTTGG
attB2_AtPFA-DSP4V5	ACCTCCTCCAGATCCGTAATCAATAGTATTAGTATACCTCTTGG
attB1_AtPFA-DSP5	AAAAAGCAGGCTTCATGGGCTTAATTGTGGATGATG
attB2_AtPFA-DSP5s	AGAAAGCTGGGTCTTATCCTTTGGTGGCTTGAGG
attB2_AtPFA-DSP5V5	ACCTCCTCCAGATCCTCCTTTGGTGGCTTGAGG
ScSIW14_C214S_F	TCAACCGATACTGATACATTCTAATAGAGGCAAACATAGAAC
ScSIW14_C214S_R	GTTCTATGTTTGCCTCTATTAGAATGTATCAGTATCGGTTGA
AtPFA-DSP1_C150S_F	GTTCTGATTCATAGTAAGCGAGGC
AtPFA-DSP1_C150S_R	GCCTCGCTTACTATGAATCAGAACA
ScSIW14pgt_PstI_F	AGCCTGCAGGATGGAGCTGCTCCTGGCTG
ScSIW14pgt_EcoRI_R	GAATTCAATATAAAGCGGGAATTTTTTTTTTTC
AtPFA-DSP1_267_F	ATACTTGTGCCCGGAGCCCT
AtPFA-DSP1_373_R	TCACAAATGGCTCCTTGTTGCCT
AtTIP41-like_F	TGGTTGGAAGCAGGAAGGGCT
AtTIP41-like_R	TGCTGAGACGGCTTGCTCCTGA
AtPP2AA3_F_qPCR	TGGTGCTCAGATGAGGGAGA
AtPP2AA3_R_qPCR	TAGCACATCTGGGGCACTTG
ScSIW14_pUG_F	CTCTTCTGGATCAATTTTTCTTTTTCATCTAAAGTTTAAAAGGAGCAGCTGAAGCTTCGTA CGC
ScSIW14_pUG_R	CATCATTTTCGAAGAGACTAGTTACGTAAAGGTAATCACTGTCTACATAGCATAGGCCAC TAGTGGATCTG
WiscDsLox_473B10_LP	TTGTTTTGCAAAACTGCAAAG
WiscDsLox_473B10_RP	TTGCCTTCAATACCAAACTGG
P745_WiscDsLox_F	AACGTCCGCAATGTGTTATTAAGTTGTC
GT1415_F	CGACTCTCCTCACCTAAAGATTCA
GT1415_R	GTTGCCTTCAATACCAAACTGG
DS3-1	ACCCGACCGGATCGTATCGGT
SAIL_116_C12_LP	TTGTTTTGCAAAACTGCAAAG
SAIL_116_C12_RP	TTGCCTTCAATACCAAACTGG
LB1_SAIL_F	GCCTTTTCAGAAATGGATAAATAGCCTTGCTTCC

[&]Present address: Department of Biomedicine, University of Basel, 4058 Basel, Switzerland

References

1. Kuo, H. F., Hsu, Y. Y., Lin, W. C., Chen, K. Y., Munnik, T., Brearley, C. A., and Chiou, T. J. (2018) Arabidopsis inositol phosphate kinases IPK1 and ITPK1 constitute a metabolic pathway in maintaining phosphate homeostasis, Plant J.
2. Stevenson-Paulik, J., Bastidas, R. J., Chiou, S. T., Frye, R. A., and York, J. D. (2005) Generation of phytate-free seeds in Arabidopsis through disruption of inositol polyphosphate kinases, Proc Natl Acad Sci U S A 102, 12612-12617.
3. Bhosale, R., Giri, J., Pandey, B. K., Giehl, R. F. H., Hartmann, A., Traini, R., Truskina, J., Leftley, N., Hanlon, M., Swarup, K., Rashed, A., Voss, U., Alonso, J., Stepanova, A., Yun, J., Ljung, K., Brown, K. M., Lynch, J. P., Dolan, L., Vernoux, T., Bishopp, A., Wells, D., von Wiren, N., Bennett, M. J., and Swarup, R. (2018) A mechanistic framework for auxin dependent Arabidopsis root hair elongation to low external phosphate, Nat Commun 9, 1409.

6.3. Other publications

Laha, D., Johnen, P., Azevedo, C., Dynowski, M., Weiß, M., Capolicchio, S., Mao, H., Iven, T., Steenbergen, M., Freyer, M., Gaugler, P., de Campos, M. K., Zheng, N., Feussner, I., Jessen, H. J., Van Wees, S. C., Saiardi, A., Schaaf, G. VIH2 Regulates the Synthesis of Inositol Pyrophosphate InsP8 and Jasmonate-Dependent Defenses in Arabidopsis. *The Plant cell* 2015, 27(4), 1082–1097. https://doi.org/10.1105/tpc.114.135160

Zhu, J., Lau, K., Puschmann, R., Harmel, R. K., Zhang, Y., Pries, V., Gaugler, P., Broger, L., Dutta, A. K., Jessen, H. J., Schaaf, G., Fernie, A. R., Hothorn, L. A., Fiedler, D., Hothorn, M. Two bifunctional inositol pyrophosphate kinases/phosphatases control plant phosphate homeostasis. *eLife* 2019, 8, e43582.
https://doi.org/10.7554/elife.43582

Riemer, E., Qiu, D., Laha, D., Harmel, R. K., Gaugler, P., Gaugler, V., Frei, M., Hajirezaei, M. R., Laha, N. P., Krusenbaum, L., Schneider, R., Saiardi, A., Fiedler, D., Jessen, H. J., Schaaf, G., Giehl, R. F. H. ITPK1 is an $InsP_6$/ADP phosphotransferase that controls phosphate signaling in Arabidopsis. *Molecular plant* 2021, 14(11), 1864–1880.
https://doi.org/10.1016/j.molp.2021.07.011

Laha, N. P., Giehl, R. F. H., Riemer, E., Qiu, D., Pullagurla, N. J., Schneider, R., Dhir, Y. W., Yadav, R., Mihiret, Y. E., Gaugler, P., Gaugler, V., Mao, H., Zheng, N., von Wirén, N., Saiardi, A., Bhattacharjee, S., Jessen, H. J., Laha, D., Schaaf, G. INOSITOL (1,3,4) TRIPHOSPHATE 5/6 KINASE1-dependent inositol polyphosphates regulate auxin responses in Arabidopsis. *Plant physiology* 2022, 190(4), 2722–2738.
https://doi.org/10.1093/plphys/kiac425

7. Acknowledgements

First and foremost, I want to thank Professor Gabriel Schaaf for giving me the opportunity to continue my work at his lab after my Master studies and to move with him to Bonn for my doctoral studies. A step that ultimately had much more impact on my life than the PhD itself.
I want to thank him for the trust and the possibility to set up the new lab in Bonn and creating a new scientific environment for us that moved from Tübingen, for the ones that joined shortly after and the ones that were already there. During all these years, I learned a lot of things, not only about science, but also about academia and especially about myself.
Thank you, Gabriel, for the great supervision during this one-decade long journey and for giving me the opportunity and the encouragement to learn a lot about science and a lot about the things that make science possible.

Thanks to all the members of the GRK2064, especially Professor Peter Dörmann and Professor Andreas Meyer, for fruitful discussions and their efforts to make my time in the GRK not only very constructive for my thesis but also very enjoyable.

I want to thank Debabrata Laha for starting this whole project and the support during all these years.
Thank you, Deb, for all the help and the fun times in and outside the lab.

Of course I want to thank all the previous and current members of Lab Schaaf and the Plant Nutrititon, with whom I had the honor and delight to work with. Way more people than I can mention here, but I want to highlight some. Marília and Philipp, for giving me a warm welcome back when I started by bachelor thesis and for all the support and nice times all the years. Esther and Robin for all the fun we had and still have during these sometimes very difficult times in and outside the lab. Brigitte for the tremendous help during my daily work.
And of course my favorite PostDoc, seat neighbor, lab partner and moving helper, Verena, who evolved quite quickly from colleague to friend to girlfriend to wife. Thank you literally for everything. I love you and I owe you much more than you can imagine.

Last but not least, a very big thank you to my whole family and friends for their support and help. Mama, Papa, thank you for all your help, encouragement, patience and understanding and giving me the opportunity and the strength to go my way.